

**Characteristics of the P2Y₁₁ nucleotide receptor:
Ligand binding characteristics and P2Y₁₁-P2Y₁ receptor
interaction**

Dissertation

zur Erlangung des akademischen Grades

doctor rerum naturalium

(Dr. rer. nat.),

genehmigt durch

die Fakultät der Naturwissenschaften
der Otto-von-Guericke Universität Magdeburg

von **Apothekerin Denise Ecke**

geb. am 25. September 1978 in Halle/S.

Gutachter:

Prof. Dr. Georg Reiser

Prof. Dr. Karen Nieber

Eingereicht am:

06.06.07

Verteidigung am:

16.11.2007

Rosemarie Geide, in ewiger Erinnerung

Danksagung

Mein Dank gilt Herrn Prof. Dr. G. Reiser, der diese Arbeit ermöglicht hat. Durch seine stete Diskussionsbereitschaft, seine Anregungen und seine Unterstützung während des gesamten Projektes hat er den erfolgreichen Fortgang dieser Arbeit mitgestaltet.

Der Platz reicht leider nicht aus, um mich angemessen bei Herrn Dr. Rainer Schäfer für seine Hilfsbereitschaft, seine Anregungen und sein Verständnis zu bedanken. Dennoch möchte ich kurz zusammenfassen, dass ich ihm für das Wissen, das er mir vermittelt hat, und dafür dass er immer zur Stelle war sehr dankbar bin.

Herrn Dr. Theodor Hanck, Frau Dr. Fariba Sedehizadeh und Herrn Dr. Rolf Stricker bin ich für die Einführung in die molekularbiologische Methodik sehr dankbar. Ohne die Hilfe dieser drei Personen wäre ich mit Sicherheit in den ‚Startblöcken‘ stecken geblieben oder auf dem Weg zum Abschluß dieser Arbeit gestrauchelt. Besonders dankbar bin ich auch für die Bereitschaft von Dr. Theodor Hanck in allen Lebenslagen als wandelndes Lexikon zur Verfügung zu stehen.

Die Arbeit im Team mit Herrn Mohan E. Tulapurkar war sehr wertvoll für diese Arbeit. Ich möchte mich bei ihm zuerst für die Unterweisung im Fluoreszenz-Imaging und der konfokalen Mikroskopie bedanken. Weiterhin hat er mir klar gemacht, dass man mit ein wenig mehr Gelassenheit meistens mehr erreicht. Für seine Unterstützung und unsere gute Zusammenarbeit bin ich sehr dankbar.

Die Versuche zu dieser Dissertation wären noch längst nicht abgeschlossen, hätte ich nicht auf die exzellente, technische Unterstützung von Dorothee Terhardt zurückgreifen können. Ich möchte mich bei ihr für ihre Aufmerksamkeit, ihr Engagement und ihre freiwillige Übernahme der Funktion: ‚mein zweites Gedächtnis‘ bedanken.

Mein Dank gilt auch allen anderen Mitarbeitern und ehemaligen Mitarbeitern unserer Arbeitsgruppe, insbesondere Frau A. Schneider, P. Grüneberg, Frau K. Christoph und E. Busse für ihre technische Unterstützung. Dankbar bin ich auch für die gute Atmosphäre im Labor, die vor allem durch Sabine Hein, Dr. Stefan Kahlert, Dr. Gregor Zündorf, Dr. Mikhail Strokin, und Claudia Borrmann aufrecht erhalten wurde. Weibo Luo bin ich für seine Kooperationsbereitschaft dankbar. Für die Unterstützung in allen organisatorischen Angelegenheiten möchte ich mich bei Frau I. Klaes und Frau M. Dullin-Viehweg bedanken. Letzteren bin ich weiterhin dankbar, dass sie mich beim Bowling immer haben gewinnen lassen. Bei Herrn Peter Ehrbarth bedanke ich mich für die prompte Reparatur von etwaigen technischen Geräten und abstürzenden Computern. Mein herzlicher Dank gilt auch den Leuten vom Mobitz-Stammtisch: Dr. U. Schröder, Dr. T. Hecht, Dr. E. Wilhelmi, J. Ullrich, D. Albrecht und Dr. C. Sabelhaus für die interessanten Debatten über reale Forschung.

Nicht zuletzt möchte ich mich bei meinen Eltern für ihr grenzenloses Verständnis und die Unterstützung während der gesamten Zeit der Promotion bedanken. Sie haben mir immer wieder Mut gemacht, wenn ich am Abschluß dieser Arbeit gezweifelt habe. Das gleiche gilt auch für Tanuja Rohatgi. Ich bin ihr dankbar, dass sie all meine Launen ertragen hat und trotzdem immer noch zu mir hält.

Table of content

1	Introduction	1
1.1	Receptor theory	1
1.2	Purinergic Signaling	3
1.3	Purinergic Receptor Family	3
1.3.1	General properties of P2Y receptors	4
1.3.2	Pharmacological characteristics of the P2Y ₁ and P2Y ₁₁ receptor	7
1.3.3	Physiological roles of the P2Y ₁₁ receptor	9
1.3.4	Ligand recognition at the P2Y receptor	11
1.4	Oligomerization of GPCRs	14
1.5	Aims of the thesis project	17
2	Materials and Methods	20
2.1	Materials	20
2.1.1	Cell lines	20
2.1.2	Bacterial strains	20
2.1.3	Plasmid vectors	20
2.1.4	Enzymes	21
2.1.5	Kits	21
2.1.6	Laboratory instruments	22
2.1.7	Chemicals and reagents	23
2.1.8	Antibodies	24
2.1.9	Molecular mass markers	24
2.1.10	Buffers and solvents	24
2.1.11	Oligonucleotides	27
2.2	Methods	30
2.2.1	Methods in molecular biology	30
2.2.2	Methods in Cell Biology	40
2.2.3	Methods in Protein chemistry	43
2.2.4	[Ca ²⁺] _i measurements	46
2.2.5	Confocal imaging	47
2.2.6	Flow cytometry	48
2.2.7	Data analysis	48

3	Results	49
3.1	Diastereoselectivity of the P2Y₁₁ receptor: P_α substituted ATP analogues	49
3.1.1	Heterologous expression of the P2Y ₁₁ GFP receptor in 1321N1 cells	49
3.1.2	Calcium measurements with pairs of different ATP diastereoisomers	50
3.1.3	Adenosine-5'-O-(α -thiotriphosphate) diastereoisomers	54
3.2	Ligand recognition at the P2Y₁₁ receptor	57
3.2.1	Selection of residues putatively involved in ligand recognition	57
3.2.2	Introduction of point mutations into the P2Y ₁₁ receptor DNA sequence	58
3.2.3	Expression of P2Y ₁₁ receptor mutants in 1321N1 cells	59
3.2.4	Pharmacological characterisation of the P2Y ₁₁ receptor mutants	59
3.3	Hetero-oligomerization of the P2Y₁ and the P2Y₁₁ receptor.....	66
3.3.1	Agonist-induced internalization of the P2Y ₁₁ GFP receptor in HEK293 cells	66
3.3.2	Co-Internalization of the P2Y ₁ and P2Y ₁₁ GFP receptor in HEK293 cells	69
3.3.3	Co-internalization of the P2Y ₁ and P2Y ₁₁ receptor in 1321N1 cells	72
3.3.4	Co-Pulldown Experiments	78
3.3.5	Co-immunoprecipitation of P2Y ₁ mycHis and P2Y ₁₁ GST receptors	81
3.3.6	Pharmacological characteristics of the receptor heterooligomer	83
4	Discussion	87
4.1	Diastereoselective activation is opposite for the P2Y₁ receptor and the P2Y₁₁ receptor	87
4.2	Ligand binding site characteristics of the P2Y₁₁ receptor deduced from mutational analysis	90
4.3	Crosstalk between two P2Y receptors: the P2Y₁ and P2Y₁₁ receptor	95
5	Zusammenfassung	102
6	Abstract	105
7	References	107
8	Abbreviations	114

Table of Figures

Figure 1:	Principles of linkage models in receptor theory (Rang et al., 2003; Colquhoun, 2006).....	1
Figure 2:	Recent developments in receptor theory (Kenakin and Onaran, 2002; Kenakin, 2004)	2
Figure 3:	Structure of a Class A GPCR	5
Figure 4:	(A) Multiple Sequence alignment (Clustal X 1.83) and (B) key residues of the human P2Y ₁ receptor involved in ligand recognition, adapted from (Ivanov et al., 2006).....	13
Figure 5:	Schematic representation of mechanisms potentially involved in GPCR oligomer formation adapted from (Kroeger et al., 2003).....	17
Figure 6:	Non-functional expression of P2X and P2Y receptors in wild type 1321N1 cells	49
Figure 7:	Western blot detection of the P2Y ₁₁ GFP receptor in stably transfected 1321N1 cells	50
Figure 8:	Concentration-response curves for ATP- α -B analogues and parent compounds at the P2Y ₁₁ receptor.....	52
Figure 9:	Concentration-response curves for 2-Cl-ATP- α -B analogues at the P2Y ₁ receptor	53
Figure 10:	Concentration-response curves for ATP- α -S analogues and parent compounds at the P2Y ₁₁ receptor	55
Figure 11:	Docked ATP and interacting residues in a molecular model of the P2Y ₁₁ receptor	57
Figure 12:	Introduction of mutations into the DNA-Sequence of the P2Y ₁₁ receptor.....	58
Figure 13:	Concentration-response curves for ATP γ S at the wild type and mutant P2Y ₁₁ GFP receptor stably expressed in 1321N1 cells	61
Figure 14:	Concentration-response curves for ATP at the wild type and mutant P2Y ₁₁ GFP receptor stably expressed in 1321N1 cells	62
Figure 15:	Concentration-response curves for ATP- α -S (A) and (B) isomers at the wild type and mutant P2Y ₁₁ GFP receptors stably expressed in 1321N1 cells	64
Figure 16:	Section of the molecular model of the P2Y ₁₁ receptor displaying a hydrophobic pocket	66
Figure 17:	Live imaging of agonist-induced internalization of the P2Y ₁₁ GFP receptor stably expressed in HEK293 cells	67
Figure 18:	Intracellular calcium rise in stably transfected HEK293 cells	68
Figure 19:	Expression levels of mRNA of different GPCRs in HEK293 cells.....	69
Figure 20:	Intracellular calcium rise in HEKP2Y ₁₁ GFP cells	70
Figure 21:	GPCR crosstalk in agonist-induced P2Y ₁₁ GFP receptor endocytosis	71
Figure 22:	Agonist-induced internalization of the P2Y ₁ GFP and P2Y ₁₁ GFP receptor in 1321N1 cells.....	72
Figure 23:	Co-internalization of the P2Y ₁ mycHis and P2Y ₁₁ GFP receptor in 1321N1 cells	73
Figure 24:	Live-imaging of the A ₂₆₈ P2Y ₁₁ GFP receptor in HEK293 cells	75
Figure 25:	Expression level of P2Y ₁ receptor mRNA in HEKP2Y ₁₁ GFP cells after siRNA treatment.....	76
Figure 26:	Treatment with P2Y ₁ -R siRNA reduces internalization of the P2Y ₁₁ GFP receptor in HEK293 cells	76
Figure 27:	Fluorescence intensities of the P2Y ₁₁ GFP receptor in cytosol of siRNA transfected HEK293 cells upon agonist stimulation	77
Figure 28:	Co-pulldown of the P2Y ₁ mycHis and P2Y ₁₁ GST receptor from HEK 293 cells	80
Figure 29:	Co-Pulldown of the P2Y ₁ mycHis and A ₂₆₈ P2Y ₁₁ receptor from HEK 293 cells	81
Figure 30:	Co-Immunoprecipitation (IP) of the P2Y ₁ mycHis and P2Y ₁₁ GST receptors from HEK293 cells	82
Figure 31:	Peak values of intracellular calcium rise induced by P2Y receptor stimulation.....	84
Figure 32:	Peak values of intracellular calcium rise induced by UDP in HEK293 cells	85
Figure 33:	Stimulation of cAMP accumulation in HEKP2Y ₁₁ GFP cells	86

1 INTRODUCTION

1.1 Receptor theory

The word ‘receptor’ originates from the Latin word ‘recipere’ – to accept, receive. Thus, in biochemistry a receptor is known to be a protein that accepts or receives signals (ligands, drugs), which then initiate a cellular response. The first step in the generation of such a signal-transduction cascade is the formation of a reversible drug-receptor complex (Paul Ehrlich: ‘Corpora non agunt nisi fixata’ ~ ‘A drug will not work unless it is bound’), where the reactions are governed by the Law of Mass Action (Rang et al., 2003). In terms of the occupation theory (linkage model), a linear relationship between receptor occupancy and cellular response was assumed because the roughly hyperbolic shape of the dose-response curves in pharmacological measurements seemed to reflect ‘Langmuirean binding’ (Fig. 1). However, there is not necessarily a linear relationship between the proportion of occupied receptors and the response which makes the use of the dose-response curves for determination of agonist affinity at a receptor impossible.

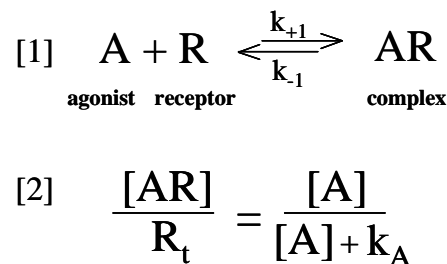


Figure 1: Principles of linkage models in receptor theory (Rang et al., 2003; Colquhoun, 2006)

[1] Schematic representation of the reaction of agonist (A) and receptor (R) in drug-receptor complex (AR) formation with a specific association (k_{+1}) and dissociation (k_{-1}) rate constant. Applying the Law of Mass Action to this reaction results in equation [2] which is known as the Hill-Langmuir equation. The proportion of receptors occupied (AR) is dependent on the total receptor density (R_t), agonist concentration (A) and the equilibrium constant (k_A). The equilibrium constant (k_A) is a characteristic of the agonist and the receptor.

This knowledge revealed the limitation of defining receptors simply by the order of agonist occupancy in a single tissue (Limbird, 2004). In the operational model, more emphasis was put on the characteristics of the tissue (e.g. nature of the coupling between the receptor and response), as well as of the agonist itself, and the concept of intrinsic efficacy was more closely related to experimentally observed behavior of pharmacological systems by the transducer function (Kenakin, 2004). Thus, this model was able to explain how differences in the transducer function and receptor density in different tissues can result in the same agonist, acting on the same receptor, appearing as a full agonist in one tissue, and as a partial agonist in another one (Rang et al., 2003).

The discovery of constitutively active G protein-coupled receptors (GPCR) and inverse agonism has led to a renaissance in receptor theory and already existing models had to be extended to describe this new receptor behaviour (Kenakin, 2004). The extended ternary complex model describes the coupling of a receptor to an agonist and/or a trimeric G protein with selective affinities of agonist/ antagonists for the active (R_a) or inactive receptor (R_i) (Fig. 2, [1]). This allowed for the theoretical characterization of an inverse agonist. Such an agent stabilizes the inactive form of the receptor thereby reducing its ‘basal’ or constitutive activity, whereas a full agonist has a high preference for the activated state of the receptor. Moreover, an antagonist shows no preference and binds to both states of a receptor, thereby not changing the existing equilibrium between both states and not eliciting an observable cellular response (Limbird, 2004).

However, the shortcoming of all linkage models is that they must pre-define the species present in a thermodynamic space. If there are more species than defined, these models fail. The probabilistic model of GPCRs assumes that a receptor possesses a particular distribution between different conformations in a resting state (Fig. 2, [2]). The binding of a ligand and/ or G protein changes this distribution by stabilizing specific conformations. Thus, agonists are ligands that shift the distribution of conformations towards those that activate G proteins. After all, GPCRs are now seen as interactive information processing units other than switches for G proteins (Kenakin, 2004).

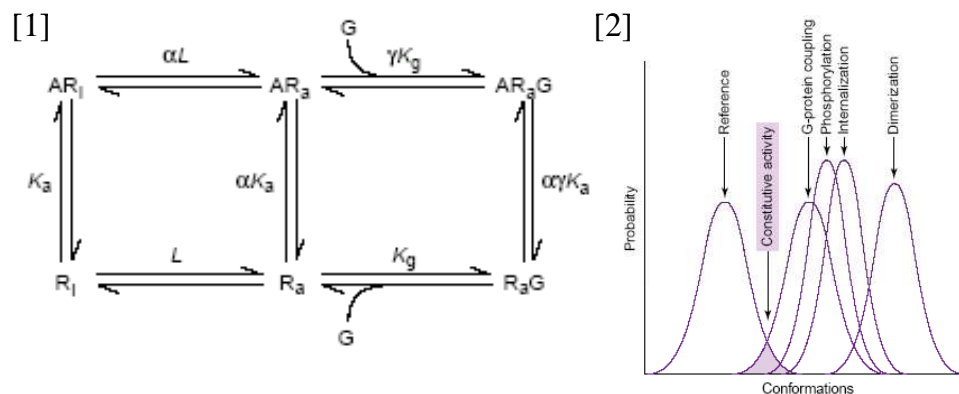


Figure 2: Recent developments in receptor theory (Kenakin and Onaran, 2002; Kenakin, 2004)

[1] The extended ternary complex model describes the coexistence of inactive (R_i) and active (R_a) receptor states according to the constant L . G proteins (G) that enter the system can bind to R_a in or without the presence of an agonist (A). The ligand can bind to both receptor states. Constitutive activity is the spontaneous formation of R_aG complexes. Affinity of ligands is described by K_a and efficacy by the two terms α and γ . [2] Example of the distribution of different receptor conformations in the probabilistic model of GPCRs. The ‘reference’ ensemble represents the collection of receptor conformations in the resting state. The intersection between the ‘reference’ and ‘G protein coupling’ ensembles indicates constitutive activity.

1.2 Purinergic Signaling

The term 'purinergic' was coined by Geoffrey Burnstock, who first introduced ATP as a signaling molecule to the scientific world (Burnstock, 1971). Since then ATP was already known to be involved in many biochemical processes, but the idea of such an universal molecule also acting as a signal transmitter was not well accepted in the beginning. Subsequently, as the existence of purinergic receptors became obvious, also sceptics became convinced (Burnstock, 1976). The idea evolved that two types of purinergic receptors can be distinguished, and they were recognized as P1 (adenosine/ nucleoside) and P2 (nucleotide) receptors. Simultaneously, the presence of ectoenzymes that metabolize ATP or ADP to produce AMP or adenosine were discovered (Cooper et al., 1979) and two different ectonucleotidases and a nucleoside diphosphate kinase were characterized (Pearson et al., 1980). This made the purinergic signaling system complete.

1.3 Purinergic Receptor Family

The purinergic receptor family consists of two different subgroups, the P1 and P2 receptors. P1/adenosine receptors (Table 1, next page) have four known members (A_1 , A_{2A} , A_{2B} , A_3) that have been cloned from a variety of species. The natural agonist is adenosine. Nonselective antagonists (but not universal) at the P1 receptors are xanthines and xanthine derivatives (e.g. caffeine, theophylline). Selective antagonists of the A_{2A} receptor are currently under investigation as novel Anti-Parkinson-Therapeutics (Jenner, 2005) due to an observed reduced affinity of agonists binding to D2 dopamine receptors upon stimulation of A_{2A} receptors (Ferre et al., 1997). P1 and P2 receptors are found to be opponents under many physiological or pathophysiological conditions, as they crossregulate their mutual function due to the degradation of ATP to adenosine by ectoenzymes or the phosphorylation of adenosine by ectokinases.

In 1985 the existence of two P2 receptor types was proposed (P2X and P2Y) (Burnstock and Kennedy, 1985) and to date seven P2X subtypes and eight P2Y receptor subtypes have been discovered (Ralevic and Burnstock, 1998). The P2X receptors are ligand-gated ion channels that, like other ion channels, are oligomeric proteins consisting of several subunits (Khakh et al., 2001). However, they are ion channels whose molecular architecture is different from any other ion channel family (Khakh and North, 2006). They have two membrane-spanning domains and most of the protein is located extracellularly. All P2X receptors are cation-selective with almost equal permeability for Na^+ and K^+ and a significant permeability for Ca^{2+} (Evans et al., 1996).

Table 1: P1 receptor effects and ligands adapted from Ralevic et.al. 1998

P1 receptor subtypes	G protein coupling effects	Selective Agonists	Selective Antagonists
A ₁	G _{i/o} cAMP↓; IP ₃ ↑	N ⁶ -cyclopentyladenosine (CPA)	1,3-dipropyl-8-cyclopentylxanthine (DPCPX)
A _{2A}	G _s cAMP↑	2-[p-(2-carbonyl-ethyl)-phenylethylamino]-5'-N-ethylcarboximidoadenosine (CGS21680)	1,3-dipropyl-8-(3,4-dimethoxystyryl)-7-methylxanthine (KF17837)
A _{2B}	G _s , G _q cAMP↑; IP ₃ ↑	-	-
A ₃	G _i , G _q cAMP↓; IP ₃ ↑	N ⁶ -(3-iodo-benzyl)-5'-(N-methylcarbamoyl)adenosine (IB-MECA)	3,6-dichloro-2'-isopropoxy-4'-isopropylflavone (MRS1067)

The receptors can exist either as homomeric or heteromeric proteins. So far eleven P2X subunit combinations are known. ATP is the natural ligand at all seven homomeric P2X receptor subtypes. Moreover, nearly all P2X receptors respond more or less to BzATP, except the P2X₆ receptor (Burnstock and Knight, 2004). Antagonists at the P2X receptor include the universal P2 receptor antagonists suramin and PPADS and the more selective antagonist TNP-ATP (Gever et al., 2006).

P2X receptor subunits are widely expressed in the nervous system, and at some central synapses ATP is a fast neurotransmitter eliciting small synaptic currents (Khakh and North, 2006). Moreover, there is evidence that ATP is involved in the chronic nociceptive behavior following nerve injury or inflammation acting through P2X₃ receptors (Burnstock, 2006).

1.3.1 General properties of P2Y receptors

The P2Y receptors are G protein-coupled receptors. They belong to the rhodopsin family of G protein-coupled receptors also called Class A GPCRs with seven predicted transmembrane (TM) domains. The N-terminus locates on the extracellular side and the C-terminus on the cytoplasmic side of the plasma membrane (Fig. 3). The TMs and extracellular loops are believed to form the ligand-binding pocket and the intracellular loops interact with the appropriate G protein to activate subsequent transduction mechanisms (Ralevic and Burnstock, 1998).

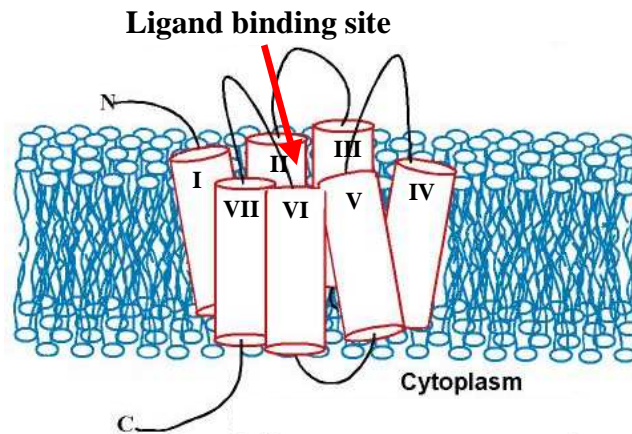


Figure 3: Structure of a Class A GPCR

As all other GPCRs, P2Y receptors are constituted by a single polypeptide chain, which crosses the cell membrane seven times, forming seven TMs (α -helical structure) connected by three extracellular and three intracellular loops. The amino terminal region is located outside the cell, while the carboxyl terminal region is located in the cytoplasm where the G proteins are activated.

To date eight different P2Y receptors have been cloned and are divided into two phylogenetically different subgroups. The P2Y_{1, 2, 4, 6, 11} receptors belong to the group that preferentially couples to G_q proteins, and the P2Y_{12, 13, 14} receptors form the second group that couples to G_i proteins (Costanzi et al., 2004). Of the first group, the P2Y₁₁ receptor also couples to G_s proteins and is less closely related to the other group members.

The natural ligands of P2Y receptors can be either adenine or uridine nucleotides. In both P2Y receptor subgroups adenine nucleotide preferring receptors (P2Y_{1, 11, 12, 13}) as well as uridine nucleotide preferring receptors (P2Y_{4, 6}) can be found. The P2Y₂ receptor is equally activated by UTP or ATP. A summary of the principal agonists and antagonists at the different P2Y receptor subtypes can be found in Table 2.

The expression of the P2Y receptors in several tissues brings along many physiological roles of these receptors. The P2Y₁ receptor is probably the most extensively studied subtype. It has a conserved macroscopic localization in the mammalian brain (Moore et al., 2000) and can function as a presynaptic inhibitor of glutamate release (Rodrigues et al., 2005). The most established function of the P2Y₁ receptor is its role in the platelet physiology next to the P2Y₁₂ receptor. The selective activation of the P2Y₁ receptor on platelets leads to cytosolic Ca²⁺ mobilization and shape change, followed by a rapidly reversible aggregation of the platelets. However, activation of the P2Y₁₂ receptor mediates sustained platelet aggregation in the absence of shape change (Oury et al., 2006).

Table 2: Human P2Y receptors: activities of agonists and affinities of antagonists (^a selective agonist/antagonist) at the different receptor subtypes and their distribution in tissues summarized from (Burnstock and Knight, 2004; von Kugelgen, 2006)

Receptor subtype	Major tissue distribution	Agonists	Antagonists
P2Y ₁	wide including platelets, heart, skeletal muscle, neuronal tissues, digestive tract	MRS2365 ^a > 2-MeS-ADP > ADP = ADPβS = ATPβS >> ATP	MRS2179, MRS2500 ^a , Suramin, Reactive Blue 2
P2Y ₂	wide including lung, heart, skeletal muscle, spleen, kidney	UTP = ATP = UTPγS > INS37217 > Ap4A > ATPγS	Reactive Blue 2, Suramin
P2Y ₄	placenta, lung, vascular smooth muscle, brain, liver	UTP	PPADS, Reactive Blue 2
P2Y ₆	wide including lung heart, aorta, spleen, placenta, thymus, intestine, brain	UDP = UDPβS = 5-Br-UDP > 2-MeS-ADP > UTP	MRS2567 ^a , Reactive Blue2, PPADS
P2Y ₁₁	spleen, intestine, immune system, brain, pituitary	ARC67085 = ATPγS = BzATP > dATP > ATP > 2-MeS-ATP	NF157, Suramin, Reactive Blue 2
P2Y ₁₂	platelets, neural tissue	2-MeS-ADP > ADP = ATPβS > 2-MeS-ATP	Clopidogrel ^a , ARC69931MX, Suramin, Reactive Blue 2
P2Y ₁₃	spleen, leucocytes, bone marrow, liver, brain	2-MeS-ADP > ADP = 2-MeS-ATP > ADPβS	ARC69931MX, Reactive Blue 2, Suramin, PPADS
P2Y ₁₄	placenta, adipose tissue, spleen, intestine, brain	UDP-glucose > UDP-galactose	-

Moreover, the P2Y₁ receptor also functions as an activator of bone resorption, regulator of the vascular tone in the placenta and together with the P2Y₂ receptor as a postsynaptic gene activator in neuromuscular junctions (Tsim and Barnard, 2002; Gallagher, 2004; Buvinic et al., 2006). Agonists at the P2Y₂ receptor, furthermore, are targets of clinical research on cystic fibrosis (CF). It is known that activation of the P2Y₂ receptor partially compensates the impaired chloride secretion in CF patients and that genetic variants of the P2Y₂ receptor contribute to phenotypic differences in the disease state of the patients (Buscher et al., 2006).

Likewise, activation of the P2Y₄ receptor can also influence epithelial ion transport. In mice jejunum and colon, P2Y₄ receptor activation induces epithelial chloride transport and K⁺ secretion, respectively (Robaye et al., 2003; Matos et al., 2005). The other pyrimidine-selective receptor P2Y₆ seems to play a role in bone resorption by enhancing osteoclast survival (Korcok et al., 2005).

The phylogenetic subgroup of P2Y receptors that comprises the receptors coupled to G_i proteins has physiological functions in the human blood system. As already mentioned, the P2Y₁₂ receptor is important for platelet aggregation and thus thrombus formation. Moreover, recently the P2Y₁₂ receptor was shown to have a role in microglial activation at early stages after injury which suggests a physiological benefit in neuronal injury and disease if the receptor function is modulated by specific antagonists. The other ADP-preferring receptor of this subgroup is the P2Y₁₃ receptor, which was found to activate a negative feedback pathway for ATP release in red blood cells (RBCs). RBCs release ATP in response to reduction in oxygen tension and pH. The released ATP then acts on P2Y receptors expressed by endothelial cells of the vessels and leads to vasodilatation. Right after hydrolysis to ADP further release of ATP is attenuated by activation of the P2Y₁₃ receptor. Thus, the P2Y₁₃ receptor acts as a regulator of ATP-induced vascular tone adaptation (Wang et al., 2005).

Moreover, the P2Y₁₄ receptor is associated to haematopoietic stem cells, where it plays a direct role in stem cell phenotype and localization to the bone marrow compartment. Stem cells expressing the receptor are capable of undergoing multilineage differentiation (Lee et al., 2003).

1.3.2 Pharmacological characteristics of the P2Y₁ and P2Y₁₁ receptor

Among the P2Y receptors, the P2Y₁ and P2Y₁₁ receptor are found to be closest homologues, sharing 33% identical amino acids (Communi et al., 1997). However, both receptors display differences in their pharmacological properties despite of being exclusively activated by adenine nucleotides. The most striking difference is the preference of the human P2Y₁ receptor for adenosine diphosphates over triphosphates, which is opposite at the human P2Y₁₁ receptor. Moreover, the P2Y₁ receptor is characterized by the high potency of 2-MeS-ADP or 2-MeS-ATP (Palmer et al., 1998), whereas at the P2Y₁₁ receptor these agonists are only weakly potent (Communi et al., 1997).

Further changes of the phosphate chain and the ribose moiety increase the potency of the 2-alkylthio-ATP derivatives for the P2Y₁₁ receptor, as was observed for ARC-67085MX (2-propylthio-beta,gamma-dichloromethylene-d-ATP) (Communi et al., 1999; Wilkin et al., 2001; White et al., 2003). Furthermore, modified ribose as in d-ATP and BzATP results in potent ligands at the P2Y₁₁ receptor (Burnstock and Knight, 2004), whereas at the P2Y₁ receptor BzATP shows antagonistic activity (Vigne et al., 1999). A selective agonist for the P2Y₁ receptor is MRS2365 ((N)-methanocarba-2MeSADP), in which a pseudo-ribose, consisting of a bicyclic structure fused into the (N)-methanocarba modification, replaces the ribose moiety (Chhatriwala et al., 2004). The constrained northern conformation of the pseudo-ribose leads to increased potency at the P2Y₁ receptor in general and to a preserved potency at the P2Y₁₁ receptor, whereas the corresponding (S) isomers display greatly reduced potency at both receptors (Kim et al., 2002).

Adenosine phosphorothioates (ATP- β -S, ATP- γ -S) are able to activate both receptors, with the P2Y₁₁ receptor preferring the γ - and the P2Y₁ receptor the β -phosphorothioates as ligands. The action of adenosine 5'-O-(1-thiotriphosphate) (ATP- α -S) was more closely investigated. Through substitution of one of the non-bridging oxygen atoms of P $_{\alpha}$ by sulfur a new chiral center in the ATP molecule is introduced. The resulting diastereoisomers were separated, and these ATP- α -S diastereoisomers were shown to display a diastereoselective activity at the P2Y₁ receptor (Major et al., 2004). The recently synthesized chiral ATP- α -B analogues, where a borano group (BH₃) substitutes a non-bridging oxygen at P $_{\alpha}$, proved agonists at the P2Y₁ receptor, As with the ATP- α -S isomers, one chiral isomer was clearly preferred at this receptor (Nahum et al., 2002).

If receptor antagonists are considered, both the P2Y₁ and P2Y₁₁ receptors show an affinity for the broad-spectrum P2Y receptor antagonists Suramin and Reactive Blue 2 (Burnstock and Knight, 2004). The recently developed P2Y₁₁ receptor antagonist NF157 represents a Suramin derivative and clearly prefers the P2Y₁₁ over the P2Y₁ receptor but is still non-selective (Ullmann et al., 2005). In contrast, there are already selective antagonists available for the P2Y₁ receptor. MRS2500 has a nucleotide-like structure and also contains a pseudoribose locked in a northern conformation as described above for the selective P2Y₁ receptor agonist (Hechler et al., 2006).

The different pharmacology of the P2Y₁ and P2Y₁₁ receptors is important to consider if cells or tissues are investigated where both receptors are co-expressed. Here selective activation of one of the receptors can be important for interfering with pathophysiological conditions. Both receptors are present in large quantities in the human central nervous system. Co-expression is found in basal ganglia, hippocampus and the cerebellum (Moore et al., 2001). Moreover, the P2Y₁ and P2Y₁₁ receptors are also found in vascular smooth muscle cells and seem to mediate smooth muscle relaxation in the gastrointestinal tract. In immune cells, both receptors are expressed in macrophages, eosinophils and lymphocytes (Abbracchio et al., 2006). So far no clear cross-talk or cross-regulation between both receptors has been observed in such tissues. However, dendritic cells express the P2Y₁ as well as the P2Y₁₁ receptor (Berchtold et al., 1999). The function of the latter has already been studied (see below), whereas no specific function has been ascribed to the P2Y₁ receptor in dendritic cells. However, a previously uncharacterized ADP receptor seems to be involved in ERK activation and calcium mobilization leading to inhibition of cytokine production in these cells (Marteau et al., 2004). It can be hypothesized that this uncharacterized receptor represents a crosstalk between the P2Y₁ and P2Y₁₁ receptor that shows a combination of both receptor pharmacologies. Moreover, the P2Y₁ receptor was found to mediate the purinergic inhibitory neuromuscular transmission in the human colon (Gallego et al., 2006). However, the specific P2Y₁ receptor antagonist MRS2179 was not able to completely block the actions of ADPβS, suggesting the involvement of another P2Y receptor which is thought to be the P2Y₁₁ receptor (Abbracchio et al., 2006). In addition, the P2Y₁ and P2Y₁₁ receptors are thought to play a role in the marked proliferation of mesangial cells in renal diseases but again a cross-talk was not confirmed (Vonend et al., 2003).

1.3.3 Physiological roles of the P2Y₁₁ receptor

The P2Y₁₁ receptor is known to couple to two different G proteins (G_s and G_q), which allows for induction of intracellular calcium rise as well as stimulation of cAMP production after receptor activation. Moreover, the P2Y₁₁ receptor can also induce the production of the signaling molecule cyclic adenosine diphosphate ribose (cADPR) via PKA and subsequent ADP-ribosylcyclase (ADPRC) activation leading to a sustained Ca²⁺ increase (Moreschi et al., 2006).

A major role of the P2Y₁₁ receptor in physiology is thought to be a control of the cellular immune system. Above all, its presence in several different dendritic cell (DC) types implies a function of the receptor in shaping an immune response. Activation of the P2Y₁₁ receptor in monocyte- and dermal-derived dendritic cells inhibits their migration. As the receptor is stimulated only at rather high ATP concentrations, the DCs are trapped at the epicenter of inflammation where due to the accumulation of ATP its concentration reaches high values. Here, DCs can internalize antigens and are exposed to maturation-inducing factors for prolonged time periods (Schnurr et al., 2003). Moreover, exposure of monocyte-derived DCs to ATP γ S and ADP β S inhibits the release of major monocyte-recruiting chemokines. At the site of inflammation, released nucleotides might regulate the activation of monocytes as well as the arrival of other immature DCs (Horckmans et al., 2006).

Langerhans cells, which are immature DCs of the skin, show an enhanced ability to present antigen upon treatment with ATP γ S, which is one of the most potent agonists at the P2Y₁₁ receptor (Table 2). These immunostimulatory properties of ATP derivatives could be used for an adjuvant activity to enhance the efficacy of vaccines (Granstein et al., 2005). Furthermore, agonists of the P2Y₁₁ receptor also influence the maturation state of monocyte derived DCs. The ATP-induced maturation of DCs represents an alternative state that rather leads to reduced inflammation and control of the immune response. Therefore, the P2Y₁₁ receptor is a preferential target to pharmacologically manipulate the immune tolerance at the DC level (Marteau et al., 2005). Additionally, in lymphocytes the P2Y₁₁ receptor is also known to influence maturation by elevating cAMP levels, thereby controlling the immune response at the level of lymphocyte proliferation or apoptosis (Conigrave et al., 2001). In contrast, in human granulocytes the P2Y₁₁ receptor was found to be involved in pro-inflammatory processes. The discovery of β -NAD⁺ being an agonist at the P2Y₁₁ receptor revealed the participation of the receptor in the cADPR/Ca²⁺ signaling system, which is causally related to enhanced chemotaxis of granulocytes at sites of inflammation (Moreschi et al., 2006).

The P2Y₁₁ receptor also seems to be involved in mast cell physiology. Known agonists of the P2Y₁₁ receptor increase cAMP levels in human mast cells, thereby initiating cAMP-dependent inhibitory signaling pathways. In the past, the function of mast cells has been understood only partially. Mast cells were thought to play a role in allergic inflammatory diseases only, but emerging evidence supports an additional role in myocardial ischemia. After cardiovascular events the plasma levels of tryptase and histamine are elevated, which are released by activated mast cells (Feng et al., 2004).

Selective P2Y₁₁ receptor agonists could be used to interfere with the activation of mast cells in cardiovascular diseases. Moreover, such agonists could also be useful in the treatment of heart failure. Mouse cardiomyocytes were found to show a significant inotropic response to ATP and derivatives via P2Y₁₁-like receptors. Unfortunately, the involvement of the P2Y₁₁ receptor could not be directly confirmed as the gene has not yet been cloned in mouse or rat (Balogh et al., 2005). However, a common dimorphism in the human gene of the receptor (Ala-87-Thr) has been associated with acute myocardial infarction probably by stimulating inflammation, underlining the role of the P2Y₁₁ receptor as a promising drug target in the prevention of cardiovascular disease (Amisten et al., 2007).

In fat tissue the function of a P2Y₁₁-like receptor was found especially in white adipocytes of the rat. Here, stimulation of the receptor increases lipolysis and decreases leptin production via protein kinase A signaling pathways. This suggests selective P2Y₁₁ receptor agonists for a new antiobesity strategy (Lee et al., 2005).

1.3.4 Ligand recognition at the P2Y receptor

All class A GPCRs for small molecule agonists are activated by binding of the agonist to a binding pocket located deep inside the upper part of the 7TM domain of the receptor molecule (Kristiansen, 2004). The actual knowledge about ligand recognition at P2Y receptors suggests that the key structure responsible for binding and activation of the receptors is the phosphate moiety of the nucleotides. The negatively charged phosphate chain is likely coordinated to basic amino acids in TM3, 6 and 7 (Jacobson et al., 2004). The first evidence supporting this suggestion was highlighted in a study focussing at the P2Y₂ receptor. Neutralization of three positively charged amino acids in TM6 and 7 (His6.52, Arg6.55, Arg7.39, highlighted in Fig. 4A) by substitution with leucine in each case caused a marked decrease in potency of ATP and UTP at the receptor (Erb et al., 1995).

Later studies focusing on the P2Y₁ receptor also showed the importance of basic residues in TM3, 6 and 7 (Arg3.29, Lys6.55, Arg7.39, highlighted in Fig. 4A+B) for receptor activity (Jiang et al., 1997; Moro et al., 1998). Moreover, docking of UDP in a molecular model of the P2Y₆ receptor revealed the binding of the phosphate moiety to the same positively charged subpocket formed by the three cationic amino acids (Fig. 4A) (Costanzi et al., 2005). Interestingly, adenosine receptors seem to lack basic residues at these positions supporting their function in binding of the phosphate chain.

Interaction of the adenine/ uracil moiety with the P2Y receptors in agonist recognition has been explored by means of molecular modelling. Hydrogen bonds between the nitrogen atoms of the base and residues in TM7 (Fig. 4A) have been predicted. For the P2Y₁ receptor Ser314 (7.43) was found to donate a hydrogen bond to the N1 position of adenine (Jiang et al., 1997). This serine residue was highly conserved among the G_q coupled P2Y receptors except for the P2Y₁₁ receptor, that displayed a proline residue at this position. The amino acid at position 7.36 is also important for the stabilization of the base. For both adenine nucleotide preferring P2Y receptors of the first subgroup (P2Y₁-R and P2Y₁₁-R) a glutamine is present at this position, which can interact with the N⁶ position of adenine by accepting a hydrogen bond. The P2Y₂, P2Y₄ and P2Y₆ receptors all display a lysine at position 7.36 that interacts with the uracil ring (Fig. 4A) (Costanzi et al., 2004). Moreover, the base moiety also seems to be coordinated by interaction with hydrophobic amino acids (Fig. 4A). In the P2Y₁ and P2Y₆ receptor the conserved phenylalanine at position 3.32 was found to be in proximity to the adenine/ uracil ring and mutation of this Phe131 in the P2Y₁ receptor caused a substantial loss in the potency of agonists (Jiang et al., 1997; Costanzi et al., 2005).

All of the aforementioned studies did not detect any specific interactions of the P2Y receptors with the ribose ring. However, structure-activity analyses of ribose-modified nucleotide derivatives revealed the importance of the 2'-OH group for the potency of nucleotides at the P2Y₂, P2Y₄ and most critically at the P2Y₆ receptor (Besada et al., 2006; Jacobson et al., 2006). Interestingly, at the P2Y₁₁ receptor, 2'-deoxy-ATP was found to be more potent than the natural agonist (Communi et al., 1999). Moreover, P2Y receptors belonging to the first subgroup except the P2Y₆ receptor have been shown to prefer nucleotides with a pseudoribose locked in a Northern (N, 2'-exo) conformation (Ravi et al., 2002). This indicates the adoption of a specific conformation of the ribose upon binding of the nucleotide to the receptor.

In contrast to the principal binding side, coordination of the ribose moiety by specific residues seems to be present in the meta-binding sites of the P2Y₁ receptor. Meta-binding sites are not involved in the activation of a receptor by the agonist, but allow the ligand to move from the extracellular space to the principal binding pocket in the TM cleft by reducing the energy barrier (Moro et al., 1999). The meta-binding sites of the P2Y₁ receptor are predominantly formed by amino acids in the extracellular loops of the receptor (Fig. 4B). Besides being part of the meta-binding sites in the P2Y₁ receptor, EL2 is also thought to build a cap over the bound ligand after its penetration into the principal binding site (Jacobson et al., 2004).

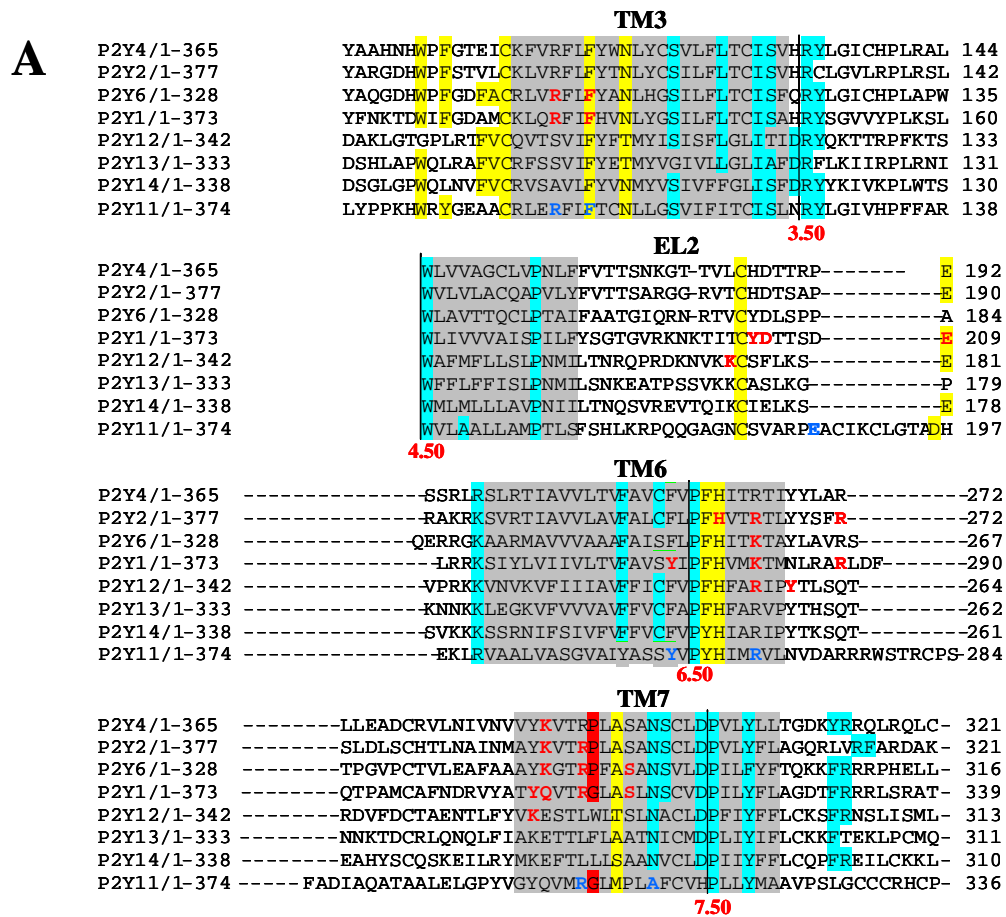
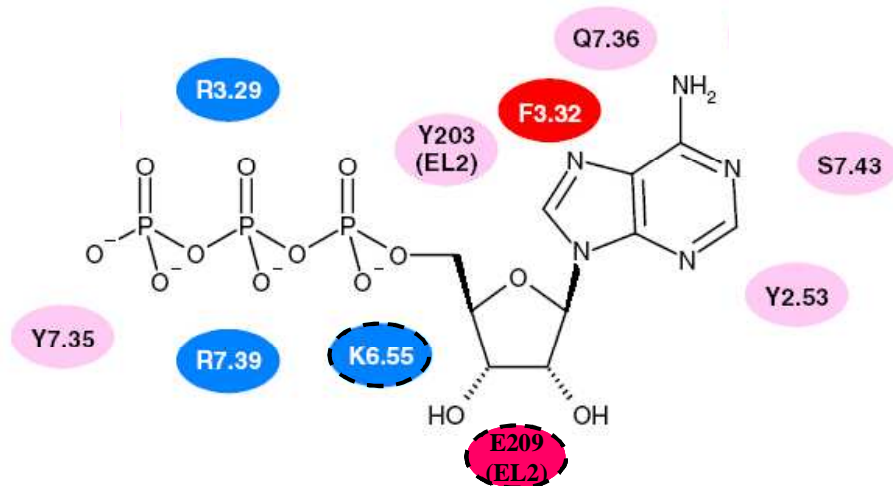
**B**

Figure 4: (A) Multiple Sequence alignment (Clustal X 1.83) and (B) key residues of the human P2Y₁ receptor involved in ligand recognition, adapted from (Ivanov et al., 2006)

(A) Alignment of the protein sequence of P2Y receptors. Grey: transmembrane domains of b-rhodopsin. Blue: conserved pattern. Yellow: similarity. Red: conserved proline/glycine residues. Red letters: residues already known to be involved in ligand recognition. Blue letters: residues included in a mutagenic analysis of the P2Y₁₁ receptor in this study. (B) Docked ATP in a molecular model of the hP2Y₁ receptor. The residues involved in ligand binding are colored as follows: pink = polar, uncharged residues (Y2.53, Y203, Y7.35, Q7.36 and S7.43); blue = positively charged residues (R3.29, K6.55, R7.39); red = non-polar residues (F3.32); magenta = negatively charged residues (E209). The black dashed ellipse surrounding two of the residues (E209, K6.55) indicates their involvement in meta-binding sites of the receptor.

Unlike the first subgroup of P2Y receptors, limited information on ligand recognition is available about the G_i coupled P2Y receptors. Molecular modelling of the P2Y₁₂ receptor revealed a similar binding mode of the ligand to that found for the members of the first subgroup. However, there was a difference in the position of the basic residues coordinating the phosphate chain. The only cationic residue in common was an arginine at position 6.55, whereas the other positively charged amino acids were located in EL2 and at position 7.35, opposed to 3.29 and 7.39 in the P2Y₁ like receptors (Fig. 4A). These three basic residues were conserved among the second P2Y receptor subgroup (Costanzi et al., 2004). The arginine in TM6 was found to be critical for normal P2Y₁₂ receptor function. A patient with a congenital bleeding disorder was found to have a point mutation in the P2Y₁₂ receptor gene that changed the Arg6.55 (Arg256) to Q, resulting in a functionally impaired receptor (Cattaneo et al., 2003).

1.4 Oligomerization of GPCRs

The currently accepted notion of GPCR organization in the plasma membrane includes the well established fact that they tend to oligomerize among each other in order to directly link distinct signalling pathways and to integrate receptor functions (Kroeger et al., 2003). Early evidence for GPCR oligomerization accumulated from ligand binding assays, where unexplained cooperativity was observed, and from SDS-PAGE analysis of GPCRs that showed multiple bands of different sizes, indicating higher-order complexes. A clear proof of GPCR oligomerization was obtained through the finding that the GABA_B receptors exist as an obligatory heterodimer (Marshall et al., 1999). Actual visualization of GPCR oligomers has been achieved by transmission electron and atomic force microscopy of native murine disc membranes from retinal rod photoreceptors, demonstrating the existence of rhodopsin (light-perceiving GPCR) dimers and higher oligomers (Fotiadis et al., 2003).

Hetero-dimerization among purinergic receptors has also been detected. The A₁ receptor was found to exert P2Y receptor like agonistic effects when co-expressed with the P2Y₁ receptor in HEK293 cells. By means of a bioluminescence resonance energy transfer (BRET) approach and co-immunoprecipitation, the two receptors were clearly shown to heterodimerize after co-expression (Yoshioka et al., 2002). Moreover, the P2Y₁ receptor could also be co-immunoprecipitated by an A₁ receptor antibody from rat brain cortical neurons, bringing evidence for a role of the hetero-dimer in vivo as well (Yoshioka et al., 2002).

Consequently, the question about GPCR oligomerization has recently changed from ‘Do GPCR oligomers really exist?’ to ‘Why do GPCRs exist as dimers?’. One hypothesis for the role of oligomerization is that two receptor molecules might be necessary to satisfy the binding requirements of a single G protein. Furthermore, oligomerization might be a common requirement for GPCRs to pass ER quality control because it can mask specific retention signals or hydrophobic patches that would otherwise retain the proteins in the ER (Terrillon and Bouvier, 2004; Bulenger et al., 2005). For example, the GABA_{B1} receptor does only reach the cell surface when co-expressed with the GABA_{B2} receptor because the ER retention signal is masked by hetero-dimerization of the receptors (Hansen and Sheikh, 2004). The same is true for the α_{1D} and α_{1B} receptors, as their hetero-dimerization is necessary for proper trafficking of the α_{1D} receptor to the plasma membrane (Bulenger et al., 2005).

In the light of drug development, a more intriguing question in receptor oligomerization is ‘what are the functional consequences?’. Hetero-oligomerization has been proposed to change the selectivity of some GPCRs towards distinct G α subunits of the G protein family. This can result in the activation of different signaling cascades following activation of the receptor hetero-dimer or monomers (Terrillon and Bouvier, 2004). Furthermore, the internalization of receptors and therewith their desensitization can be modulated by hetero-oligomerization. For example the co-expression of the β_2 receptor with either the β_1 or β_3 receptor reduces the internalization of the β_2 receptor (Prinster et al., 2005; Milligan, 2006). In contrast, the endocytosis-resistant somatostatin receptor SSTR1 could be efficiently internalized upon agonist-stimulation when co-expressed with the SSTR5 receptor (Prinster et al., 2005).

This cross-internalization phenomenon might be a very important consequence of GPCR hetero-dimerization in regulating the desensitization or resensitization of the receptor responses. In case of Parkinson’s disease the hetero-dimerization of D₂ and A_{2A} receptors seems to accelerate the developing tolerance against L-DOPA, as adenosine levels are increased in patients treated with L-DOPA, and therefore the chronic activation of both receptors leads to a greater extent of desensitization. Thus, simultaneous treatment with A_{2A} antagonists could improve the activity range in the L-DOPA therapy (Kroeger et al., 2003).

Perhaps even more interesting in relation to drug development is the observation that co-expression of two GPCRs can alter the potency of drugs in inducing a response. For the A₁-P2Y₁ receptor hetero-dimer a ligand binding assay showed that the potent P2Y₁ receptor antagonist MRS2179 (Table 2) failed to displace a bound A₁ agonist, whereas the P2Y₁ agonist ADPβS was sufficient in displacing the ligands from the A₁ binding site. Thus, providing an explanation for the theophylline-sensitive P2Y receptors observed in brain that are insensitive to known P2Y receptor antagonists (Yoshioka et al., 2001). More recently, interaction of the P2Y₂ receptor with the A₁ receptor was also shown to influence the A₁ receptor signaling. UTP was able to reduce A₁ receptor radioligand binding and attenuated A₁ receptor mediated inhibition of cAMP production (Suzuki et al., 2006). However, the regulation of A₁ receptor signaling by P2Y₁ or P2Y₂ receptor agonists is different. ADPβS seems to act like a real A₁ receptor agonist in the A₁-P2Y₁ receptor hetero-dimer, whereas UTP is not able to mediate A₁ receptor signaling but interferes with binding of specific A₁ receptor agonists in the A₁-P2Y₂ receptor hetero-dimer.

The last but not the least important question in the receptor oligomerization remaining is ‘how do GPCRs oligomerize?’. Experimental data implicate that all TMs of a receptor could be involved in oligomerization, and a conserved dimer interface may be less likely. For rhodopsin it seems to be clear that only a TM4-TM5 dimeric interaction is possible (Hansen and Sheikh, 2004). However, currently there are two theories how the TMs of rhodopsin-like GPCRs (Class A) interact to form dimers. The first is the ‘Contact dimerization (lateral packing)’ theory, which would enable the maintenance of the heptahelical bundle for each monomer, but requires additional interaction sites on the exterior of the receptor (Fig. 5a). The second theory is called ‘Domain swapping’ and would force the separation of two independent folding units, which then interact via the sites used in forming the monomers for dimerization (Fig. 5b) There is indication that different receptors are likely to utilize different oligomerization mechanisms because unique residues are involved in the formation of different dimers (Kroeger et al., 2003).

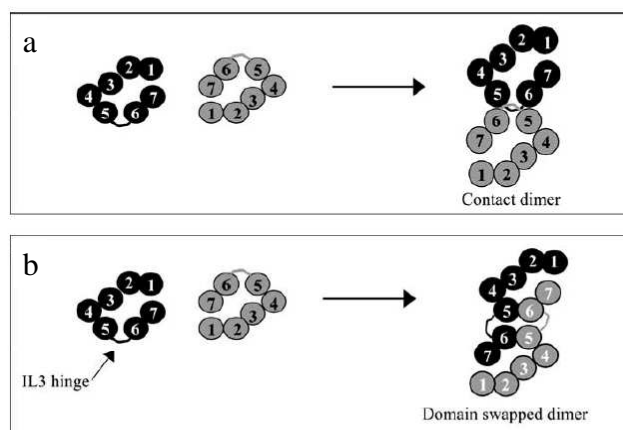


Figure 5: Schematic representation of mechanisms potentially involved in GPCR oligomer formation adapted from (Kroeger et al., 2003)

(a) In the contact dimer, GPCRs directly contact each other via exterior residues. (b) The domain swapping model requires the exchange of independently folded TM domains between monomeric units using the same interaction sites as for the formation of monomers.

1.5 Aims of the thesis project

The main focus of the thesis project was to characterize a metabotropic nucleotide receptor, namely the P2Y₁₁ receptor. We were interested in the P2Y₁₁ receptor subtype because limited work has been done on the receptor pharmacology and function despite of being a promising drug target. Therefore, we undertook the present study to characterize this little explored member of the P2Y receptor family in terms of pharmacology, ligand recognition and interaction with other P2Y receptor subtypes.

Aim 1: To study the pharmacological properties of a receptor, it is necessary that the receptor is heterologously expressed in an expression system that is devoid of endogenous nucleotide receptors to exclude contaminating signals during the pharmacological measurements. Towards this end, the 1321N1 astrocytoma cell line was selected because it does not express any P2Y receptor subtypes endogenously (Lazarowski et al., 1995). The P2Y₁₁ receptor with a C-terminal green fluorescent protein (GFP) tag was stably expressed in the 1321N1 cells and used for the pharmacological characterization.

Aim 2: Most of the agonists acting on the P2Y₁₁ receptor are also potent P2Y₁ receptor agonists, since the P2Y₁₁ receptor is most closely related to the P2Y₁ receptor (Costanzi et al., 2004). Also, earlier studies have shown that knowledge about stereoselective preferences of P2Y receptors can be of great help in establishing new lead compounds for the development of specific ligands (Kim et al., 2002; Costanzi et al., 2005). Hence, we decided to concentrate on the stereochemic differences in the ligands that are preferred by the P2Y₁₁ or the P2Y₁ receptor.

The P2Y₁ receptor was shown to prefer one chiral isomer of P_α substituted ATP derivatives (Nahum et al., 2002; Major et al., 2004). Thus, it was interesting to know whether the P2Y₁₁ receptor would show the same preference or whether the stereoselective discrimination would be different between the two receptors. The 1321N1 cells stably expressing the P2Y₁₁GFP receptor were used for testing the potency of several ATP diastereoisomers in inducing intracellular calcium rise. P_α borano (ATP- α -B) or sulfur (ATP- α -S) substituted ATP analogues were selected as chiral probes to investigate the stereoselectivity of the P2Y₁₁ receptor.

Aim 3: Furthermore, to gain insight into the structural determinants of the activity of adenine nucleotides at the receptor, mutational analysis based on a molecular model of the P2Y₁₁ receptor was initiated. Amino acid residues putatively involved in the binding of ligands at the P2Y₁₁ receptor were selectively mutated and then the activity of agonists at these receptor mutants was determined. Structural differences between the P2Y₁ and P2Y₁₁ receptors were kept in consideration while designing the mutations, since these differences will be essential for further studies focusing on the development of P2Y₁₁ receptor selective drugs. In addition, some receptor mutants were also tested for stereoselective activation by ATP- α -S diastereoisomers.

Aim 4: Moreover, the emerging fact that GPCRs can form homo- or hetero-oligomers has provided a new view on receptor organization and signaling in recent times. GPCR oligomerization was shown to have functional consequences. Among others these consequences can affect the agonist-induced internalization and ligand selectivity of GPCRs (Hansen and Sheikh, 2004). Both P2Y₁ and P2Y₁₁ receptors are co-expressed by several tissues, but it has not been studied so far whether a crosstalk or functional interaction is present between these receptors. Additionally, there are indications that such an interaction might exist, because the pharmacology of the endogenously expressed receptors not always resembles the profile found at the heterologously expressed receptors. Thereby, we were interested to know if the P2Y₁ and P2Y₁₁ receptors interact to form a hetero-oligomer. Moreover, with our experimental approach we wanted to test the hypothesis that the discrepancy between the behavior of endogenous and heterologously expressed receptors is due to the formation of this hetero-oligomer. Specifically, we focused on the physical association of the receptors in cells and the functional outcome of this interaction.

The experiments of the project were carried out in the following order:

1. Functional expression of the P2Y₁₁ receptor in 1321N1 cells as a GFP fusion protein.
2. Investigation of the stereoselective preference of agonists at the P2Y₁₁ receptor by measuring intracellular calcium concentration using fura-2 in stably transfected 1321N1 cells. ATP- α -B and ATP- α -S derivatives were used as chiral probes.
3. Mutational analysis of amino acid residues putatively involved in ligand recognition at the P2Y₁₁ receptor. Receptor mutants were tested for loss or gain of function using intracellular calcium measurements.
4. To study the probable organization of the P2Y₁ and P2Y₁₁ receptor in hetero-oligomers by biochemical means and investigate functional consequences of the interaction in inducing receptor endocytosis and in alteration of ligand selectivities.

2 MATERIALS AND METHODS

2.1 Materials

2.1.1 Cell lines

Human Embryonic Kidney cells (HEK293, epithelial), Human astrocytoma cells (1321N1, glioma)

2.1.2 Bacterial strains

	Strain	Genotype	Reference
Bacteria: <i>E coli</i>	XL1-Blue	<i>supE44, hsdR17, recA1, endA1, gyrA46, thi, relA1, lac, [F' proAB, lacI^q, ZΔM15, Tn10(ter^f)]</i>	Sambrook et al., 1989
	DH5αF'	<i>F'endA1, hsdR17 (r_k⁻m_k⁺), glnV44, thi-1, recA1, gyrA (Nal^r), relA1, Δ(lacIZYA-argF)U169, deoR, (φ80dlacΔ(lacZ)M15)</i>	Woodcock et.al., 1989

2.1.3 Plasmid vectors

Name	Size(Kb)	Antibiotic resistance	Manufacturer
pcDNA3.1 (+)	5.5	ampicillin/ neomycin	Invitrogen, Karlsruhe, Germany
pcDNA3.1/Myc-His (A)	5.5	ampicillin/ neomycin	Invitrogen, Karlsruhe, Germany
pCMV-HA	3.8	ampicillin	Clontech, Heidelberg, Germany
pEGFP-N1	4.7	kanamycin/ neomycin	"
pEYFP-N1	4.7	kanamycin/ neomycin	"
pGEX	4.9	ampicillin	GEHealthcare, München, Germany
pmCerulean-C1	4.7	kanamycin/ neomycin	David W. Piston, VUMC, Nashville, USA
pVL1392	9.6	ampicillin	BD Biosciences, Heidelberg, Germany

2.1.4 Enzymes

Enzymes and buffer	Manufacturer
Shrimp Alkaline Phosphatase	Boehringer, Mannheim, Germany
T4 DNA Ligase	Invitrogen
T4 DNA Polymerase	“
BamHI	MBI Fermentas, St. Leon-Roth, Germany
BglII	“
EcoRI	“
EcoRV	“
HindIII	“
NotI	“
SmaI	“
XhoI	“
O ⁺ buffer	“
Y/Tango ⁺ (10X) buffer	“
dNTP mix	“
Apal	New England Biolabs, Beverly, MA, USA
BlpI	“
BspEI	“
NEBuffer 1-4	“

2.1.5 Kits

Type of kit	Usage	Manufacturer
cAMP EIA kit	determination of cellular cAMP content	assay designs, Ann Arbor, Michigan, USA
BigDye Terminator Cycle Sequencing Ready Reaction kit	DNA sequencing	Applied Biosystems, Warrington, UK
iScript cDNA synthesis kit	Making of cDNA for Real-Time PCR	BioRAD, München, Germany
iQ SYBr Green supermix	Real-Time PCR	“
AccuPrime	PCR (proof reading polymerase)	Invitrogen, Karlsruhe, Germany
HiSpeed Plasmid Midi kit	Plasmid isolation	Qiagen, Hilden, Germany
MinElute Gel extraction kit	Purification of DNA from Agarose-Gel	“
QIAquick PCR purification kit	Purification of PCR products	“
Taq Master Mix kit	PCR with Taq DNA polymerase	“
Omniscript Reverse Transcription kit	Making of cDNA	“
RNase-Free DNase Set	Removal of genomic DNA during RNA isolation	“
RNeasy Mini kit	Isolation of RNA	“
Supersignal West Pico kit	Detection of western blot	Pierce, Rockford, IL, USA
QuikChange Site-directed Mutagenesis kit	Generation of point-mutations in plasmid vectors	Stratagene, LaJolla, CA, USA

2.1.6 Laboratory instruments

Instrument	Manufacturer
ABI PRISM™ 310 Genetic Analyzer	Applied Biosystems Division, Foster City, CA, USA
Mighty Small II (for western blotting electrophoresis)	Amersham Pharmacia Biotech Buckinghamshire, UK
Sonoplus sonicator	Bandelin electronic, Berlin, Germany
Avanti 30 centrifuge	Beckman Coulter, Krefeld, Germany
T3 Thermocycler	Biometra, Göttingen, Germany
Electrophoresis power supply	Bio-Rad Laboratories, München, Germany
Gel electrophoresis system	“
Semi-dry Transfer Cell	“
GS-800 Calibrated Densitometer	“
iCycler (Real-Time PCR)	“
LSM510 laser scanning confocal microscope Axiovert 135 fluorescence microscope	Carl Zeiss, Jena, Germany
Axiovert 135 fluorescence microscope (calcium imaging)	“
CTI Controller 3700 digital (CO ₂ controller confocal microscope)	“
temp control-37-2 digital (temperature controller confocal microscope)	“
Sorvall RC-5B Refrigerated Superspeed Centrifuge	Dupont Instruments, Hamburg, Germany
Thermomixer comfort	Eppendorf, Wesseling-Berzdorf, Germany
Biofuge A, 13 R, 3.2 RS (centrifuge)	Heraeus, Hamburg, Germany
HB2448 LaminAir (clean bench)	“
Function line incubator (5% CO ₂)	“
Rotina 35 R centrifuge	Hettich Zentrifugen, Leipzig, Germany
Magnet plate	IBA, Göttingen, Germany
Discovery 90 Ultracentrifuge	Kendro, Langenselbold, Germany
pH Meter (pH763)	Knick, Berlin, Germany
Vacuum oven	Memmert, Schwabach, Germany
Microplate reader	Molecular Devices
Innova 4230 Refrigerated incubator shaker	New Brunswick Scientific, Nürtingen, Germany
UV/visible Spectrophotometer	Pharmacia Biotech
Gel-blotting-papers	Schleicher & Schuell, Dassel, Germany
Protran BA83 Cellulosenitrat (E) (0.2 µm)	“
Liquid blocker, Super Pap pen	Sigma, Deisenhofen, Germany
Eagle Eye Still video system	Stratagene, Heidelberg, Germany
Polychrom II monochromator	TILL Photonics, Gräfelfing, Germany
CCD camera IMAGO type VGA	“
TILLvision version 4.0	“
Nuaire CO ₂ -Water-Jacketed Incubator (10% CO ₂)	Zapf Instruments, Sarstedt, Germany
Ismatec Reglo pump	Windaus Labortechnik, Magdeburg, Germany

2.1.7 Chemicals and reagents

Chemicals	Manufacturer
2-MeS-ATP- α -S	Bilha Fischer, Bar-Ilan University, Ramat-Gan, Israel
2-neopentenyl-thio-ATP	Bilha Fischer, Bar-Ilan University, Ramat-Gan, Israel
Ampicillin	Biochrom, Berlin, Germany
ATP- α -B, 2-Cl-ATP- α -B, 2-MeS-ATP- α -B	Bilha Fischer, Bar-Ilan University, Ramat-Gan, Israel
Bacto Agar	BD Bioscience (Clontech), Heidelberg, Germany
Bacto Tryptone	BD Bioscience (Clontech), Heidelberg, Germany
Bacto Yeast extract	BD Bioscience (Clontech), Heidelberg, Germany
Bio-Rad protein assay dye reagent concentrate	Bio-Rad Laboratories, München, Germany
CaCl ₂ + EDTA	Roth, Karlsruhe, Germany
Complete Protease Inhibitor Cocktail	Roche Diagnostic, Mannheim, Germany
Deoxycholic acid	SERVA, Heidelberg, Germany
Dimethyl sulfoxide (DMSO)	SIGMA, Deisenhofen, Germany
DMEM + HAM'S F12 (1:1)	Biochrom, Berlin, Germany
DOTAP transfection reagent	Roche Diagnostic, Mannheim, Germany
Dulbecco's Modified Eagle's Medium (DMEM)	Biochrom, Berlin, Germany
Fetal calf serum (FCS)	Biochrom, Berlin, Germany
FuGENE TM 6 transfection reagent	Roche Diagnostic, Mannheim, Germany
Fura-2AM	Molecular Probes Invitrogen, Karlsruhe, Germany
G418 Sulphate	Calbiochem, La Jolla, CA, USA
Glücksklee, non-fat dry milk	Nestle, Germany
Glucose*H ₂ O + Glycine + Glycerol	Roth, Karlsruhe, Germany
Glutathione Sepharose 4 Fast Flow	GE Healthcare, München, Germany
HBSS (w/o Ca ²⁺ and Mg ²⁺)	Biochrom, Berlin, Germany
HEPES	Roth, Karlsruhe, Germany
Igepal CA630	SIGMA, Deisenhofen, Germany
Immersol TM 518N (Immersion oil for microscopy)	Carl Zeiss, Oberkochen, Germany
Kanamycin sulphate	Biochrom, Berlin, Germany
KCl	Roth, Karlsruhe, Germany
KH ₂ PO ₄	Merck, Darmstadt, Germany
MATra solution	IBA, Göttingen, Germany
MgCl ₂	Roth, Karlsruhe, Germany
MgSO ₄	Roth, Karlsruhe, Germany
MRS2179	SIGMA, Deisenhofen, Germany
Na ₂ HPO ₄ *2H ₂ O	Roth, Karlsruhe, Germany
NaCl	Roth, Karlsruhe, Germany
NaHCO ₃	Roth, Karlsruhe, Germany
NF157	M.U. Kassack, Universität Bonn, Germany
Penicillin and Streptomycin	Biochrom, Berlin, Germany
PFA	Fluka Chemika, Sigma, Germany
Pluronic acid	Molecular Probes Invitrogen, Karlsruhe, Germany
Poly-L-Lysine	SIGMA, Deisenhofen, Germany
Ponceau S solution (0.2% in acetic acid)	Boehringer, Mannheim, Germany
Protein A/G Plus Agarose	Santa Cruz, Heidelberg, Germany
Purine-/ pyrimidine nucleotides and derivatives	SIGMA, Deisenhofen, Germany
Rp/Sp-ATP- α -S	Biolog, Bremen, Germany
Saccharose + SDS	Roth, Karlsruhe, Germany
TEMED	SIGMA, Deisenhofen, Germany
Template Suppression Reagent (TSR)	Applied Biosystems Division, Foster City, CA, USA
Triton-X-100	SERVA, Heidelberg, Germany
Trypanblue	Biochrom, Berlin, Germany
Trypsin/EDTA	Biochrom, Berlin, Germany
Tween 20	SIGMA, Deisenhofen, Germany
β -mercaptoethanol	SIGMA, Deisenhofen, Germany
RNase	Roth, Karlsruhe, Germany

2.1.8 Antibodies

Antibody	Manufacturer
rabbit polyclonal anti-hP2Y ₁	Alomone labs, Jerusalem, Israel
rabbit polyclonal anti-hP2Y ₁₁	“
mouse monoclonal IgG against HA-tag	Cell Signalling, Danvers, MA, USA
peroxidase-conjugated anti-mouse and anti-rabbit IgG	Dianova, Hamburg, Germany
mouse monoclonal antibody anti-Myc	Invitrogen, Karlsruhe, Germany
rabbit polyclonal anti-GFP	“
Alexa ₅₅₅ anti-mouse IgG and Alexa ₄₈₈ anti-rabbit IgG	Molecular Probes, Invitrogen, Karlsruhe, Germany
rabbit polyclonal anti-GST	Santa Cruz, Heidelberg, Germany
rabbit polyclonal anti-myc	Sigma, Deisenhofen, Germany

2.1.9 Molecular mass markers

2.1.9.1 Nucleic acid standard marker

GeneRuler 100bp DNA Ladder (1 kb)	MBI Fermentas, St. Leon-Rot, Germany
GeneRuler DNA Ladder Mix (10 kb)	“ - “

2.1.9.2 Protein standard marker

Precision Plus (All Blue) (250-10 kDa)	Bio-Rad, München, Germany
--	---------------------------

2.1.10 Buffers and solvents

2.1.10.1 Cell culture media and solutions

- **HEK-293 cells** - DMEM/HAM'S F12 (1:1) with 2 mM Glutamine, 10% FCS, 100 U/ml Penicillin, 100 µg/ml Streptomycin
- **1321N1 cells** – DMEM with 2 mM Glutamine, 5% FCS, 100 U/ml Penicillin, 100 µg/ml Streptomycin
- HBSS (Hanks' balanced salt solution) without Ca²⁺ and Mg²⁺
- PBS
- Trypsin/EDTA
- G418 Sulphate- stock solution: 500 mg/ml, working concentration: 500 µg/ml
- Poly-L-Lysine: 0.1 mg/ml H₂O

2.1.10.2 Microbial Media and solutions

- Luria bertini (LB)- 1 lt

Bacto-tryptone	10 g
Bacto yeast extract	5 g
NaCl	10 g
pH 7.0	
bacto agar (for plates)	15 g
Ampicillin	100 µg/ml (final conc.)
Kanamycin	50 µg/ml (final conc.)

- SOC – 250 ml

Bacto tryptone	5 g
Yeast extract	1.25 g
NaCl	0.15 g
KCl	0.125 g
1M Glucose	5 ml (final 20 mM)
1M MgCl ₂	2.5 ml (final 10 mM)
1M MgSO ₄	2.5 ml (final 10 mM)

- TSB buffer-150 ml

2x LB-media	75 ml	1x LB (final conc.)
DMSO	7.5 ml	5% (final conc.)
1 M MgCl ₂	1.5 ml	10 mM (final conc.)
1 M MgSO ₄	1.5 ml	10 mM (final conc.)
PEG 4000	15 g	10% (final conc.)
Sterile filtered with 0.2 µm Filter		

- 2x LB-100 ml

bacto tryptone	2 g
Yeast extract	1 g
NaCl	2 g
pH	7.0-7.4

- Mini-Prep Solutions

Solution I	50 mM Glucose
	25 mM Tris/HCl (pH 8.0)
	10 mM EDTA (pH 8.0)
	100 µg/ml RNase
Solution II	0,2 N NaOH
	1% SDS
Solution III	3 M Potassiumacetat
	11,5 % Acetic acid
TER	10 mM Tris/HCL (pH 8.0)
	1 mM EDTA
	200 µg/ml RNase

- 5xKCM buffer: 0.5 M KCl
0.15 M CaCl₂
0.25 M MgCl₂

2.1.10.3 Molecular Biology: buffers and solutions

<u>1x PBS:</u>	137 mM NaCl, 2.6 mM KCl, 8.1 mM Na ₂ HPO ₄ , 1.4 mM KH ₂ PO ₄ , pH 7.4
<u>1x NaHBS:</u>	145 mM NaCl, 5,4 mM KCl, 1mM MgCl ₂ , 1.8 mM CaCl ₂ 25 mM Glucose, 20 mM HEPES, pH 7.4
<u>1x TAE:</u>	40 mM Tris, 5 mM NaOAc, 1 mM EDTA, pH 7.4
<u>1x TE:</u>	10 mM Tris/HCl, pH 7.4, 1 mM EDTA, pH 8.0
<u>Ethidium bromide solution:</u>	10 mg/ml
<u>4% PFA solution:</u>	4% PFA (Paraformaldehyde), 120 mM sodium phosphate, pH 7.4, 4% Saccharose
<u>FSBB:</u>	Blocking and Wash buffer (immunostaining)-12 ml FCS 2 ml 10% Triton-X100 0.365 ml 240 mM Na ₃ PO ₄ 1 ml 4 M NaCl 1.35 ml H ₂ O ad 12 ml
<u>High Salt buffer:</u>	500 mM NaCl, 20 mM Na ₂ HPO ₄
<u>Low Salt buffer:</u>	150 mM NaCl, 10 mM Na ₂ HPO ₄
<u>RIPA-buffer:</u>	50 mM Tris (pH 7.4), 1% Igepal CA630, 0.25% Na-deoxycholate, 150 mM NaCl, 1 mM EDTA, 1 mM NaF, one tablet Complete Protease Inhibitor Cocktail per 50 ml
<u>Hypotonic buffer pH 8.1:</u>	5 mM Tris/HCl (pH 8.1), 50 μM CaCl ₂ , 3 mM MgCl ₂ , 0.1% Igepal CA630, 2 mM DTT, one tablet Complete Protease Inhibitor Cocktail per 50ml
<u>60% Acrylamid/Bis:</u>	Acrylamid 58.4 g/100ml N,N'-Methylen-bisacrylamid 1.6 g/100ml
<u>Resolving buffer:</u>	750 mM Tris/HCl, pH 8.8 (SDS-PAGE-Laemmli)
<u>Stacking buffer:</u>	250 mM Tris/HCl, pH 6.8 (SDS-PAGE-Laemmli)
<u>SDS solution:</u>	10% (w/v) SDS in H ₂ O

- PER solution: 10% (w/v) Ammoniumperoxodisulfat in H₂O
- 4x Laemmli Sample buffer: 500 mM Tris/HCl, pH 6.8, 8% SDS, 40% Glycerol, 0.005% Bromophenolblue
- 1x Running buffer: 25 mM Tris, 192 mM Glycin, 0.1% SDS, pH 8.5 (SDS-PAGE-Laemmli)
- 1x Transfer buffer: 25 mM Tris, 192 mM Glycine, 20% (v/v) Methanol (for Laemmli gels with NC membrane)

Membrane Stripping buffer: 62.5 mM Tris, pH 6.8, 100 mM β -Mercaptoethanol, 2% SDS

2.1.11 Oligonucleotides

All oligonucleotides were from Operon/ Qiagen, except the RT-PCR and sequencing primers (MWG), DECERFRETRV (Invitrogen) and GST cloning primers (MWG).

2.1.11.1 RT-PCR primer

Primer	Accession-Nr.	Sequence	Tm (°C)	PCR product
hGAPDH5	NM_002046	5'-TCC AAA ATC AAG TGG GGC GAT GCT-3'	60	600 bp
hGAPGH3		5'-ACC ACC TGG TGC TCA GTG TAG CCC-3'		
hsP2X4Fw	NM_002560	5'-GCC TTC CTG TTC GAG TAC GAC-3'	55	420 bp
hsP2X4Rev		5'-CGC ACC TGC CTG TTG AGA CTC-3'		
hsP2X7Fw	NM_002562	5'-GTC ACT CGG ATC CAG AGC ATG-3'	55	532 bp
hsP2X7Rev		5'-TTG TTC TTG ATG AGC ACA GTG-3'		
hsP2Y1Fn	NM_002563	5'-TCT TCC ACA TGA AGC CC-3'	55	531 bp
hsP2Y1Rn		5'-AGA GGA GAG TTG TCC AGA-3'		
hsP2Y2Fn	NM_002564	5'-CTT CAA CGA GGA CTT CAA GT-3'	55	579 bp
hsP2Y2Rn		5'-CAC GTA ACA GAC AAG GAT GA-3'		
hsP2Y6Fn	NM_176797	5'-CGC TGA ACA TCT GTG TCA TT-3'	55	409 bp
hsP2Y6Rn		5'-ATA GCA GAC AGT GCG GTT AC-3'		
NHSP2Y11Fw	NM_002566	5'-CGA GGT GCC AAG TCC TGC CCT-3'	60	809 bp
NHSP2Y11Rv		5'-CGC CGA GCA TCC ACG TTG AGC-3'		
hsPAR2-sense	U61373	5'-GCCATCCTGCTAGCAGCCTCTC-3'	60	341 bp
hsPAR2-antisense		5'-GATGACAGAGAGGAGGTCAGCC-3'		

2.1.11.2 Cloning primers

Primer	Accession-Nr.	Sequence	Tm (°C)	Usage
DECERATGFW	-	5'-TC CCG CTG GAT CCA CCG GTC GCC ACC ATG GTG-3'	58	Subcloning of Cerulean from pmCer-C1 in pP2Y ₁ N1
DECERATGRV		5'-CTT GAG CGC GGC CGC TGA GTC CTT ACT TGT AC-3'		
DECERFRETRV		5'-ACC GTC GAC TGC AGG ATC CGA AGC TTG AGC-3'		
THGSTFW	-	5'-GAT CTG ATA TCA TGT CCC CTA TAC TAG-3'	60	Cloning of GST from pGEX vector
THGSTRV		5'-GAA GAT CTT CAA TCC GAT TTT GGA GGA TGG TCG CC-3'		
DEHSP2Y1ATGFW	NM_002563	5'-GATC GAA TTC ATG ACC GAG GTG CTG TGG CCG-3'	58	Cloning of the hP2Y ₁ receptor
DEHSP2Y1SMAIRV		5'-CAG AAT GGA GAT ACA AGC CTG GGC CCG GGG TGA C-3'		

2.1.11.3 Mutagenesis primer

Primer	Sequence	Usage
DEP2Y1K280A-Fw	5'-CCT TTC CAT GTG ATG GCC ACG ATG AAC TTG AGG-3'	Mutagenesis-PCR: P2Y ₁ -R K280A mutant
DEP2Y1K280A-Rv	5'-CCT CAA GTT CAT CGT GGC CAT CAC ATG GAA AGG-3'	
DEP2Y11F109IUP	5'-CTG GAG CGC TTC CTC ATC ACC TGC AAC CTG CTG-3'	Mutagenesis-PCR: P2Y ₁₁ -R F109I mutant
DEP2Y11F109ILOW	5'-CAG CAG GTT GCA GGT GAT GAG GAA GCG CTC CAG-3'	
DEP2Y11E186AUP	5'-AGC GTG GCC AGG CCC GCG GCC TGC ATC AAG TGT-3'	Mutagenesis-PCR: P2Y ₁₁ -R E186A mutant
DEP2Y11E186ALOW	5'-ACA CTT GAT GCA GGC CGC GGG CCT GGC CAC GCT-3'	
DEP2Y11R106AUP	5'-GCG TGC CGC CTG GAG GCC TTC CTC TTC ACC TGC-3'	Mutagenesis-PCR: P2Y ₁₁ -R R106A mutant
DEP2Y11R106ALOW	5'-GCA GGT GAA GAG GAA GGC CTC CAG GCG GCA CGC-3'	
DEP2Y11Y261AUP	5'-CTC TAC GCC AGC TCC GCG GTG CCC TAC CAC ATC-3'	Mutagenesis-PCR: P2Y ₁₁ -R Y261A mutant
DEP2Y11Y261ALOW	5'-GAT GTG GTA GGG CAC CGC GGA GCT GGC GTA GAG-3'	
DEP2Y11R268AUP	5'-CCC TAC CAC ATC ATG GCG GTG CTC AAC GTG GAT-3'	Mutagenesis-PCR: P2Y ₁₁ -R R268A mutant
DEP2Y11R268ALOW	5'-ATC CAC GTT GAG CAC CGC CAT GAT GTG GTA GGG-3'	
DEP2Y11R268QUP	5'-CCC TAC CAC ATC ATG CAG GTG CTC AAC GTG GAT-3'	Mutagenesis-PCR: P2Y ₁₁ -R R268Q mutant
DEP2Y11R268QLOW	5'-ATC CAC GTT GAG CAC CTG CAT GAT GTG GTA GGG-3'	
DEP2Y11R307AUP	5'-GGC TAC CAG GTG ATG GCG GGC CTC ATG CCC CTG-3'	Mutagenesis-PCR: P2Y ₁₁ -R R307A mutant
DEP2Y11R307ALOW	5'-CAG GGG CAT GAG GCC CGC CAT CAC CTG GTA GCC-3'	
DEP2Y11A313NUP	5'-GGC CTC ATG CCC CTG AAC TTC TGT GTC CAC CCT-3'	Mutagenesis-PCR: P2Y ₁₁ -R A313N mutant
DEP2Y11A313NLOW	5'-AGG GTG GAC ACA GAA GTT CAG GGG CAT GAG GCC-3'	
DECitrinemutaFW	5'-TTC GGC TAC GGC CTG ATG TGC TTC GCC CGC TAC-3'	Mutagenesis-PCR: mutate YFP to Citrine (YFP-Q69M mutant)
DECitrinemutaRV	5'-GTA GCG GGC GAA GCA CAT CAG GCC GTA GCC GAA-3'	

2.1.11.4 Sequencing primers

Primer	Sequence	Usage
DEpeGFPN1-fw	5'-GAT CCA CCG GTC GCC ACC ATG G-3'	Sequencing of fluorescent tags in N1 Clontech vectors
DEpeGFPN1-rv	5'-CCT CTA CAA ATG TGG TAT GGC-3'	
T7 fw	5'-TAA TAC GAC TCA CTA TAG GGA-3'	sequencing of vectors with T7 promotor
BGH rv	5'-TAG AAG GCA CAG TCG AGG-3'	sequencing of vectors with BGH polyadenylation site
THHSP2Y1FW1	5'-AGG TTC ATC TTT CAT GTG AAC-3'	Sequencing of the hP2Y ₁ receptor
THHSP2Y1FW3	5'-TAC CTG GTA ATC ATT GTA CTG-3'	
THHSP2Y1RV2	5'-CAG TTT ACA CAT GGC ATC CCC-3'	
THHSP2Y1RV4	5'-CCT CAG AGG AGA GTT GTC CAG-3'	
THP2Y11FW1	5'-ACC TGC ATC AGC CTC AAC CGC-3'	Sequencing of the hP2Y ₁₁ receptor
THP2Y11FW2	5'-TGG CCC TCT ACG CCA GCT CCT A-3'	
THP2Y11FW3	5'-TGT GTC CAC CCT CTA CTC TAC A-3'	
THP2Y11RV1	5'-AGC GGT TGA GGC TGA TGC AGG T-3'	
THP2Y11RV2	5'-TAG GAG CTG GCG TAG AGG GCC A-3'	
THP2Y11RV3	5'-TGT AGA GTA GAG GGT GGA CAC A-3'	

2.1.11.5 siRNA

DEP2RY1_1 siRNA sense r(CUC UCC UCU GAG GAG AAA A)dTdT
control (non-silencing) siRNA sense r(UUC UCC GAA CGU GUC ACG U)dTdT

2.2 Methods

2.2.1 Methods in molecular biology

2.2.1.1 Isolation of nucleic acids

2.2.1.1.1 RNA isolation from animal cells

Total RNA was isolated from cultured cells (wild type and transfected) using the RNeasy Mini kit (Qiagen, Hilden). The medium was aspirated from the culture dish (5 cm) and cells were lysed with 350 μ l Buffer RLT. Cells were homogenized completely by pipetting with 1 ml tip, and to this homogenized suspension 700 μ l of 70% ethanol was added and mixed well by pipetting. The sample (700 μ l) was applied to a RNeasy mini spin column sitting in a 2-ml collection tube, and centrifuged for 1 min at 10,000 rpm. For washing, 350 μ l Buffer RW1 was pipetted onto the RNeasy column, and centrifuged for 1 min at 10,000 rpm to wash the silica-gel-membrane. Now on-column DNase digestion was performed to remove genomic DNA using the RNase-Free DNase kit (Qiagen, Hilden). Therefore, 10 μ l of DNase I stock solution (2.73 Kunitz units/ μ l) mixed in 70 μ l Buffer RDD (DNase I incubation mix) was added directly onto the spin-column membrane and incubated at room temperature for 15 min. For a second washing step 350 μ l Buffer RW1 was pipetted into the spin column and centrifuged for 1 min at 10,000 rpm. The RNeasy column was transferred into a new 2-ml collection tube. Buffer RPE (500 μ l) was pipetted onto the RNeasy column, and centrifuged for 1 min at 10,000 rpm. This step was repeated but this time the column was centrifuged for 2 min at maximum speed to dry the RNeasy membrane. The RNeasy column was transferred into a new 1.5-ml collection tube, and 30 μ l RNase-free water was pipetted onto the RNeasy membrane. Incubated at room temperature for 10 min and then centrifuged for 2 min at 12,000 rpm to elute. Stored at -80°C .

2.2.1.1.2 Plasmid DNA isolation from bacteria (Mini-Preparation, Mini-Prep)

Single colonies were picked from agar plates and grown overnight in 5 ml of selective LB medium (LB-Medium with 100 µg ampicillin or 50 ng kanamycin/ ml). About one third of the bacteria culture (1.5 ml) was transferred into a suitable reaction tube and centrifuged for 30 s at maximum speed. The supernatant was discarded and the pellet was resuspended in 100 µl of solution I. Solution II (200 µl) was added to the bacteria suspension and mixed carefully by inverting the tube 5-6 times. After 5 min incubation at room temperature, 150 µl of Solution III was added and again mixed carefully. The tubes were placed on ice for 15 min to allow quantitative precipitation of bacterial proteins. The precipitate was removed by centrifugation for 15 min at maximum speed and the supernatant was transferred to a new reaction tube without taking along any precipitate. Then 300 µl of isopropanol was added and the mixture incubated for 5 min at room temperature to precipitate plasmid DNA. After centrifugation for 10 min at maximum speed the supernatant was discarded and the pellet washed with 250 µl of 70% Ethanol. The tubes were again centrifuged at maximum speed for 10 min, the ethanol containing supernatant discarded and the pellets dried at 37°C for 30 min. After all remaining ethanol had evaporated, the pellets were dissolved in 50 µl TER buffer and the DNA-solution incubated at 37°C for 1 h to destroy contaminating RNA. At this step the mini-preps were analyzed with the appropriate restriction enzymes to check for successful plasmid isolation and positive clones after cloning. For this, 2-5 µl of the DNA-solution was analyzed in a single or double digestion (section 2.2.1.2.2).

Positive clones were once more precipitated with 50 µl 4M NH₄OAc, plus 300 µl absolute ethanol. The mixture was centrifuged for 10 min at maximum speed and the supernatant discarded. The pellet was washed with 70% Ethanol and again centrifuged. After the pellet was fully dried it was resuspended in 30 µl H₂O or 10 mM Tris/HCl (pH 8.0) depending on the further usage (H₂O: Sequencing with ABI PRISMTM 310 Genetic Analyzer; Tris/HCl: Sequencing at Seqlab GmbH, Göttingen, Germany).

2.2.1.1.3 Plasmid DNA isolation from bacteria (Midi-preparation)

Plasmid DNA from transformed bacteria was harvested using the HiSpeed Plasmid Midi Kit (Qiagen, Hilden). 50 ml of overnight grown transformed bacteria culture was centrifuged for 15 min at 5000 rpm to recover cell pellet. Bacterial pellet was resuspended in 6 ml of Buffer P1 containing RNase A. Buffer P2 (6 ml) was added, mixed gently, and incubated at room temperature for 5 min.

Then 4 ml of chilled Buffer P3 was added, mixed immediately but gently and the lysate was poured into the barrel of the QIAfilter Midi Cartridge. Incubated at room temperature for 10 min to allow precipitation of protein and genomic DNA at the top of the solution. In the mean time Buffer QBT (4 ml) was applied to equilibrate a Qiagen-tip 500 and the column was allowed to empty by gravity flow. Then the cap from the QIAfilter outlet nozzle was removed and the plunger gently inserted into the cartridge. The cell lysate was filtered into an already equilibrated Qiagen-tip. The cleared lysate was allowed to enter the resin by gravity flow. The Qiagen-tip was washed with 2 x 10 ml Buffer QC. After washing the cartridge was placed in a fresh falcon tube and plasmid DNA was eluted with 5 ml of Buffer QF. DNA was precipitated with 3.5 ml of isopropanol (room temperature) and transferred onto a QIAprecipitator. The filter was washed with 2 ml 70% Ethanol and dried by pressing air through it using a 20 ml syringe. The DNA was eluted with 500 μ l - 1 ml of Buffer TE. Stored at -20°C.

2.2.1.1.4 Isolation of DNA fragments from agarose gel

To isolate DNA fragments (PCR or cDNA-insert in plasmid) from agarose gel, the MinElute Gel Extraction kit (Qiagen) was used. The area containing the DNA fragment was cut from the gel. Care was taken to minimize the surrounding agarose excised with the fragment. For 1% agarose gel maximum 400 mg of gel slices was used per 1.5 ml tube. The gel slice was weighed and 3 volumes of Buffer QG to 1 volume of gel (100 mg ~ 100 μ l) was added. The gel slices were incubated in buffer at 50°C for minimum 10 min at 500 rpm (Eppendorf Thermomixer). The tubes were additionally mixed every 3 min. After the gel slice appeared to be dissolved 1 volume of isopropanol was added and mixed carefully.

To bind DNA the sample was applied to a QIAquick column and centrifuged for 1 min at 13,000 rpm. The flow-through was discarded and 500 μ l of Solubilization buffer (QG) was added to the cartridge and centrifuged again. Discarded the flow-through. Wash buffer PE (750 μ l) was added (containing ethanol) to the cartridge and incubated for 5 min at room temperature. Then centrifuged for 1 min at 13,000 rpm. Discarded the flow-through. Centrifuged again to remove residual wash buffer. The cartridge was placed into a fresh 1.5 ml recovery tube and 15 μ l of Buffer EB was added directly to the center of the silica-gel-membrane. After an incubation of 10 min at room temperature the cartridge was centrifuged for 1 min at 13,000 rpm. Discarded the cartridge and stored the DNA at -20°C.

2.2.1.1.5 Cleaning of DNA fragment

DNA fragments after PCR amplification and restriction digestion were cleaned using the QIAquick PCR purification kit (Qiagen). Five volumes of buffer PB (Binding Solution) was added to 1 volume of amplification reaction. The sample mix was applied to the cartridge placed in a 2.0 ml wash tube and centrifuged for 1 min at 13,000 rpm. Discarded the flow-through. Wash Buffer PE (700 μ l, containing ethanol) was added to the cartridge and centrifuged for 1 min at 13,000 rpm. Discarded the flow-through and centrifuged again to remove the residual wash buffer. The cartridge was placed into a new 1.5 ml receiver tube and 30 μ l of Buffer EB was added directly onto the center of the cartridge. After incubation for 10 min at room temperature the cartridge was centrifuged for 1 min at 13,000 rpm. Discarded the cartridge and stored the cleaned DNA at -20°C.

2.2.1.1.6 Precipitation of Sequencing PCR DNA

Sequencing PCR product was precipitated with sodium acetate and 100% ethanol. Briefly, to 80 μ l H₂O added 10 μ l of 3 M sodium acetate. To this 20 μ l of sequencing PCR reaction mixture was added and mixed thoroughly. Then added 250 μ l of chilled 100% ethanol and incubated on ice for 5 min. Centrifuged for 15 min at 14,000 rpm. Supernatant discarded and pellet resuspended in 300 μ l of 70% ethanol. Centrifuged again for 15 min at 14,000 rpm. Discarded the supernatant carefully and allowed the pellet to air-dry or at 37°C. DNA sample prepared for Sequencer (ABI PRISM™ 310 Genetic Analyzer). DNA pellet was then resuspended in 25 μ l of Template Suppression Reagent (TSR) buffer (ABI PRISM, Applied Biosystems Division, Foster City, CA, USA). Vortexed and centrifuged briefly. Sample denatured for 2 min at 95°C and then kept on ice for 2 min. Reaction mixture then transferred to the small 0.5 ml sequencing tube (without lid) and capped with rubber stopper suitable for the capillary in the sequencing machine.

2.2.1.1.7 Quantification of Nucleic acids

Quantity of Isolated DNA and RNA was measured by the UV absorption ratio 260 nm /280 nm using an Ultrospec 2000 UV/visible spectrophotometer (Pharmacia Biotech, Freiburg, Germany). A 1:10 dilution of sample was prepared and measured in a quartz cuvette (5.00 mm thickness). Measurement at 260 nm gave the absorption of nucleic acid, at 280 nm the protein absorption and 320 nm gave the salt present in the sample. The sample concentration was obtained in μ g/ ml. A factor of 2 was used to calculate the actual concentration of the nucleic acid present in sample in μ g/ ml. Absorption ratio of 260 nm/ 280 nm gave the quality of the nucleic acid (ratio > 1.7 considered okay). Quality of the nucleic acid was checked on a 1% agarose/TAE gel pre-stained with ethidium bromide (10 mg/ml).

2.2.1.2 Molecular cloning techniques

2.2.1.2.1 Generation of DNA insert by PCR

To clone a particular DNA fragment into plasmid vector for generating a recombinant plasmid, PCR was done to amplify the full coding sequence interest from the gene. Cloning primers were designed from the sequences available in the Genbank. 30-33 bp long primers were designed flanking the 5' and 3' region of interest. Care was taken to have similar annealing temperature for the primer pair. Suitable restriction enzyme sites were included in the primer based on the multiple cloning site (MCS) of the plasmid vector into which the fragment was to be cloned. DNA fragment to be cloned was checked for the presence of sequence matching the restriction site. Primers were designed in a way to ensure that the right amino acid codon frame remained intact in the recombinant plasmid. For cloning the full cDNA, stop codon was mutated in the 3' primer when cloned into a vector with a 3' detection tag.

The cloning PCR was done using the AccuPrime kit (Invitrogen). The following reaction setup was used:

cDNA or recombinant plasmid	1-2 μ l (~ 200 ng)
10 x AccuPrime reaction mix	1 x
sense primer	20 pmol
antisense primer	20 pmol
Pfx DNA Polymerase	1 μ l
H ₂ O	<u>variable</u>
	50 μ l

The PCR reaction was done using the following programme (for Pfx DNA polymerase):

Lid temperature:	110°C		
Preheating:	On		
Initial denaturation	95°C	2 min	
Denaturation	94°C	30 sec	35 cycles from this step
Annealing	variable	30 sec	
Extension	68°C	1 min per kb	
Final extension	68°C	10 min	
pause	4°C		

The total amount of PCR product was loaded on an agarose gel and the fragment with the correct size was cut from the gel and purified using the MinElute Gel extraction kit (Qiagen, chapter 2.2.1.1.4). Then the cleaned fragment was digested with the appropriate restriction enzymes, again purified (QIAquick PCR purification, Qiagen) to remove the digestion buffer and finally quantified to calculate the volume needed to set the ligation reaction.

2.2.1.2.2 Hydrolysis of DNA with restriction endonucleases

Restriction digestion of DNA was done with restriction enzyme and its appropriate 10x reaction buffer. Recombinant plasmids were cut either with one or two enzymes simultaneously. In general, for single digestion appropriate reaction buffer (10x) was used at a final concentration of 1x, while for double digestion Y⁺/Tango buffer (10x) used at a final concentration of 2x (see scheme below).

	Single digestion	Double digestion
DNA	1-2 µg	2-3 µg
Enzyme 1 (10 u/µl)	2 µl	2 µl
Enzyme 2 (10 u/µl)	-	2 µl
Buffer (10x)	1x	2x
H ₂ O	<u>variable</u>	<u>variable</u>
	20 µl	30 µl
Incubation time	1-2 h at 37°C	

For double digestion with SmaI, samples were first digested with smaI at 30°C. After heat inactivation of the enzyme the second restriction endonuclease was added plus additional 10x buffer and samples were incubated at 37°C. Double digestion with ApaI and BspEI was done in separation due to incompatibility of 10x buffers and incubation temperature. Samples were first treated with ApaI in NEBuffer 4 plus 1% BSA at 25°C. Then the enzyme was heat inactivated and the linearized DNA precipitated with 3 M NaOAc, plus absolute ethanol. The pelleted DNA was then resuspended in H₂O and digested with BspEI in NEBuffer 3 at 37°C. Single digestion with BamHI was always done in 2x Y⁺/Tango buffer.

2.2.1.2.3 Formation of blunt ends by fill-in of 5' overhang

For subcloning of DNA fragments from one plasmid vector into another, it was sometimes necessary to fill-in 5' overhangs after digestion with a sticky end producing restriction enzyme, when the target vector had only a suitable blunt end restriction site. After digestion and heat inactivation of the restriction enzyme (sticky ends) 1 µl of each, dNTP mix and T4 DNA Polymerase were directly added to the digestion mixture and incubated for 20 min at 25°C. Then the polymerase was heat inactivated and the DNA digested with a second enzyme or purified by agarose gel extraction.

2.2.1.2.4 Dephosphorylation of digested plasmid

The restriction enzyme treated plasmid was dephosphorylated with Shrimp Alkaline Phosphatase (Boehringer) to remove the phosphate groups from the linear plasmid and avoid self-ligation during the ligation process.

Restriction digested DNA	1-2 µg
Shrimp Alkaline Phosphatase (1 U/µl)	2 µl
Dephosphorylation buffer (10x)	3x
H ₂ O	<u>variable</u>
	30 µl

Incubated for 1 h at 37°C followed by 10 min at 65°C for denaturing the enzyme. After phosphatase reaction, plasmid vector was purified again to remove the dephosphorylation reaction buffer.

2.2.1.2.5 Ligation of plasmid and DNA insert

To generate recombinant plasmid, restriction digested plasmid (dephosphorylated, when 5' and 3' end were similarly cut) was ligated with the DNA insert having the appropriate restriction sites at their 5' and 3' end using the T4 DNA Ligase (Invitrogen).

Plasmid vector	15 fmol
DNA insert	45 fmol
T4 DNA Ligase (1 u/µl)	2 µl
5x Ligase buffer	4 µl (1x)
H ₂ O	<u>variable</u>
	20 µl

Ligation was done in T3 Thermocycler (Biometra) at 16°C for 18 h. The ligation mixture was then used to transform bacteria to generate recombinant plasmid.

2.2.1.3 Gel electrophoresis

2.2.1.3.1 Agarose gel electrophoresis of DNA

To check the quality of DNA (PCR product, recombinant plasmid DNA, restriction analysis) a 1.5% agarose (SIGMA) gel in 1x TAE buffer was made. The gel was pre-stained with ethidium bromide (10 mg/ml). DNA samples were prepared in 6x loading buffer (containing bromophenol blue dye, MBI Fermentas). Gel was run in 1x TAE for around 30 min at 80 V. Depending on the fragment size either GeneRuler 100bp DNA Ladder (1 kb) or GeneRuler DNA Ladder Mix (10 kb) was used as standard marker. DNA bands were visualized under UV-Transilluminator in an Eagle Eye II video system (Stratagene, Heidelberg, Germany).

2.2.1.4 Polymerase Chain Reaction (PCR)

To check for the expression of genes of interest on RNA level in cell lines used in this study, PCR was applied. For non-quantitative analysis of RNA-expression in cells, isolated RNA was reverse transcribed using the Omniscript kit and PCR was performed with the Taq Master Mix kit (Qiagen). In case of quantitative analysis of RNA-expression in relation to a reference gene, Real-time PCR was carried out. Here, cDNA was generated using the iScript kit and the Sybr Green kit used to perform PCR (Bio-Rad).

2.2.1.4.1 Non-quantitative RT-PCR

To reverse transcribe (RT) the isolated total RNA from cells, 1 µg of total RNA was used to make cDNA in a 0.5 µl tube with Omniscript Reverse Transcription kit. RT reaction was set as follows:

RNA	1 µg
RT Buffer (10x)	2 µl
dNTP mix (5 mM each)	2 µl
Oligo-dT primer (0.5 µg/µl)	2 µl
Omniscript Reverse Transcriptase (4 U/µl)	1 µl
H ₂ O	<u>variable</u>
	20 µl

RT was done in T3 Thermocycler (Biometra). The reaction was incubated for 1 h at 37°C, followed by 5 min at 95°C and then rapidly cooled to 4°C. cDNA was stored at -20°C.

PCR was done with the cDNA generated from the RT step using the Taq Master Mix kit.

The reaction mixture was pipetted as follows:

cDNA	1 µl
Taq Master Mix	25 µl
5' primer (10 pmol/µl)	2 µl
3' primer (10 pmol/µl)	2 µl
H ₂ O	<u>variable</u>
	50 µl

The following programme was applied to do the PCR reaction (for Taq polymerase):

Lid temperature:	110°C	
Preheating:	On	
Initial denaturation:	98°C	2 min
Denaturation	94°C	1 min (35 cycles from here)
Annealing	variable	90 sec
Extension	72°C	2 min
Final extension	72°C	10 min
pause	4°C	

8 µl of the amplification was used for agarose gel electrophoresis to check for the presence of the desired gene product.

2.2.1.4.2 *Real-time PCR*

For analysis of the relative expression of genes of interest in various cell lines (wild type or transfected) the Real-time PCR approach was chosen. Total isolated RNA (1 µg) from cells was reverse transcribed using the iScript kit. The reaction setup is shown below:

RNA	1 µg
iScript mix (5x)	1x
Reverse Transcriptase	1 µl
RNase free H ₂ O	<u>variable</u>
	20 µl

The reaction mix was put in the T3 Thermocycler and kept for 5 min at 25°C, then heated to 42°C for 30 min, followed by a 5 min incubation at 85°C and finally cooled to 4°C. Generated cDNA was stored at -20°C.

PCR was done in 25 µl reaction volume with the generated cDNA (described above) applying the following reaction setup:

SYBR Green supermix	12.5 µl
primer mix	2 µl
cDNA	1 µl
H ₂ O	9.5 µl

Samples were put in the iCycler (Bio-Rad) and a gradient programme was run:

40 cycles	}	Initial denaturation:	95°C	4 min 30 sec
		Denaturation	94°C	30 sec
		Annealing	Gradient	90 sec
		Extension	72°C	1 min
			95°C	1 min
			56°C	1 min

The specificity of amplification was proved by melting curve analysis and agarose gel electrophoresis. Relative expression was calculated, using the number of cycles, determined from a preset threshold value, referred to the GAPDH cycles.

2.2.1.4.3 *Mutagenesis-PCR*

For site-directed mutagenesis the QuikChange kit (Stratagene) was used to make point mutations. Plasmid DNA (100 ng) was used as template. Primer containing the mutated codon were designed so that 15 bp were flanking the codon both up- and downstream and the primer pairs being complementary to opposite strands of the vector. After annealing of the mutagenesis oligonucleotides to the template they were extended by Pfu Turbo DNA Polymerase (high fidelity) to generate a mutated plasmid containing staggered nicks. After digestion of the parental plasmid DNA by DpnI restriction endonuclease, half of the reaction setup was transformed into bacteria. Isolated plasmid DNA (Mini-Prep) was then checked for incorporation of the mutation by sequencing.

The reaction setup was done following the scheme below:

10x Reaction buffer	1x
Plasmid DNA	100 ng
primer Fw	12.5 pmol
primer Rv	12.5 pmol
dNTP mix	1 μ l
H ₂ O	<u>variable</u>
	50 μ l

+ 1 μ l PfU Turbo DNA Polymerase

Samples were put in the T3 Thermocycler (Biometra) and a specific programme applied:

15 cycles	}	Initial denaturation:	98°C	30 sec
		Denaturation	95°C	30 sec
		Annealing	55°C	1 min
		Extension	68°C	12 min
		pause	4°C	

Directly after programme was finished, 1 μ l of DpnI was added and samples incubated at 37°C for 1 h. Transformation of the products was done using the KCM method.

2.2.1.4.4 Sequencing-PCR

For sequencing reaction, 150-300 ng of recombinant plasmid DNA was used with 2 μ l primer (10 pmol/ μ l) and 4 μ l Big dye reagent (contained DNA polymerase, fluorescent dye-labeled dNTPs, buffer) (Applied Biosystems), diluted with H₂O to a final volume of 20 μ l. The PCR conditions were:

25 cycles	}	Initial Denaturation	98°C	2 min
		Denaturation	96°C	30 sec
		Annealing	55°C	30 sec
		Extension	60°C	4 min
				+ 25 sec increment/cycle
		pause	4°C	

After PCR, DNA was precipitated and prepared for capillary electrophoresis and analysis in the ABI PRISM™ 310 Genetic Analyzer (Applied Biosystems).

2.2.1.5 Transformation of bacteria

2.2.1.5.1 Making of competent cells

A single colony of XL1-Blue or DH5 α F E.coli strain was allowed to grow overnight in 5 ml LB media (without antibiotic) at 37°C, shaking at 250 rpm. Then 1 ml of overnight bacterial culture was transferred to 150 ml of fresh LB media and allowed to grow till an OD₆₀₀ of 0.6. The cell suspension was then centrifuged for 10 min at 5000 rpm at room temperature. The supernatant was discarded and the pellet resuspended in 15 ml (1/10 volume) of TSB buffer. After a 10 min incubation of the suspension on ice it was aliquoted to 500 μ l each in Eppendorf safelock tubes. Tubes were frozen in liquid nitrogen and stored at -80°C.

2.2.1.5.2 KCM Transformation method

To transform KCM competent cells using plasmid DNA, 20 μ l of KCM buffer was added to either 20 μ l of ligation mix or 10-20 ng of super-coiled plasmid DNA and diluted with H₂O to 100 μ l. Mixed nicely and left on ice. In the mean time the KCM competent cells were put on ice for thawing. The transformation reaction was mixed properly with 100 μ l of competent cells and incubated on ice for 10 min (re-trafo) or 50 min (ligation). Afterwards the mix was incubated for 10 min at room temperature (very important). Then 1 ml of SOC media was added and incubated for 1 h at 37°C with shaking at 300 rpm. Thereafter, the complete transformation mixture was pelleted for transformation of ligation reaction and plated on LB-agar containing suitable antibiotic. The plates were incubated up-side down at 37°C overnight to allow for growth of transformants. For retrafo and subsequent plasmid Midi preparation, 50 ml of LB media + antibiotic was inoculated with the transformation mixture.

2.2.2 Methods in Cell Biology

2.2.2.1 Cell culture

The medium used for culturing of cells was sterile and ready-to-use (Biochrom). Thawing of cells (HEK293, 1321N1): frozen cells were rapidly thawed in 37°C water bath and the cryo-preserved cell suspension + 9 ml of complete cell culture medium were centrifuged at 200 g for 3 min at room temperature. The cell pellet was resuspended in complete medium and seeded on a tissue culture dish (10 cm) (Nunc, Denmark). HEK293 (Human embryonic kidney, epithelial) cells were cultured in DMEM (Dulbecco minimum essential medium) / HAM'S F12 (1:1) with 2 mM Glutamine, 10% FCS (fetal calf serum), 100 U/ml Penicillin and 100 μ g/ml Streptomycin (Biochrom) in a Function line incubator (Heraeus) with humidified atmosphere of 95% air, 5% CO₂ at 37°C.

1321N1 astrocytoma cells were cultured in DMEM containing 3.7 g/L NaHCO₃, 4.5 g/L D-glucose, 1.028 g/L N-Acetyl L-alanyl-L-glutamine and 5% FCS, 100 U/ml Penicillin, 100 µg/ml Streptomycin in a Nuair incubator (Zapf Instruments) with humidified atmosphere of 90% air, 10% CO₂ at 37°C. Culture medium was changed every 2-3 days.

For cell passage, HEK293 cells were detached from the culture dish with Trypsin/EDTA (Biochrom) for 5 min at room temperature after aspirating the medium. For 1321N1 cells, the cells were first washed twice with HBSS or PBS and then incubated in the cell incubator with Trypsin/EDTA 1 ml per 10 cm dish for 1 min at 37°C. Cells were centrifuged at 200 g for 3 min, resuspended in medium and seeded 1:20 in fresh complete medium.

2.2.2.2 Freezing of cells

Cells were frozen in DMSO for long storage. Briefly, cells grown in 10 cm culture dish were frozen in 3 cryo tubes (Nunc). To each cryo tube 100 µl DMSO (sterile) was added. Already detached, centrifuged and resuspended cells (900 µl) were added and fastly mixed with DMSO in the cryo tube and immediately stored at -20°C for 24 h. Then shifted to -80°C and soon after to liquid nitrogen for long storage.

2.2.2.3 Transfection of cells

2.2.2.3.1 DOTAP Lipofection

HEK293 cells were stably transfected with the P2Y₁GFPN1 or P2Y₁₁GFPN1 constructs using the Liposomal transfection reagent DOTAP (Roche Diagnostic). Plasmid DNA was isolated using the HiSpeed Midi kit (Qiagen) to obtain DNA of best quality. Cells were grown 50-70% confluent for 2-3 days. The transfection mix was prepared using 5 µg of plasmid DNA made to 50 µl with 20 mM HEPES in a siliconized reaction tube. In another tube, 30 µl DOTAP was mixed with 70 µl of 20 mM HEPES. After a 5 min incubation both solutions were mixed nicely and incubated for 30 min at room temperature. Meanwhile, the medium of the cells was aspirated and replaced by serum- and antibiotic-free medium. After 30 min, the transfection mixture was given drop wise onto the cells. Cells were incubated in the transfection media for 8 h and then replaced by full medium containing serum (FCS) and antibiotics. 24-48 h after transfection cells were visualized under the fluorescent microscope to check for expression of fusion protein containing the GFP tag (green fluorescent protein). For stable transfection G418 Sulphate antibiotic (kanamycin and neomycin derivative) was added after 48 h at a rate of 500 µg/ml (stock: 500 mg/ml).

2.2.2.3.2 *Fugene 6 Lipofection*

1321N1 astrocytoma cells were transfected with various plasmids using the Fugene 6 transfection reagent. This is a multi-component lipid-based reagent that complexes with DNA and enables high transfection efficiency. Cells were seeded at a density of 100,000 cells/ 35 mm² a day prior to transfection. Before preparation of the transfection mix, the normal growth medium of the cells was replaced by serum- and antibiotic free medium. The Fugene 6 reagent (3µl) was added to serum-free medium to make a volume of 100 µl in a siliconized reaction tube. To this mixture 2 µg of plasmid DNA was added (Fugene 6 : DNA ratio = 3:2), mixed properly and incubated for 30 min at room temperature. The complex mixture was then added drop wise to the cells and they were incubated for 8 h in the transfection medium. Then transfected cells were changed to normal growth medium. After 24-48 h cells were checked for positive transfection or further used for experiments. For stable transfection G418 Sulphate antibiotic (kanamycin and neomycin derivative) was added after 24-48 h at a rate of 500 µg/ml (stock: 500 mg/ml).

2.2.2.3.3 *Magnet assisted transfection*

For transient expression of proteins in HEK293 cells and siRNA transfection for gene silencing the Magnet assisted transfection (MATra) method was applied. Cells were prepared as described above (2.2.2.3.1). 5 µg of plasmid DNA (for double transfection: 2.5 µg of each plasmid) or 20µl of a 100 µM siRNA stock solution was diluted with 400 µl of serum-free medium. Then 6.6 µl of magneto beads suspension (MATra A solution) was added and mixed carefully by pipetting and gently tapping the siliconized reaction tube. The mixture was incubated for 20 min at room temperature and then applied to the cell culture dish. Culture dishes were put on a magnet plate (placed in the incubator) and incubated for 15 min at 37°C. Then transfection medium was replaced by full growth medium and cells put back in the incubator. Experiments were done 48 h post-transfection.

2.2.2.3.4 *Selection of stably transfected cell clones*

Stably transfected cell clones were separated from non-transfected, G418 resistant cell clones by flow cytometry. Cells transfected with fusion proteins containing a GFP tag were sorted with a FACS diva cells sorter (Becton Dickinson, equipped with a 488 nm laser) 3-4 days post-transfection. Positive clones were collected and depending on the number of cells seeded in an appropriate dish. Quality of the clones was checked with a fluorescent microscope and after two passages, part of the cells were frozen for long-time storage in liquid nitrogen.

2.2.3 Methods in Protein chemistry

2.2.3.1 Whole Cell lysate

To make whole cell lysate, 80% confluent cells (6 cm dish) were washed 2x with ice-cold PBS and lysed in 0.5 ml of RIPA buffer during a 10 min incubation on ice. Cell debris was collected in 1.5 ml tubes using a cell scraper. The cell lysate was gently mixed on a rotator for 15 min at 4°C. The lysate was then sonicated on ice in an Ultrasonicator for 3 x 10 sec (40% power). Afterwards centrifuged at 14,000 x g for 15 min at 4°C. The supernatant was transferred into a fresh tube and pellet discarded. Protein concentration was determined by Bradford method using 1% bovine serum albumin as standard. Lysate stored at -20°C.

2.2.3.2 Subfractionation of cells (cell membrane preparation)

Confluent cells (10 cm dish) were washed twice with 3 ml ice-cold PBS and incubated in 1 ml of hypotonic buffer pH 8.1 for 10 min on ice. Then cells were scraped from the dish and the lysate sonicated for 5 x 1 sec (40% power). Thereafter, the lysate was centrifuged at 1000 x g for 5 min in a 4°C cold centrifuge. Supernatant was saved and the pellet, containing nuclei and mitochondria, discarded. The collected supernatant was centrifuged again at 50,000 x g for 30 min at 4°C. The resulting supernatant contained the cytosolic fraction and the pellet plasma membrane, endoplasmic reticulum and microsomes. The cytosolic fraction was transferred to a fresh tube and the pellet resuspended in 250 µl of hypotonic buffer. Fractions were subjected to protein estimation and stored at -20°C.

2.2.3.3 Co-Pulldown

Lysates (containing GST fusion proteins) were diluted with RIPA-buffer to a final protein concentration of 500 µg/ml in a predefined end volume (500-800 µl). Then 20 µl of a pre-equilibrated GSH-bead suspension (50%) (Glutathion Sepharose) was added and incubated overnight on a rocker (15 rpm) at 4°C. Next day, the beads were washed 2x with RIPA-buffer after centrifugation for 5 min at 500 rpm in a pre-cooled centrifuge. After a further washing step beads were centrifuged at 13.000 rpm for 5 min to destroy bead structure and allow for total removal of the supernatant. Then 15 µl of 2x Laemmli sample buffer was added to denature adherent proteins and prepare for loading on a SDS-PAGE.

2.2.3.4 Co-Immunoprecipitation

Lysates (containing myc fusion proteins) were diluted with RIPA-buffer to a final protein concentration of 250 µg/ml in a predefined end volume (500-800 µl). Then 1.5 µg of anti-myc antibody (mouse monoclonal, Invitrogen) was added and incubated with the lysate overnight on a rocker (15 rpm) at 4°C. Next morning, 20µl of Protein A/G Plus Agarose suspension was added and lysates were again incubated for at least 2 hours at 4°C. Thereafter, the beads were washed 2x with RIPA-buffer after centrifugation for 5 min at 2000 rpm in a pre-cooled centrifuge. After a further washing step beads were centrifuged at 13.000 rpm for 5 min to destroy bead structure and allow for total removal of the supernatant. Then 15 µl of 2x Laemmli sample buffer was added to denature adherent proteins and prepare for loading on a SDS-PAGE

2.2.3.5 SDS PAGE (Laemmli) Gel preparation

(for 2 gels with 1 mm thickness and 8 cm width)

Components	10% Resolving gel (ml)	4% Stacking gel (ml)
60% acrylamide/Bis	2.0	0.335
Resolving gel buffer	6.0	-
Stacking gel buffer	-	2.5
H ₂ O	3.8	2.065
10% SDS solution	0.12	0.05
1x PER solution	0.06	0.04
TEMED	0.024	0.01
Bromophenol blue	-	0.002

2.2.3.6 SDS-PAGE and immunoblotting

Defined amounts of cell lysates were precipitated (directly loaded on the gel, if protein concentration sufficient) using Methanol/Aceton 1:1 in 4-fold excess and then denatured in 1x Laemmli sample buffer. For immunoprecipitation or co-pulldown, beads were washed and denatured in 2x sample buffer. Protein samples were denatured without boiling but incubation at 4°C overnight or 15 min at room temperature in sample buffer. The gel-electrophoretic resolution of the proteins was done in a Vertical-Minigel apparatus (Bio-Rad) using 10% SDS-PAGE. Proteins were transferred to nitrocellulose membrane (Protran BA79, 0.2 µm) using a semi-dry transfer system (Bio-Rad) at constant voltage (10 V) and 200 mA current for 60 min. Successful transfer was checked, visualizing the protein bands on the membrane by 0.2% Ponceau S staining.

The membrane was blocked in 5% non-fat dry milk (made in PBS-Tween, 0.1%) overnight at 4°C. Depending on the antibody used for specific detection of protein bands, membrane was incubated at room temperature for 1 h or at 4°C overnight. Then the membrane was washed three times with PBS-Tween 0.1% and incubated with secondary antibody (peroxidase-conjugated anti-mouse IgG or anti-rabbit IgG; Dianova) for 1 h at room temperature. The membrane was again washed as described before and then incubated with ECL reagent (Supersignal West Pico kit, Pierce). Chemiluminescence signals were detected on chemiluminescence film (Hyperfilm ECL, GEHealthcare) after developing.

2.2.3.7 Stripping of membrane for reprobing

To reprobe the membrane with a second primary antibody this procedure was followed: ECL reagent was washed out by washing for around half an hour in PBS-Tween (0.1%). Then the membrane was incubated in stripping buffer for 30 min at 55°C. Afterwards, the membrane was first washed extensively in H₂O and then in PBS-Tween to remove β-mercaptoethanol. The blocking procedure was repeated and then the membrane was reprobated with another primary antibody as described above.

2.2.3.8 Immunocytochemistry

Cells (wild-type or transfected) cultured on 22 mm coverglasses or in glass bottom dishes (MatTek, Ashland MA, USA) were fixed in 4% paraformaldehyde for 20 min at room temperature, then washed and stored in 120 mM Sodiumphosphate solution. Fixed cells were blocked and permeabilised in FSBB buffer for 20 min. Then incubated in mouse monoclonal anti-myc 0.8 µg/µl (Invitrogen) overnight at 4°C. The cells were washed 3x 10 min in High salt buffer. Then secondary antibodies were applied (Alexa IgG Goat-anti-mouse A₅₅₅-1:200; Molecular Probes) for 2 h at room temperature. The washing step was repeated 1x in High salt buffer and further washing was done 1x with 120 mM Sodiumphosphate solution and 3x with 5 mM Sodiumphosphate solution. Cells were mounted in Vectashield mounting media (Axxora, Grünberg, Germany) and visualized with a LSM510 Confocal laser scanning microscope (Carl Zeiss).

2.2.3.9 cAMP-EIA

HEK293 cells stably expressing the P2Y₁₁GFP receptor were seeded in a 6-well plate at a density of 100.000 cells/ well and grown for 2 days till 80% confluency. Prior to stimulation the medium was aspirated and replaced by NaHBS buffer containing 0.5 M IBMX (isobutyl-methyl-xanthine). Cells were incubated in this buffer for 30 min at 37°C either with or without P2Y receptor antagonists. Then cells were stimulated with various agonists for 10 min. After stimulation, the buffer was aspirated and cells were lysed with 0.1 M HCL. Cells were scraped from the dish and collected in a 1.5 ml safelock reaction tube. A 100 µl aliquot was kept for later protein estimation. The rest of the tube was centrifuged at 1000 x g for 10 min and supernatant transferred into a fresh tube.

Determination of intracellular cAMP was done using the Direct cAMP EIA kit (assay designs). The appropriate amount of EIA strips coated with goat anti-rabbit IgG was placed in a suitable rack. In all wells 50 µl of neutralizing reagent was pipetted. Then 100 µl standards or samples were pipetted in the appropriate wells (for determination of nonspecific binding (NSB) and maximal binding, 100 µl of 0.1 M HCL was pipetted in the appr. wells). To that came 50 µl of alkaline phosphatase solution conjugated with cAMP as tracer plus 50 µl of a rabbit polyclonal antibody directed against cAMP (except NSB wells). After an incubation of 2 h with shaking at 500 rpm the plate was washed 3x with wash buffer. Then 200 µl of p-nitrophenyl phosphate as enzyme substrate was added and incubated in the dark for 1 h. At the end 50 µl stop solution (Na₃PO₄) was added and the optical density was read at 405 nm with correction at 595 nm. The cAMP concentration (pmol/ml) was calculated by interpolating the percentage of bound tracer for each sample on the simultaneously determined standard curve. The resulting values were normalized to the protein concentration of each sample, so that results were expressed as pmol cAMP/ mg protein. At last, results for all stimulated samples were normalized to unstimulated control, expressed as n-fold stimulation.

2.2.4 [Ca²⁺]_i measurements

The cells were plated on coverslips (diameter = 22 mm), and single cell measurement was done after 3 days, when the cells were 30-50% confluent. The changes of free intracellular Ca²⁺ concentration ([Ca²⁺]_i) were measured, as described before (Ubl *et al.*, 1998).

Briefly, cells were preincubated with 2 μ M fura-2AM at 37°C for 30 min in NaHBS (for 1321N1 cells 0.02% Pluronic acid was added for better solubility of fura-2AM) and then stimulated under continuous superfusion of pre-warmed NaHBS at 37°C with different concentrations of various agonists. Fluorescence intensity was recorded alternatively at 340 and 380 nm excitation and 520 nm emission. Changes were monitored in single cells bathed in a perfusion chamber which was placed on the microscope stage of a fluorescence imaging system from TILL Photonics with a X40/ 1.30 oil immersion objective and a flow rate of 1 ml/min (Vöhringer *et al.*, 2000).

Calcium data were analyzed with the Excel program applying basal deduction to the calcium traces and calculating the peak height (R_{\max}) for each cell. Concentration-response data obtained with average values from 40 to 70 single cells were further analyzed to derive EC_{50} values (half-maximal response) using the SigmaPlot program (Jandel). Calculation of the EC_{50} values and curve fitting was performed using the following equation with a standard slope: $y = R_{\min} + \frac{R_{\max} - R_{\min}}{1 + 10^{(\log EC_{50} - x)}}$. If the free curve fit extended beyond the experimental data the maximal response (R_{\max}) was adjusted to the experimentally obtained plateau value for the other experiments.

2.2.5 Confocal imaging

All images were taken on a Zeiss inverted LSM 510 META laser scanning confocal microscope.

2.2.5.1 Immunocytochemistry

1321N1 cells transiently co-transfected with P2Y₁₁GFP and P2Y₁mycHis and stained with anti-myc antibody and Alexa Fluor 555 IgG Goat-anti-mouse as secondary antibody were visualized using a Plan-Apochromat x63 objective. The GFP-tag was excited with a 488-nm argon/krypton laser and fluorescence detected using a 505-530 nm band pass filter. The Alexa Fluor 555 was detected using a 543-nm helium/neon laser for excitation and a 560-nm long-pass filter. Ten sections 0.5 μ m apart along the Z-axis were taken from the bottom to the top of each cell. Images were processed using the Zeiss confocal microscopy software (LSM Image examiner). Sections were projected onto XZ- and YZ-plane images using the Ortho option of the software.

2.2.5.2 Agonist-induced internalization

HEK293 cells stably expressing the P2Y₁₁GFP receptor were seeded on coverslips (30 mm diameter) precoated with 0.01% PLL and grown for 3 days till 40-50% confluency. Cells were then placed in a POC-chamber (PeCon GmbH, Erbach, Germany) and incubated on stage in a chamber of 5% CO₂ at 37°C in complete culture medium. Images were taken using a Plan-Apochromat x63 objective, a 488-nm argon/krypton laser and a 505 nm long pass filter. Thirteen to fifteen sections 1 µm apart were taken serially every ten minutes from the bottom to the top of each cell after stimulation. Cells were stimulated with various agonists and live-imaging was done for 90 minutes.

2.2.5.3 Analysis of fluorescence intensities

Fluorescence intensities of confocal images were analyzed using the Zeiss LSM 510meta software histo macro. Region of interests (ellipse 30-39 µm²) were set in the cytosol of single cells and the average fluorescence intensity in the ROI determined over time (0 min, 10 min, 30 min, 60 min). The intensity values for 10-60 min were normalized to the starting value at 0 min which was set to be 1.

2.2.6 Flow cytometry

The expression levels of wild type and mutant receptors in 1321N1 cells were analyzed by flow cytometry using a FACS LSR (BD Biosciences, Heidelberg). Cells were grown in 5 cm culture dishes (Nunc, Wiesbaden) to 80 % confluency, harvested and resuspended in culture medium. The expression levels of 10.000 cells were analyzed by determining the intensity of the GFP fluorescence per cell using the Flow Jo software.

2.2.7 Data analysis

Statistical analysis of the data was done using Graph pad prism. First data were checked for Gaussian distribution. In the case of Gaussian distributed data, further analysis was done using the one-way ANOVA test and the Tukey test as a post test. For non-Gaussian distributed data the Kruskal-Wallis test was applied using the Dunns test as a post test. Significant difference appeared at a P value < 0.05.

3 RESULTS

3.1 Diastereoselectivity of the P2Y₁₁ receptor: P_α substituted ATP analogues

3.1.1 Heterologous expression of the P2Y₁₁GFP receptor in 1321N1 cells

To express the P2Y₁₁ receptor as a GFP construct in 1321N1 astrocytoma cells, the DNA sequence of the receptor was cloned between the EcoRI and BamHI restriction sites of the eGFPN1 expression vector. The DNA of the human P2Y₁₁ receptor (GenBank™/EBI accession number AF030335) was kindly provided by Dr. Communi. The P2Y₁₁GFP receptor construct was used to transfect 1321N1 astrocytoma cells. The 1321N1 astrocytoma cell line lacks endogenously expressed P2Y receptors (Lazarowski et al., 1995; Gendron et al., 2003), which was also confirmed by us for the currently used cell batch. By RT-PCR the mRNA expression level of P2X and P2Y receptors in the cells was investigated. We detected signals for the P2Y₆, P2Y₁₁, P2X₄ and P2X₇ receptor mRNA (Fig. 6A). However, wild type cells as well as mock-transfected 1321N1 cells did not display any significant Ca²⁺ responses when challenged with 100 μM UDP or ATP. The wild type cells responded only sporadically (5 out of 53 cells) to 100 μM ADP (Fig. 6B). This confirmed the lack of functionally expressed P2 receptors in the 1321N1 cell batch used in this study.

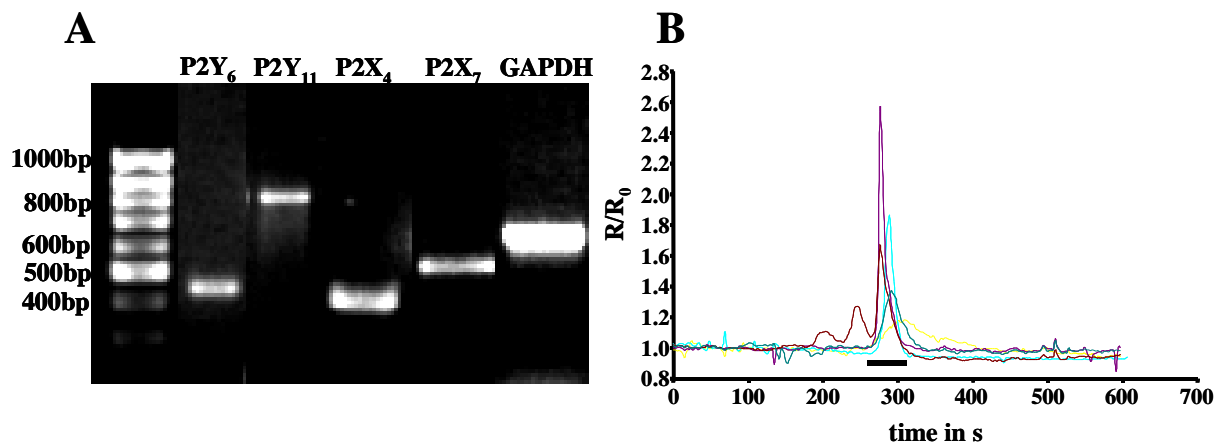


Figure 6: Non-functional expression of P2X and P2Y receptors in wild type 1321N1 cells

[A] Agarose gel resolved RT-PCR products generated from cDNA of 1321N1 wild type cells. Signals were detected for the P2Y₆ (409 bp), P2Y₁₁ (809 bp), P2X₄ (420 bp), P2X₇ (532 bp) receptors and GAPDH (600 bp). [B] Calcium traces of wild type 1321N1 cells stimulated with 100 μM ADP (black bar). Displayed are 5 out of 53 cells that significantly responded with an increase in intracellular calcium, detected with fura-2 calcium indicator.

The well characterized batch of 1321N1 cells was then transfected with the GFP-tagged human P2Y₁₁ receptor. The protein expression was verified by western blot analysis of cytosol and membrane fractions from stably transfected cells (Fig. 7). To demonstrate functional expression of the P2Y₁₁-GFP receptor in stably transfected cells, various agonists were tested for their ability to induce an intracellular [Ca²⁺]_i increase. The cells were monitored for the change in fluorescence intensity of the calcium indicator fura-2 after agonist stimulation, as described in the methods section. The obtained EC₅₀ values ± s.e.m (n = 3-4, as indicated) for ATPγS, BzATP, ATP and 2-MeS-ATP were 1.3±0.3 μM (4), 1.5±0.3 μM (3), 3.0±0.87 μM (4) and 13.8±5.58 μM (3), respectively. The order of potency was found to be ATPγS = BzATP > ATP > 2-MeS-ATP, which is similar to previously reported findings (Communi et al., 1999).

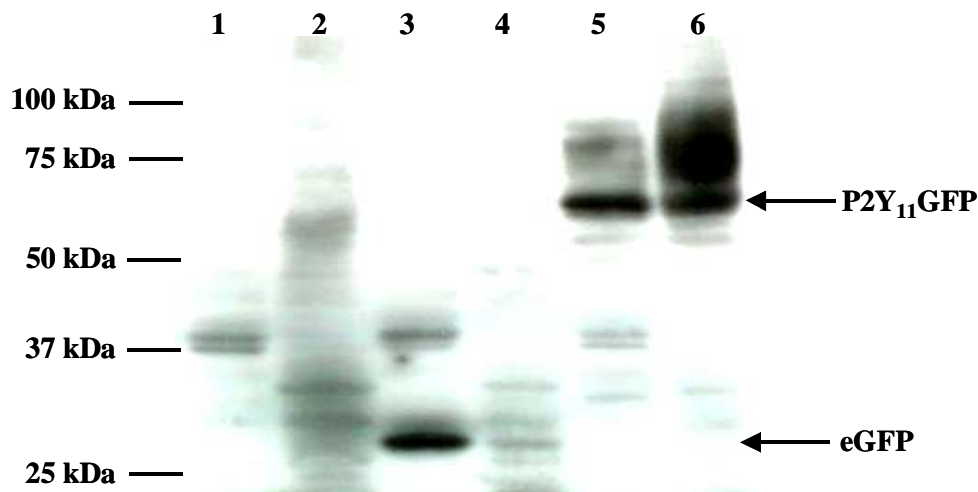


Figure 7: Western blot detection of the P2Y₁₁GFP receptor in stably transfected 1321N1 cells

Cell lysates of wild type and transfected cells were subfractionated and resolved on SDS-PAGE. After immunoblotting, protein expression was checked using an anti-GFP antibody (dilution 1:1000), as described in the methods section. The blot displays the cytosol fractions (1, 3 and 5) as well as the membrane fractions (2, 4 and 6) of differently transfected 1321N1 cells. **(1)** Cytosolic and **(2)** membrane fraction of untransfected 1321N1 cells. **(3)** Cytosolic and **(4)** membrane fraction of mock-transfected 1321N1 cells (eGFP ~27 kD). **(5)** Cytosolic and **(6)** membrane fraction of P2Y₁₁GFP (~ 69 kD) transfected 1321N1 cells.

3.1.2 Calcium measurements with pairs of different ATP diastereoisomers

3.1.2.1 Adenosine-5'-O-(α -boranotriphosphate) diastereoisomers

To characterize the diastereoselectivity of the stably expressed P2Y₁₁ receptor in 1321N1 cells, several borano-modified diastereoisomers of ATP were tested by analyzing the calcium responses (described in methods section). These ATP analogues had been chosen, as they exhibited a stereoselective activation of the P2Y₁ receptor (Nahum et al., 2002).

The diastereoisomers show substitution of one of the non-bridging oxygen atoms of P_{α} by borane. Thereby, a new chiral centre in the ATP molecule is introduced. The absolute configuration around the P_{α} was assigned to the resulting diastereoisomers, and the R_p configuration was attributed to the (A) isomers and the S_p configuration to the (B) isomers of the borano-modified analogues (Major et al., 2004).

All the different ATP- α -B diastereoisomeric pairs (ATP- α -B (A/B), 2-MeS-ATP- α -B (A/B), 2-Cl-ATP- α -B (A/B)) displayed the same stereoselective preference in activating the $P2Y_{11}$ receptor. The concentration response curves obtained for the different ATP- α -B derivatives and the parent compounds are displayed in Fig. 8, A-C. The corresponding (A) and (B) isomers of the ATP- α -B derivatives exhibited a clear difference in potency for elevation of intracellular calcium. All (B) isomers were found to be more potent than the (A) isomers, ranging from 3- to 10-fold, as seen by the EC_{50} values in Table 3 (page 56).

The (B) isomer of ATP- α -B ($EC_{50} = 340 \pm 53.0$ nM) displayed a 7-fold higher potency than ATP ($EC_{50} = 2.83 \pm 0.82$ μ M) and its corresponding (A) isomer ($EC_{50} = 2.38 \pm 0.56$ μ M) was equipotent with ATP (Fig. 8A). The tendency that the (B) isomers are preferred by the $P2Y_{11}$ receptor was the same for all the other ATP- α -B derivatives tested. The (B) isomer of 2-MeS-ATP- α -B was the most potent ligand of all compounds tested in this study with an EC_{50} value of 260 ± 33.0 nM. The corresponding (A) isomer ($EC_{50} = 1.35 \pm 0.52$ μ M) was 5-fold less potent, but displayed a much higher potency than 2-MeS-ATP ($EC_{50} = 13.8 \pm 5.58$ μ M). The difference in potency was one order of magnitude (Fig. 8B).

The 2-Cl-substitution had a negative influence on the potency of ATP- α -B at the $P2Y_{11}$ receptor. The (A) isomer of 2-Cl-ATP- α -B ($EC_{50} = 4.19 \pm 3.41$ μ M) displayed the lowest potency of all the diastereoisomers used in this study. Only the (B) isomer ($EC_{50} = 467 \pm 246$ nM) showed a potency that was comparable to that of the other α -borano (B) isomers. The parent compound 2-Cl-ATP, where the phosphate moiety was left unchanged, was too weak an agonist at the $P2Y_{11}$ receptor to determine a complete concentration response curve using single cell calcium measurements. At a concentration of 100 μ M only 60% of the maximal ATP response were obtained. Therefore, in Fig. 8C the concentration-effect curve of ATP is displayed for comparison as well as the incomplete curve for 2-Cl-ATP ($EC_{50} > 30$ μ M).

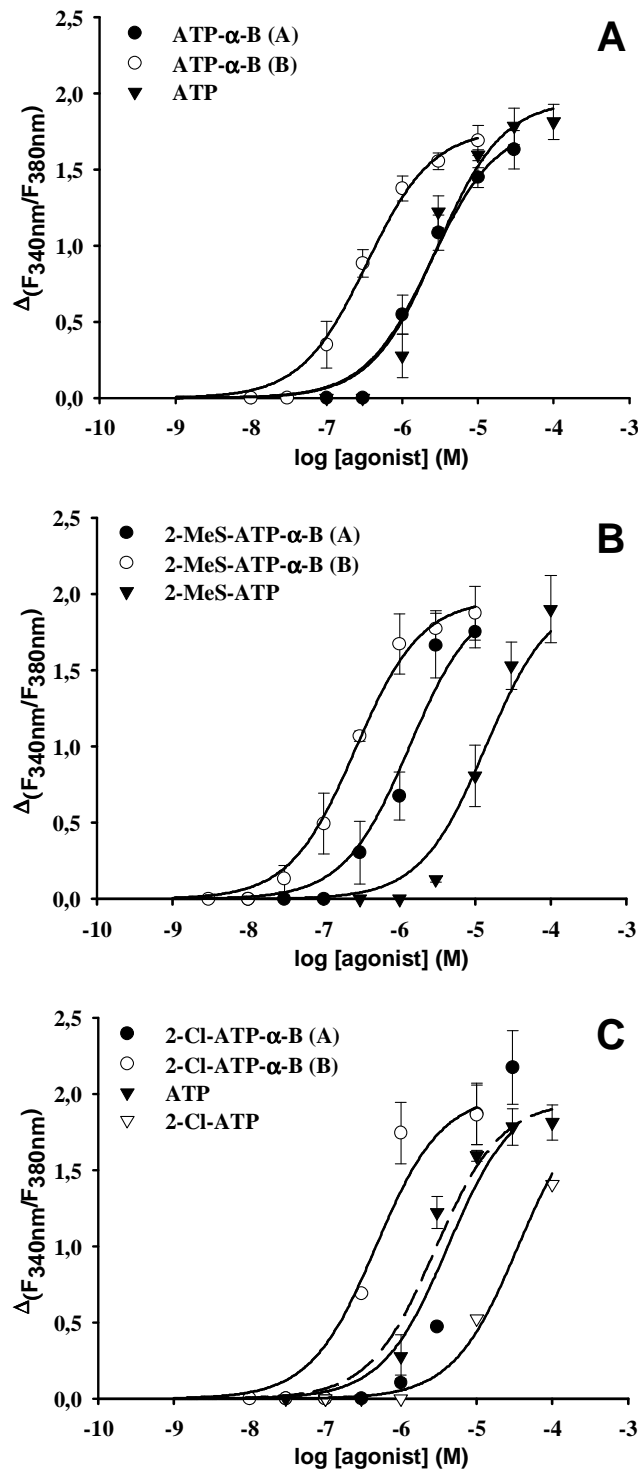


Figure 8: Concentration-response curves for ATP- α -B analogues and parent compounds at the P2Y₁₁ receptor

1321N1 cells stably expressing the P2Y₁₁ receptor GFP fusion protein, preincubated with 2 μ M fura-2-AM, were stimulated with varying concentrations of agonists and the change in fluorescence ($\Delta F_{340\text{nm}}/F_{380\text{nm}}$) was detected. Data represent the mean values and standard error from 40 to 70 single cells and were obtained in at least three separate experiments. [A]: Curves for 2-unsubstituted ATP- α -B diastereoisomers. [B]: Data obtained with the 2-MeS-ATP- α -B isomers. The maxima of the curve for the (A) isomer and the parent compound have been fixed as described in methods. [C]: Curves for 2-Cl-ATP- α -B diastereoisomers. The ATP curve is shown for comparison as well as the incomplete curve for 2-Cl-ATP. The maxima of the curve for both isomers have been fixed as described in methods.

The action of the ATP- α -B diastereoisomers at the P2Y₁₁ receptor presented here stands in contrast to the diastereoselectivity at the P2Y₁ receptor, as seen previously by us. At the P2Y₁ receptor the (A) isomers were more potent than the (B) isomers in inducing a calcium response (Nahum et al., 2002) or in causing receptor endocytosis (Tulapurkar et al., 2004). For comparison, the EC₅₀ values for the ATP- α -B derivatives at the P2Y₁ receptor are also included in Table 3. However, it should be noted that in that study the P2Y₁ receptor was heterologously expressed in HEK293 cells. For a better and more valid comparison, the action of 2-Cl-ATP- α -B isomers at the P2Y₁-GFP receptor protein stably expressed in 1321N1 cells was additionally investigated (Fig. 9). It was not possible to carry out a complete investigation of the potencies of all ligands used in this study, as the amount of compounds was not sufficient. The stereoselectivity of the 2-Cl-ATP- α -B diastereoisomers at the P2Y₁ receptor was conserved, whether the receptor was expressed in 1321N1 cells or in HEK293 cells. Thus, the diastereoselectivity is independent of the receptor expression system used. The (A) isomer displayed a higher potency (EC₅₀ = 20±5.0 nM, n=3) than the (B) isomer (EC₅₀ = 649±51.7 nM, n=3). Moreover, the difference in potency of the (A) isomer at the P2Y₁ receptor compared to the potency at the P2Y₁₁ receptor is striking.

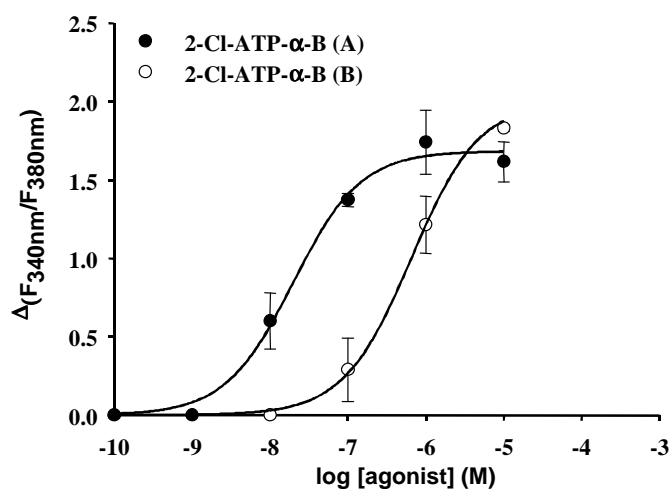


Figure 9: Concentration-response curves for 2-Cl-ATP- α -B analogues at the P2Y₁ receptor

Concentration-response curves obtained with 1321N1 cells stably expressing the P2Y₁ receptor GFP fusion protein for 2-Cl-ATP- α -B isomers in inducing intracellular [Ca²⁺]_i rise. The maximum of the curve for the (B) isomer has been fixed as described in methods. Cells preincubated with 2 μ M fura-2-AM were stimulated with varying concentrations of agonist and the change in fluorescence ($\Delta F_{340nm}/F_{380nm}$) was detected. Data represent the mean values and standard error from 40 to 70 single cells and were obtained in at least three separate experiments.

3.1.3 Adenosine-5'-O-(α -thiotriphosphate) diastereoisomers

The action of adenosine 5'-O-(1-thiotriphosphate) derivatives (ATP- α -S) at the P2Y₁₁ receptor was also investigated. The diastereoisomers show substitution of one of the non-bridging oxygen atoms of P $_{\alpha}$ by sulphur. Again, a new chiral centre in the ATP molecule is introduced. The absolute configuration around the P $_{\alpha}$ was assigned to the resulting diastereoisomers, and the Sp configuration was attributed to the (A) isomers and the Rp configuration to the (B) isomers of the thio-modified analogues. The difference in assignment for the borane-/sulphur modified isomers is due to the group priorities around P $_{\alpha}$, which are opposite for the ATP- α -B and ATP- α -S derivatives. Sulphur is of higher priority in the chemical nomenclature compared to oxygen, and borane is of lower priority than oxygen.

The concentration-response curves for each ATP- α -S diastereoisomeric pair are presented in Fig. 10, in comparison to the respective parent compound, which has an unchanged phosphate moiety. The two different pairs (ATP- α -S (A/B) and 2-MeS-ATP- α -S (A/B)) displayed the same diastereoselective activity at the P2Y₁₁ receptor as the ATP- α -B derivatives. The (B) isomers were found to be more potent than the (A) isomers, as shown by the summary of the resulting EC₅₀ values in Table 3 (page 56). However, the difference between these diastereoisomers was not as pronounced as with the α -borano substituted ATP analogues.

The (B) isomer of ATP- α -S (EC₅₀ = 270±64.0 nM) was found to be the most potent of the α -sulfur substituted compounds tested, whereas the corresponding (A) isomer with an EC₅₀ value of 1.71±0.55 μ M displayed a 6-fold lower potency (Fig. 10A). However, both substances had a higher potency at the P2Y₁₁ receptor than ATP itself. The (B) isomer of 2-MeS-ATP- α -S (EC₅₀ = 640±128 nM) showed only a 4-fold increase in potency, compared to its corresponding (A) isomer (EC₅₀ = 2.64±1.10 μ M) but was found to be 20-fold more potent than the parent compound, 2-MeS-ATP (EC₅₀ = 13.8±5.58 μ M) (Fig. 10B). Nevertheless, the maxima of the concentration effect curves for both isomers were considerably lower than the other agonist-evoked maxima, which makes a definite comparison of the EC₅₀ values rather difficult.

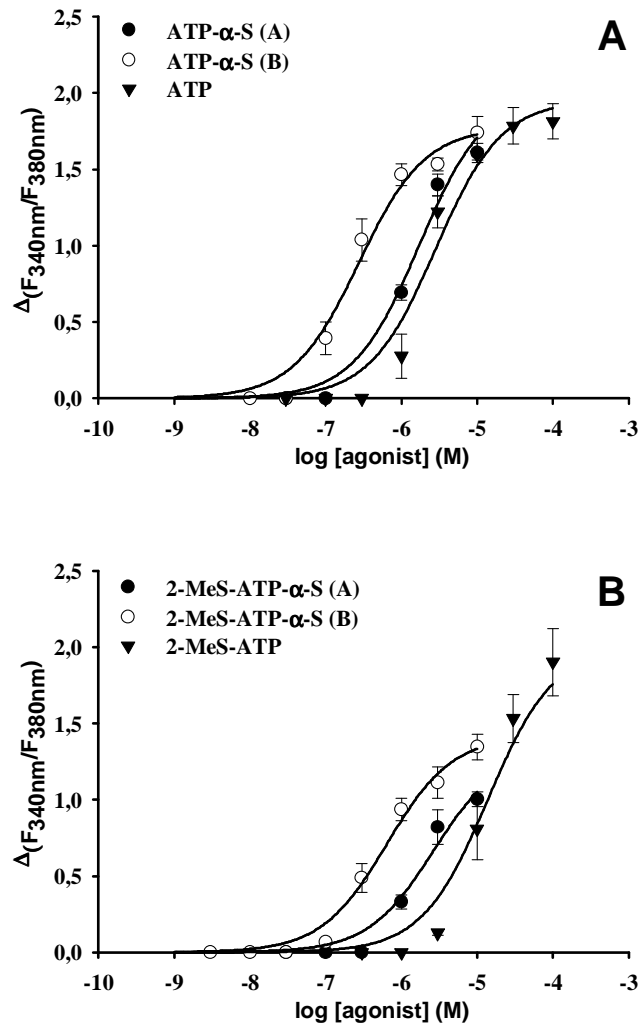


Figure 10: Concentration-response curves for ATP- α -S analogues and parent compounds at the P2Y₁₁ receptor

1321N1 cells stably expressing the P2Y₁₁ receptor GFP fusion protein, preincubated with 2 μ M fura-2, were stimulated with varying concentrations of agonists and the change in fluorescence ($\Delta F_{340\text{nm}}/F_{380\text{nm}}$) was detected. Data represent the mean values and standard error from 40 to 70 single cells and were obtained in at least three separate experiments. [A]: Curves for 2-unsubstituted ATP- α -S diastereoisomers. The maximum of the curve for the (A) isomer has been fixed as described in methods. [B]: Curves for 2-MeS-ATP- α -S diastereoisomers. The maximum of the 2-MeS-ATP curve has been fixed as described in methods.

Results

Importantly, the stereoselective activity at the P2Y₁₁ receptor is again in contrast to the activity of the α -thio-modified compounds at the P2Y₁ receptor. The P2Y₁ receptor was found to prefer the (A) over the (B) isomers of these substances (Major et al., 2004). The EC₅₀ values for the ATP- α -S derivatives at the P2Y₁ receptor are also included in Table 3. Again, in that study the P2Y₁ receptor was stably expressed in HEK293 cells. Therefore, we also investigated the action of ATP- α -S diastereoisomers at the P2Y₁GFP receptor stably expressed in 1321N1 cells. Like for the 2-Cl-ATP- α -B isomers, we obtained similar results with 1321N1 cells as with HEK293 cells concerning the stereoselective preference. The (A) isomer (EC₅₀ = 21.9±10.1 nM, n=6) of ATP- α -S was more potent than the (B) isomer (EC₅₀ = 108±14.7 nM, n=5).

Table 3: Potencies of ATP- α -B analogues and ATP- α -S analogues, respectively, and the parent compounds at P2Y₁₁ and P2Y₁ receptor for [Ca²⁺]_i rise. Data are expressed as EC₅₀ values ± s.e.m. (μ M). They represent the mean and standard error and were obtained from at least three separate experiments (n = 3-6, as indicated) with 40 to 70 single cells per concentration of agonist investigated. *For the GFP-tagged P2Y₁ receptor data are from previous analysis (see reference (Nahum et al., 2002; Major et al., 2004)), where the receptor was analyzed similarly stably expressed in HEK293 cells.

Nucleotide	Isomer	Absolute configuration	Receptor	
			P2Y ₁₁	*P2Y ₁
			Potency (EC ₅₀ value; μ M)	
ATP			2.83±0.82 (4)	0.20±0.04 (4)
2-MeS-ATP			13.8±5.58 (3)	0.001±0.001 (3)
2-Cl-ATP			>30 μ M	n.d.
P α -borano analogues				
ATP- α -B	A	Rp	2.38±0.56 (6)	0.12±0.02 (3)
	B	Sp	0.34±0.05 (6)	1.20±0.18 (3)
2-MeS-ATP- α -B	A	Rp	1.35±0.52 (3)	0.002±0.001 (3)
	B	Sp	0.26±0.03 (4)	0.06±0.01 (3)
2-Cl-ATP- α -B	A	Rp	4.19±3.41 (3)	0.004±0.002 (3)
	B	Sp	0.47±0.25 (3)	0.04±0.01 (3)
P α -thio analogues				
ATP- α -S	A	Sp	1.71±0.55 (4)	0.009±0.002 (3)
	B	Rp	0.27±0.06 (5)	0.07±0.02 (3)
2-MeS-ATP- α -S	A	Sp	2.64±1.10 (6)	0.001±0.001 (3)
	B	Rp	0.64±0.12 (5)	0.02±0.005 (3)

3.2 Ligand recognition at the P2Y₁₁ receptor

3.2.1 Selection of residues putatively involved in ligand recognition

The residues considered to be involved in ligand recognition at the P2Y₁₁ receptor were selected using the data obtained by molecular modelling. The P2Y₁₁ receptor model was constructed in collaboration with Prof. B. Fischer from the Department of Chemistry, Gonda-Goldschmied Medical Research Center, Bar-Ilan University in Ramat-Gan, Israel. Bovine rhodopsin and the previously generated P2Y₁-R:ATP complex model (Major and Fischer, 2004) were both used as templates. The P2Y₁₁ receptor model displays a binding pocket with specific residues interacting with the docked ATP molecule (Fig. 11). Most of these residues (Arg106, Phe109, Arg268, Arg307) were selected for mutational analysis. Moreover, Ala313 of the P2Y₁₁ receptor was also selected as all other P2Y receptors have an asparagine at the corresponding position (7.45) (Fig. 4A). This alanine residue might be responsible for the low potency of 2-alkylthio-ATP derivatives at the P2Y₁₁ receptor. The Ala313 is located near to a hydrophobic pocket of the nucleotide binding pocket and could interfere with the coordination of 2-alkylthio substituents at the ATP molecule into this pocket.

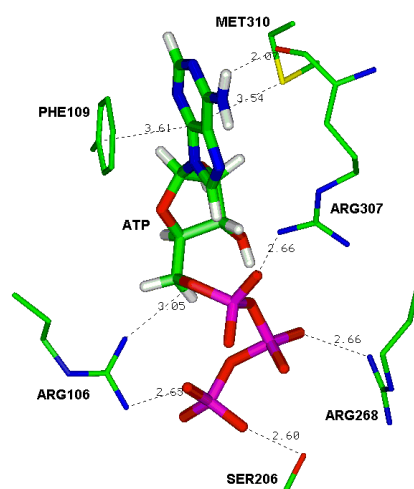


Figure 11: Docked ATP and interacting residues in a molecular model of the P2Y₁₁ receptor

The ATP molecule is surrounded by interacting residues that are involved in shaping the binding pocket of the P2Y₁₁ receptor. Distances (Å) between interacting atoms (heavy atoms: N, P, O) are indicated.

In addition, other residues selected for a site-directed mutagenesis approach were identified by sequence comparison of the P2Y₁ and P2Y₁₁ receptors. A tyrosine residue (Tyr261) in the TM6 of the P2Y₁₁ receptor was chosen because the corresponding tyrosine in the P2Y₁ receptor (6.48) was found to be a molecular switch for receptor activation (Costanzi et al., 2004). Glu186 (EL2) was mutated, as it was considered to take part in determining the diastereoselectivity of the P2Y₁₁ receptor.

3.2.2 Introduction of point mutations into the P2Y₁₁ receptor DNA sequence

Site-directed-mutagenesis was performed by PCR using specifically designed primers (listed in materials). Mutations were introduced at the preselected positions in the P2Y₁₁ receptor sequence which was present in the eGFPN1 vector.

```

      GCCAGCAATGGCCTGGCCCTGTACCGCTTCAGCATCCGGAAGCAGCGCCCATGGCACCCC
121 -----+-----+-----+-----+-----+-----+-----+ 180
      GCCGTGGTCTTCTCTGTCCAGCTGGCAGTCAGCGACCTGCTCTGCGCTCTGACGTGCC
181 -----+-----+-----+-----+-----+-----+-----+ 240
      CCGCTGGCCGCTACCTCTATCCCCCAAGCACTGGCGCTATGGGGAGGCCGCGTGCCG
241 -----+-----+-----+-----+-----+-----+-----+ 300
R106A - - - - -GCC
F109I - - - - - ATC
      CTGGAGCGCTTCCTCTTCACCTGCAACCTGCTGGGCAGCGTCATCTTCATCACCTGCATC
301 -----+-----+-----+-----+-----+-----+-----+ 360
      AGCCTCAACCGCTACCTGGGCATCGTGCACCCCTTCTTCGCCCCAAGCCACCTGCGACCC
361 -----+-----+-----+-----+-----+-----+-----+ 420
      AAGCACGCCTGGGCCGTGAGCGCTGCCGGCTGGGTCTGGCCGCCCTGCTGGCCATGCC
421 -----+-----+-----+-----+-----+-----+-----+ 480
      ACACTCAGCTTCTCCACCTGAAGAGGCCGAGCAGGGGGCGGGCAACTGCAGCGTGGCC
481 -----+-----+-----+-----+-----+-----+-----+ 540
E186A - - - - -GCG
      AGGCCCGAGGCCTGCATCAAGTGTCTGGGGACAGCAGACCACGGGCTGGCGCCTACAGA
541 -----+-----+-----+-----+-----+-----+-----+ 600
      GCGTATAGCCTGGTGTCTGGCGGGTTGGGCTGCGGCCTGCCGCTGCTGCTCACGCTGGCA
601 -----+-----+-----+-----+-----+-----+-----+ 660
      GCCTACGGCGCCCTCGGGCGGGCCGTGCTACGCAGCCCAGGCATGACTGTGGCCGAGAAG
661 -----+-----+-----+-----+-----+-----+-----+ 720
Y261A - - - - - GCG
      CTGCGTGTGGCAGCGTTGGTGGCCAGTGGTGTGGCCCTCTACGCCAGCTCCTATGTGCC
721 -----+-----+-----+-----+-----+-----+-----+ 780
R268A - - - - -GCG
R268Q - - - - -CAG
      TACCACATCATGCGGTGCTCAACGTGGATGCTCGGCGGCGCTGGAGCACCCGCTGCCCG
781 -----+-----+-----+-----+-----+-----+-----+ 840
      AGCTTTCAGACATAGCCCAGGCCACAGCAGCCCTGGAGCTGGGGCCCTACGTGGGCTAC
841 -----+-----+-----+-----+-----+-----+-----+ 900
R307A - - - - - GCG
A313N - - - - - AAC
      CAGGTGATGCGGGGCCTCATGCCCTGGCCCTTCTGTGTCCACCCTCTACTCTACATGGCC
901 -----+-----+-----+-----+-----+-----+-----+ 960

```

Figure 12: Introduction of mutations into the DNA-Sequence of the P2Y₁₁ receptor

Partial DNA sequence (single strand) of the P2Y₁₁ receptor (GenBank accession number: AF030335; cds 121-960). Selected positions (codons) for a mutational analysis are shown in blue. The change of amino acids upon site-directed mutation is indicated on the left side and the introduced codon is displayed in orange. The restriction sites of ApaI (red) and BspEI (green) are also highlighted.

The preselected residues were: Arg106 (3.29), Phe109 (3.32), Glu186 (EL2), Tyr261 (6.48), Arg268 (6.55), Arg307 (7.39) and Ala313 (7.45). Most of these residues were mutated to alanine, except Phe109 and Ala313 (Fig. 12). The phenylalanine Phe109 was mutated to isoleucine to retain the hydrophobic and spatial properties at this position, and to only delete the aromatic nature. Ala313 was mutated to asparagine as this was the conserved residue at the corresponding position (7.45) in all other P2Y receptors. For the arginine at position 6.55 (Arg268) an additional conservative mutation to glutamine was generated.

The DNA constructs of the mutated clones were digested with *Apa*I and *Bsp*EI restriction enzymes and ligated into the mother vector to avoid unwanted mutations in the vector sequence. For subcloning of the Arg307 and Ala313 mutants, plasmids were cut with *Eco*RI and *Bam*HI restriction endonucleases as the point mutations were located downstream of the *Bsp*EI restriction site.

3.2.3 Expression of P2Y₁₁ receptor mutants in 1321N1 cells

1321N1 cells were used to stably express the mutant receptors as GFP fusion proteins. The expression level was analyzed by flow cytometry detecting the GFP fluorescence intensity per cell. While three of the mutant receptors (Phe109Ile, Arg268Gln, Ala313Asn) displayed fluorescence intensities comparable to that of the wild type receptor, two receptor mutants (Glu186Ala, Arg268Ala) showed a higher expression level and three other mutants (Arg106Ala, Tyr261Ala, Arg307Ala) had around 80% expression level as compared to the wild type receptor (Table 4, next page).

The subcellular localization of the mutant receptors was also determined by taking confocal images from the stably transfected cells. The localization of the mutant P2Y₁₁ receptors was found to be comparable to that of the wild type receptor for the Glu186Ala, Arg268Ala, Arg268Gln, Ala313Asn mutants. Although the Phe109Ile mutant receptor was only partially located at the plasma membrane, it still exhibited a significant potency for ATP (section 3.2.4.1). Therefore, the potency of ATP found at the Phe109Ile mutant as well as the potency at the mutants with a similar subcellular localization (Arg106Ala, Tyr261Ala, Arg307Ala) likely reflects the intrinsic activity of these constructs.

3.2.4 Pharmacological characterisation of the P2Y₁₁ receptor mutants

The functional activity of the mutant receptors was determined by monitoring in stably transfected cells the intracellular [Ca²⁺]_i rise induced after agonist stimulation employing the calcium indicator fura-2 (described in methods section).

3.2.4.1 Potency of ATP and ATPγS

To functionally characterize the mutant receptors, we investigated the potency of ATP as the natural agonist and ATPγS as one of the most potent agonists at the P2Y₁₁ receptor. The concentration response curves obtained for ATPγS and ATP with the different P2Y₁₁ receptor mutants are displayed in Figs. 13 and 14, respectively. The EC₅₀ values resulting from these curves are summarized in Table 4.

Results

A strong influence on the potency of ATP was found after mutation of three cationic residues to alanine located in TM3, 6 and 7. The two arginine residues at positions 3.29 and 7.39 were found to be most critical for P2Y₁₁ receptor activation. After mutation to alanine, the ability of ATP to trigger a calcium signal at these receptors was almost abolished. Only at concentrations ≥ 10 mM an increase in calcium levels could be observed (Table 4). Mutation of the cationic residue in TM6 (Arg268) did not lead to a complete loss of receptor activation as for the other two arginines but resulted in a drastically decreased potency of ATP at the mutant receptor (Table 4, Fig. 14). The change in potency was about three orders of magnitude as compared to the wild type P2Y₁₁ receptor. Interestingly, when this arginine was substituted by glutamine, the potency of ATP at this receptor could be partially rescued. ATP γ S, as one of the most potent P2Y₁₁ receptor agonists, did also show a clear decrease in potency at both Arg268 mutant receptors but this decrease was far less pronounced than that for ATP (compare Figs. 13 and 14).

Table 4: Functional characteristics of mutant P2Y₁₁GFP receptors: intracellular calcium rise induced by receptor stimulation. Receptor expression levels in 1321N1 cells were analyzed by flow cytometry detecting the GFP fluorescence intensity. Data represent mean EC₅₀ values (μ M) \pm s.e.m. and (n) numbers obtained from concentration response curves of 1321N1 cells stably expressing the wild type or mutated receptor. ^a ATP induced no significant increase in intracellular calcium up to concentrations of 10 mM. n.d. = not determined.

construct	residue	EC ₅₀ values (μ M)		Receptor expression level (%)
		ATP	ATP γ S	
wt		2.37 \pm 0.88 (4)	1.04 \pm 0.38 (4)	100
Arg106Ala	3.29	^a	n.d.	76.05 \pm 4.70 (4)
Phe109Ile	3.32	10.7 \pm 2.29 (5)	n.d.	102 \pm 13 (7)
Glu186Ala	EL2	32.8 \pm 21.1 (5)	4.92 \pm 1.07 (4)	111 \pm 10 (9)
Tyr261Ala	6.48	^a	n.d.	77.35 \pm 3.91 (4)
Arg268Ala	6.55	1806 \pm 354 (3)	247 \pm 178 (8)	143 \pm 23 (3)
Arg268Gln	6.55	102 \pm 20 (5)	10.3 \pm 2.59 (3)	95.59 \pm 8.07 (7)
Arg307Ala	7.39	^a	n.d.	87.53 \pm 5.94 (4)
Ala313Asn	7.45	4.52 \pm 0.99 (7)	n.d.	97.63 \pm 11.98 (4)

Another residue in TM6 (Tyr261) also seems to be critical for normal receptor function. After mutation of Tyr261 (6.48) to alanine, ATP was not able to elicit a response at this receptor at concentrations up to ≥ 10 mM. Therefore, this tyrosine seems to play an important role in P2Y₁₁ receptor activation. It can be assumed that Tyr261 is solely involved in receptor activation, since it was not found to be directly interacting with the docked ATP in the P2Y₁₁-R model.

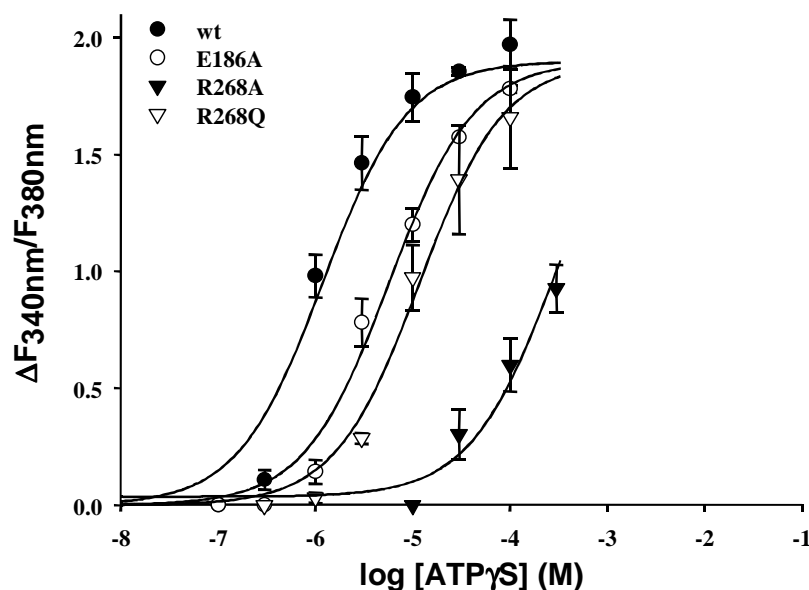


Figure 13: Concentration-response curves for ATP γ S at the wild type and mutant P2Y₁₁GFP receptor stably expressed in 1321N1 cells

Cells preincubated with 2 μ M fura-2-AM were stimulated with varying concentrations of ATP γ S and the change in fluorescence ($\Delta F_{340\text{nm}}/F_{380\text{nm}}$) was detected. Data represent the mean values and standard error from 40 to 70 single cells. Results were obtained in at least three separate experiments. The maxima of the curves were fixed to the plateau value of the ATP γ S curve at the wild type receptor.

The nucleotide binding pocket of P2Y receptors has been shown to consist not only of residues located in the transmembrane domains of the receptors but also of residues from the extracellular loop 2 (EL2). For this reason we selected a glutamate residue in the EL2 of the P2Y₁₁ receptor putatively involved in ligand recognition. Mutation of Glu186 to alanine resulted in a decreased potency of ATP at the receptor. The shift was more than one order of magnitude (Table 4, Fig. 14). However, for the more potent P2Y₁₁ receptor agonist ATP γ S the shift in potency was only 5-fold, compared to the wild type receptor (Fig. 13). This suggests that Glu186 interacts with phosphates P $_{\alpha\beta}$ of the triphosphate moiety.

The potency of ATP at two (Phe109, Ala313) out of all the other mutant receptors was only slightly affected. The aromatic amino acid in TM3 (Phe109) that was indicated from the P2Y₁₁-R model (Fig. 11) to possibly interact with the adenine moiety via π -stacking interaction seems to be not very critical for receptor activation. The EC₅₀ value of ATP was increased only by a factor of 4 after mutation of phenylalanine to isoleucine (Table 4, Fig. 14). The mutation of Phe109 to isoleucine at the P2Y₁₁ receptor did probably not much disturb the recognition of ATP, since isoleucine is also a bulky, hydrophobic amino acid and therefore the loss in potency was not dramatic.

The alanine residue at position 7.45 (Ala313) is a unique feature of the P2Y₁₁ receptor, as all other P2Y receptors have an asparagine amino acid at this position (Fig. 4A, page 13). At the Ala313Asn mutant receptor, recognition of ATP was not much influenced. ATP was only 2-fold less potent as compared to the wild type receptor (Table 4, Fig. 14).

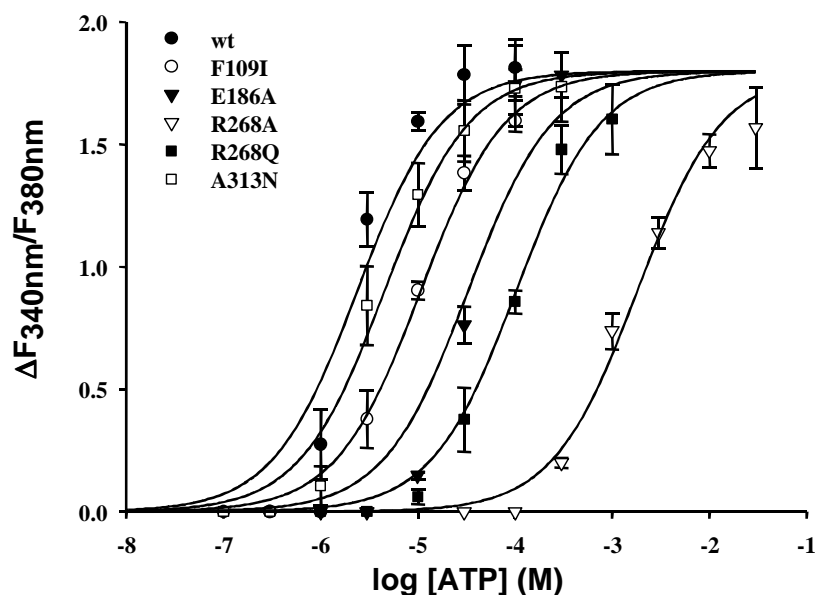


Figure 14: Concentration-response curves for ATP at the wild type and mutant P2Y₁₁GFP receptor stably expressed in 1321N1 cells

Cells preincubated with 2 μ M fura-2-AM were stimulated with varying concentrations of ATP and the change in fluorescence ($\Delta F_{340\text{nm}}/F_{380\text{nm}}$) was detected. Data represent the mean values and standard error from 40 to 70 single cells. Results were obtained in at least three separate experiments. The maxima of the curves were fixed to the plateau value of the ATP curve at the wild type receptor.

3.2.4.2 Diastereoselectivity of the P2Y₁₁ receptor mutants

To decipher the molecular basis of the diastereoselectivity of the P2Y₁₁ receptor (as described in section 3.1), two mutant receptors were selected to test if the preference of the ATP- α -S (B) isomer is lost after mutation of the selected residues. The glutamate residue (Glu186) in the EL2 of the receptor was considered to be a putative candidate to take part in the determination of the P2Y₁₁ receptor's diastereoselectivity. The corresponding residue in the P2Y₁ receptor (Asp204) was found to coordinate a Mg²⁺ ion in the vicinity of the phosphate binding pocket which in turn is responsible for the diastereoselective discrimination at the P2Y₁ receptor (Major et al., 2004). In addition, the arginine (Arg268) at position 6.55 in the P2Y₁₁ receptor was also selected as it was facing the glutamate residue (Glu186) in the P2Y₁₁ receptor model. Therefore, both residues could be involved in the preferential interaction with one of the P α conformations, as they are on opposite sites of the phosphate chain from the ATP docked in the model.

Table 5: Intracellular calcium rise induced by stimulation of mutant P2Y₁₁GFP receptors with ATP- α -S isomers. Data represent mean EC₅₀ values (μ M) \pm s.e.m. obtained from concentration response curves of 1321N1 cells stably expressing the wild type or mutated receptor in (n) numbers of experiments.

construct	EC ₅₀ values of ATP- α -S (μ M)	
	(A) isomer	(B) isomer
wt	1.71 \pm 0.55 (4)	0.27 \pm 0.06 (5)
Glu186Ala	10.2 \pm 4.52 (6)	0.85 \pm 0.26 (7)
Arg268Ala	30.8 \pm 16.3 (5)	26.4 \pm 16.0 (4)
Arg268Gln	3.28 \pm 1.04 (4)	2.69 \pm 0.79 (4)
Glu186Ala, Arg268Gln	19.8 \pm 3.27 (4)	13.7 \pm 2.00 (5)

The Glu186Ala P2Y₁₁ mutant receptor did not show a loss in preference of the ATP- α -S (B) isomer. On the contrary, the difference in potency between the (A) and (B) isomer was even increased as compared to the difference at the wild type receptor (Table 5, Fig. 15A). Interestingly, the EC₅₀ value of the (B) isomer at the Glu186Ala mutant receptor (EC₅₀ = 854 \pm 260 nM) was decreased only 3-fold, as compared to the wild type receptor (EC₅₀ = 270 \pm 64.0 nM). However, the shift in potency for the (A) isomer was more pronounced. At the Glu186Ala receptor mutant the EC₅₀ value for the ATP- α -S (A) isomer was 10.2 \pm 4.52 μ M compared to 1.71 \pm 0.55 μ M at the wild type receptor. This suggests that the recognition of the (B) isomer of ATP- α -S is not much disturbed after substitution of the glutamate in EL2 by alanine, whereas the (A) isomer is recognized to a lesser extent.

After mutation of Arg268 (6.55) to alanine or glutamine a loss of preference for the ATP- α -S (B) isomer was observed (Table 5, Fig. 15B). For the Arg268Ala P2Y₁₁ receptor mutant the decrease in potency for the (B) isomer (EC₅₀ = 26.4 \pm 16.0 μ M) was about two orders of magnitude, whereas the shift in potency for the (A) isomer (EC₅₀ = 30.8 \pm 16.3 μ M) was only 20-fold as compared to the wild type receptor. Taken together, at the Arg268Ala receptor mutant both isomers were found to be equipotent.

The shift in potency for the ATP- α -S (A) isomer at the Arg268Ala mutant receptor is least pronounced in comparison with all other agonists tested. Thus, the recognition of the (A) isomer is less disturbed by mutation of this important cationic residue, and the binding mode is apparently different from that for the other agonists. Furthermore, at the Arg268Gln P2Y₁₁ receptor mutant, the activity of the ATP- α -S (A) isomer (EC₅₀ = 3.28 \pm 1.04 μ M) was nearly rescued. The change in potency compared to the wild type receptor (EC₅₀ = 1.71 \pm 0.55 μ M) was only 2-fold. The (B) isomer (EC₅₀ = 2.69 \pm 0.79 μ M) was 10-fold less potent at the Arg268Gln receptor mutant than at the unmutated P2Y₁₁ receptor. Thus, the activity of both isomers was affected to the same degree after substitution of the arginine by glutamine and again both isomers appeared to be equipotent at this receptor mutant.

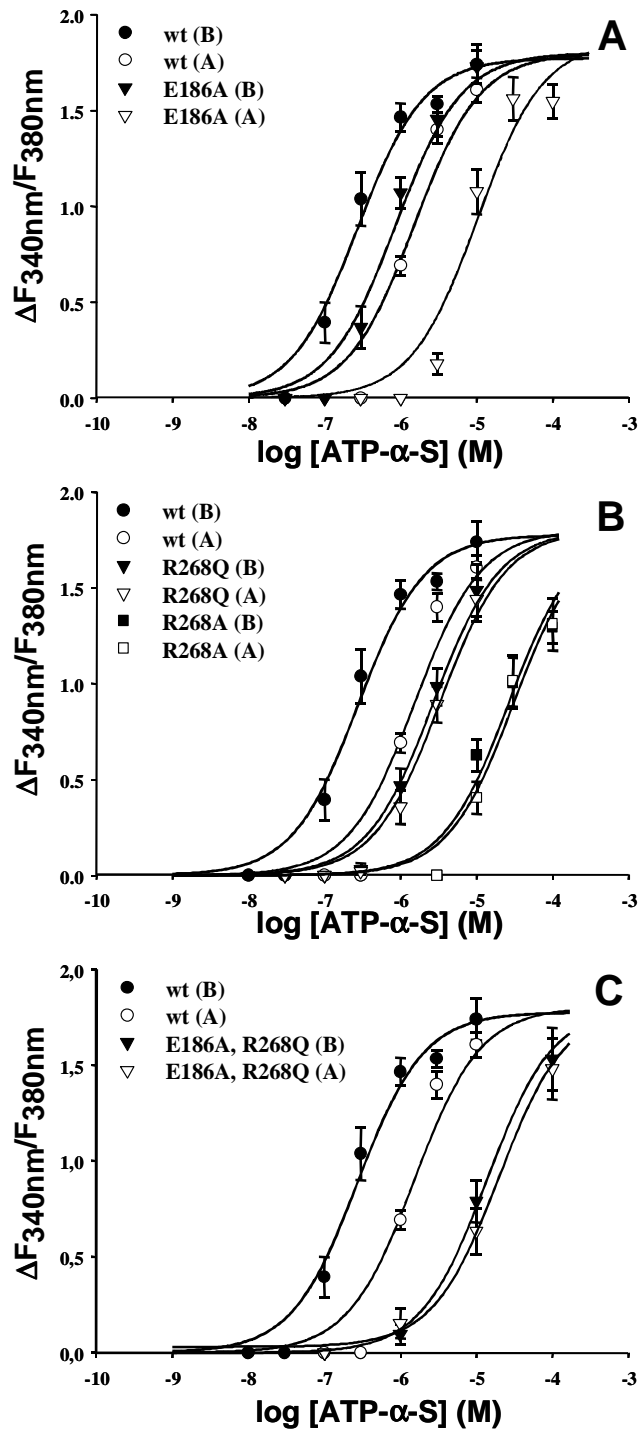


Figure 15: Concentration-response curves for ATP- α -S (A) and (B) isomers at the wild type and mutant P2Y₁₁GFP receptors stably expressed in 1321N1 cells

Cells preincubated with 2 μ M fura-2-AM were stimulated with varying concentrations of ATP- α -S (A) and (B) isomers and the change in fluorescence ($\Delta F_{340\text{nm}}/F_{380\text{nm}}$) was detected. Data represent the mean values and standard error from 40 to 70 single cells. Results were obtained in at least three separate experiments [A] Curves obtained at the E186A receptor mutant. The maxima of the curves for the (B) isomer at the E186A mutant and the (A) isomer at the wild type receptor were fixed to the plateau value of the ATP curve at the wild type receptor. [B] Curves obtained at the R268A and R268Q receptor mutants. The maxima of the curves for the isomers at the R268 mutants and the (A) isomer at the wild type receptor were fixed to the plateau value of the ATP curve at the wild type receptor. [C] Curves obtained at the E186A, R268Q double mutant receptor. The maxima of the curves for the isomers at the double mutant and the (A) isomer at the wild type receptor were fixed to the plateau value of the ATP curve at the wild type receptor.

A double mutant was constructed, to test whether a further change in the diastereoselectivity of the P2Y₁₁ receptor can be seen after simultaneous mutation of the glutamine in EL2 and the arginine in TM6. The mutant receptor contained the Glu186Ala and Arg268Gln mutations. In addition to the potency of the ATP- α -S diastereoisomers, the activity of ATP was also tested at this mutant receptor. The loss in potency for ATP at the double mutant receptor ($EC_{50} = 886 \pm 231 \mu\text{M}$, $n = 4$) was more than two orders of magnitude as compared to the wild type receptor ($EC_{50} = 2.37 \pm 0.88$). Therefore, the right shift of the concentration response curve was additive for the double mutant in comparison to the two corresponding single point mutants (Table 4). The diastereoselectivity of the Glu186Ala, Arg268Gln mutant receptor showed characteristics similar to the ones found for the single Arg268Gln and single Arg268Ala mutant. Both ATP- α -S isomers (A and B) were found to be equipotent at the double mutant receptor. The change in potency for the (A) isomer ($EC_{50} = 19.8 \pm 3.27 \mu\text{M}$) was about one order of magnitude and for the (B) isomer ($EC_{50} = 13.7 \pm 2.0 \mu\text{M}$) the change was 50-fold as compared to the unmutated P2Y₁₁ receptor (Table 5, Fig. 15C). After mutating two positions in the P2Y₁₁ receptor, the additive effect concerning the loss in potency for the (B) isomer was very clear, whereas the additive decrease in potency for the (A) isomer was only 2-fold when compared to the Glu186Ala single mutant receptor.

3.2.4.3 Recognition of 2-alkylthio substituted ATP derivatives

At the entrance to a hydrophobic pocket which is located in the vicinity of the ATP C2 position in the P2Y₁₁-R model (Fig. 16) an alanine residue (Ala313) is situated. This Ala313 is a unique feature of the P2Y₁₁ receptor, as all other P2Y receptors have an asparagine amino acid at this position (Fig. 4A). It was expected, that this Ala313 might be involved in the reduction in potency for C2-substituted ATP derivatives at the P2Y₁₁ receptor. Therefore, we investigated the potency of 2-MeS-ATP at the Ala313Asn receptor mutant and compared it to the potency at the wild type receptor.

As already described in section 3.2.4.1, ATP was found to be 2-fold less potent at the Ala313Asn receptor mutant as compared to the unmutated receptor. Interestingly, 2-MeS-ATP ($EC_{50} = 8.37 \pm 2.05 \mu\text{M}$, $n=8$) displayed a slight gain in potency as compared to the wild type receptor ($EC_{50} = 11.1 \pm 6.30 \mu\text{M}$, $n=3$). This gain in potency is not statistically significant, but obvious, when we consider the slightly reduced potency of ATP itself.

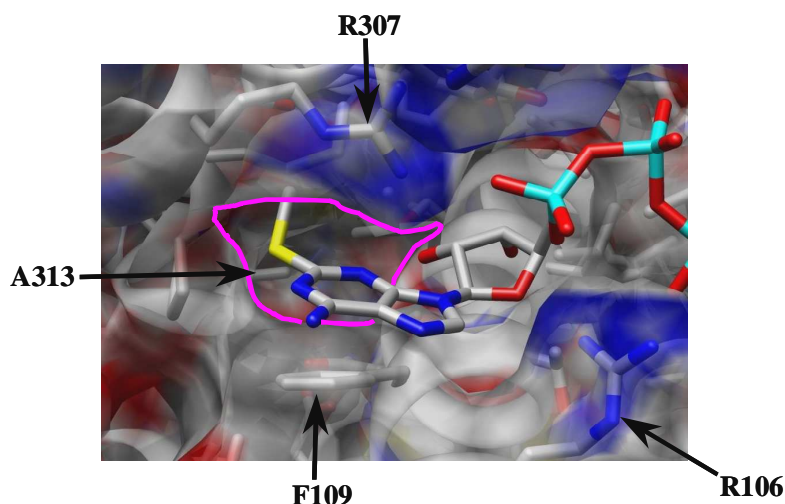


Figure 16: Section of the molecular model of the P2Y₁₁ receptor displaying a hydrophobic pocket

Nucleotide binding pocket of the P2Y₁₁ receptor with docked 2-MeS-ATP. The entrance to the hydrophobic pocket is highlighted in pink. The A313 residue is positioned directly at the entrance to the hydrophobic pocket. Other important residues for ligand recognition at the receptor are also indicated.

Unexpectedly, 2-neopentylS-ATP, did not have any activity at the Ala313Asn mutated receptor. The 2-neopentylS substituent did not fit into the hydrophobic pocket of the P2Y₁₁-R model, consistent with the inactivity of the analogue at the wild type receptor. The mutation of Ala313 to asparagine was suggested to improve the fit of 2-neopentylS-ATP into the binding pocket. However, a clear influence on the recognition of the 2-alkylthio-ATP derivatives at the P2Y₁₁ receptor could not be verified for the unique alanine residue in TM7.

3.3 Hetero-oligomerization of the P2Y₁ and the P2Y₁₁ receptor

3.3.1 Agonist-induced internalization of the P2Y₁₁GFP receptor in HEK293 cells

In order to decipher the characteristics of the P2Y₁₁ receptor endocytosis, we fused a GFP tag to the C-Terminus of the receptor and stably expressed the receptor in HEK293 cells. The expression of the receptor was visualized by confocal microscopy and it was found to localize clearly to the plasma membrane (Fig. 17). For detection of endocytosis of the P2Y₁₁GFP receptor, live cell imaging was done on a Zeiss inverted LSM 510 META laser scanning confocal microscope before and during agonist stimulation, as described in the methods section.

The HEK293 cell line used was found to express endogenously several P2Y receptor mRNA transcripts (P2Y₁, P2Y₂, P2Y₄) (Schafer et al., 2003). Therefore, the P2Y₁₁GFP receptor internalization was induced by the most potent and relatively specific receptor agonist BzATP to avoid stimulation of the endogenous P2Y receptors.

After continuous stimulation with 100 μ M BzATP for 60 min no endocytosis of the P2Y₁₁GFP receptor was observed (Fig. 17, A3). However, a clear response in intracellular calcium rise and cAMP accumulation was found upon stimulation of the cells with 100 μ M BzATP, suggesting the expression of a fully functional P2Y₁₁GFP receptor. The calcium response is given in Fig. 18 in comparison to the response of mock transfected cells (dotted line). The cAMP response is displayed in Fig. 33.

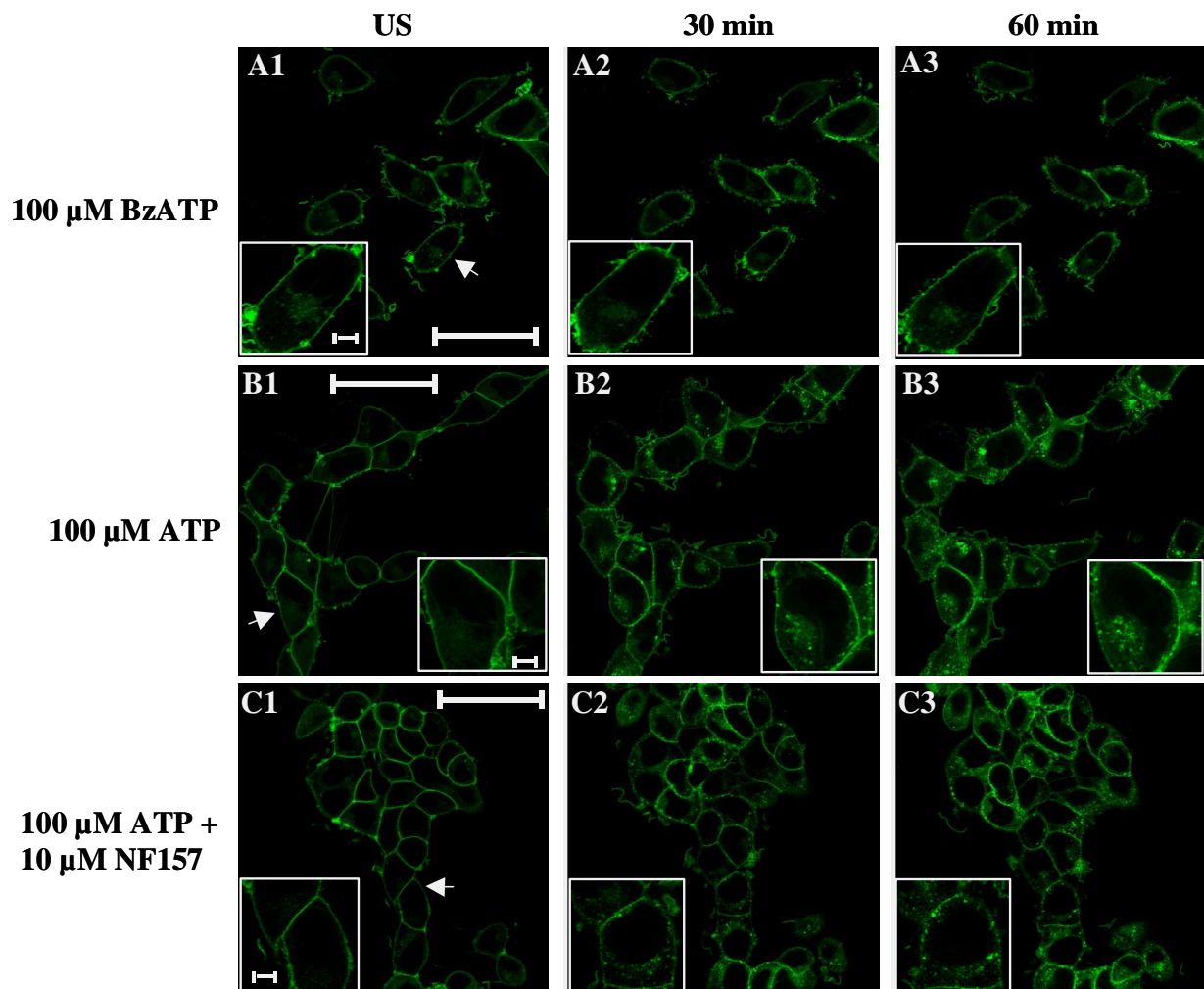


Figure 17: Live imaging of agonist-induced internalization of the P2Y₁₁GFP receptor stably expressed in HEK293 cells

HEKP2Y₁₁GFP cells were visualized with a LSM510meta confocal microscope and stimulated with various agonists for up to 60 min at 37°C (5% CO₂) as described in methods. Pictures show unstimulated (US) cells and cells after 30 and 60 min of agonist stimulation, as indicated. (A1-3) Stimulation with 100 μ M BzATP (n=3). (B1-3) Stimulation with 100 μ M ATP (n=5). (C1-3) Cells preincubated for 30 min with 10 μ M NF157 and stimulated with 100 μ M ATP (n=3). Scale bars indicate 50 μ m in the overall picture and 5 μ m in the zoomed picture. The arrow points to cells selected for the inserted zoomed picture.

To test if the lack of internalization was an agonist-specific feature, cells were stimulated with the natural agonist of the P2Y₁₁ receptor, namely ATP. A slight endocytosis of the receptor was seen after 30 min of continuous stimulation with 100 μ M ATP (Fig. 17, B2). Further stimulation until 60 min increased the amount of endocytosed receptor, but the internalization remained incomplete, as part of the receptor was still visible at the plasma membrane (Fig. 17, B3). Preincubation of the cells with the specific P2Y₁₁ receptor antagonist NF157 (10 μ M) was done 30 min before the ATP-induced internalization to prove that endocytosis of the P2Y₁₁GFP receptor was a result of its direct stimulation. However, as shown in Fig. 17, C2-3, preincubation with NF157 did not inhibit the internalization of the receptor induced by stimulation with 100 μ M ATP for 30 or 60 min. In addition, the calcium response to ATP also remained unaffected by NF157 pretreatment (Fig. 18). Thus, the results of these endocytosis experiments did not mirror the pharmacology known for the P2Y₁₁ receptor. Therefore, the involvement of a crosstalk between the P2Y receptors was hypothesized.

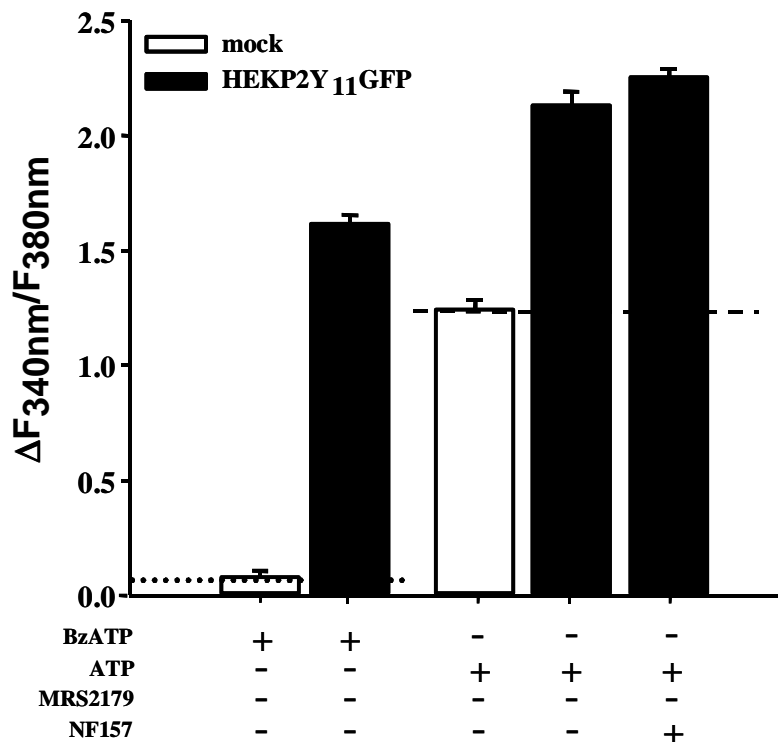


Figure 18: Intracellular calcium rise in stably transfected HEK293 cells

Peak values of $[Ca^{2+}]_i$ rise of mock-transfected (blank bars) and HEKP2Y₁₁GFP transfected (black bars) cells stimulated with 100 μ M agonist (BzATP, ATP) +/- preincubation with 100 μ M MRS2179 or 10 μ M NF157. Data represent the mean values \pm s.e.m from 30-100 cells obtained in at least three separate experiments. The dotted and dashed line in the graph indicate the response upon expression and stimulation of the P2Y₁₁GFP receptor compared to mock transfected HEK293 cells.

3.3.2 Co-Internalization of the P2Y₁ and P2Y₁₁GFP receptor in HEK293 cells

First the quantitative expression of mRNA transcripts of P2Y receptors responsive to ATP was analyzed by real time PCR to test our hypothesis of a receptor crosstalk. As expected, the HEKP2Y₁₁GFP cells were found to express the P2Y₁ and P2Y₂ receptor (Fig. 19) but the latter was only weakly expressed. Therefore, further experiments concentrated on the P2Y₁ receptor as a putative crosstalk partner in the P2Y₁₁GFP receptor endocytosis.

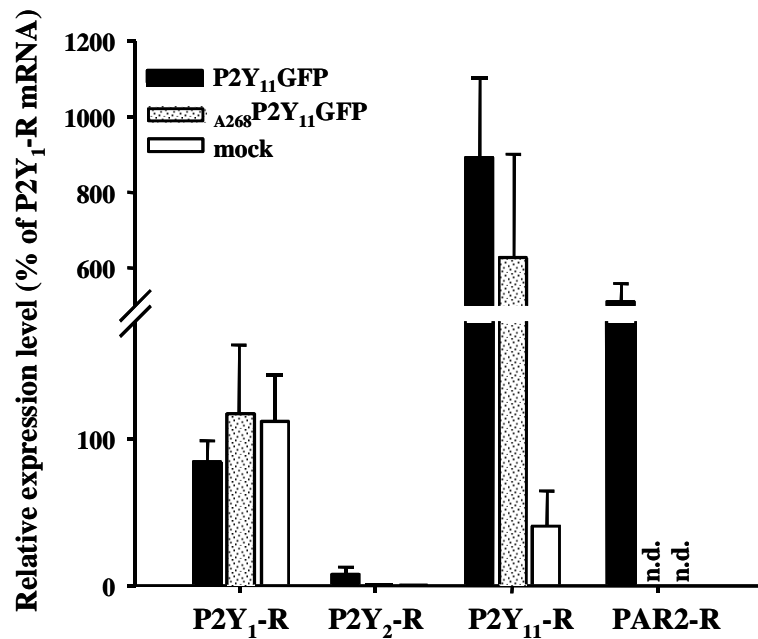


Figure 19: Expression levels of mRNA of different GPCRs in HEK293 cells

Real time PCR was done using cDNA generated from total RNA of HEKP2Y₁₁GFP, HEK_{A268}P2Y₁₁GFP or mock-transfected cells, as described in the material and methods section. The expression of several GPCRs was normalized to GAPDH. Bar graphs show relative expression (%) in relation to the expression of the P2Y₁ receptor in each of the differently transfected cells. n.d. = not determined

The possible involvement of the P2Y₁ receptor in contributing to the P2Y₁₁ receptor internalization was investigated using the specific P2Y₁ receptor antagonist MRS2179. Preincubation of HEKP2Y₁₁GFP cells with 100 μM MRS2179 for 30 min followed by subsequent stimulation with 100 μM ATP completely abolished the receptor endocytosis (Fig. 21, A1-3). In addition, stimulation of the cells with the natural P2Y₁ receptor agonist ADP (100 μM) resulted in complete internalization of the P2Y₁₁ receptor (Fig. 21, B2-3). As ADP at this concentration is also able to stimulate the P2Y₁₁ receptor, the effect of a more selective P2Y₁ receptor agonist was also tested. 2-MeS-ADP was found to be inactive at the P2Y₁₁ receptor at concentrations up to 100 μM (Communi et al., 1997), whereas it is highly potent at the P2Y₁ receptor (Palmer et al., 1998).

Stimulation of HEKP2Y₁₁GFP cells with 10 μ M 2-MeS-ADP resulted in complete internalization of the P2Y₁₁ receptor (Fig. 21, C2-3), comparable to the pattern observed after ADP stimulation. Thus, the agonist profile found strongly supports the hypothesis of a crosstalk between the P2Y₁ and P2Y₁₁ receptor.

The specificity of the functional interaction between the P2Y₁₁GFP receptor and the endogenous P2Y₁ receptor in HEK293 cells was tested next. HEKP2Y₁₁GFP cells were found to express the P2Y₂ receptor and the protease-activated-receptor 2 (PAR2) receptor, as analyzed by real time PCR. Treatment of the cells with 100 μ M UTP acting on the endogenous P2Y₂ receptor and simultaneous imaging of P2Y₁₁ receptor trafficking showed no movement of the P2Y₁₁GFP receptor even after 60 min of stimulation (Fig. 21, D3). Also, stimulation of the PAR2 receptor did not result in endocytosis of the P2Y₁₁GFP receptor when the PAR2 receptor was activated with the protease trypsin (50 nM) in serum-free medium (Fig. 21, E3). Moreover, stimulation with the PAR2-activating peptide (PAR2-AP, 100 μ M) which activates the PAR2 receptor without cleavage (Luo et al., 2005), did also not result in P2Y₁₁GFP endocytosis (Fig. 21, F3). However, a clear increase in intracellular calcium was observed after stimulation of the cells with 100 μ M UTP, 50 nM trypsin and 100 μ M PAR2-AP (Fig. 20). The latter confirms the functional expression of the endogenous P2Y₂ and PAR2 receptors in HEK293 cells.

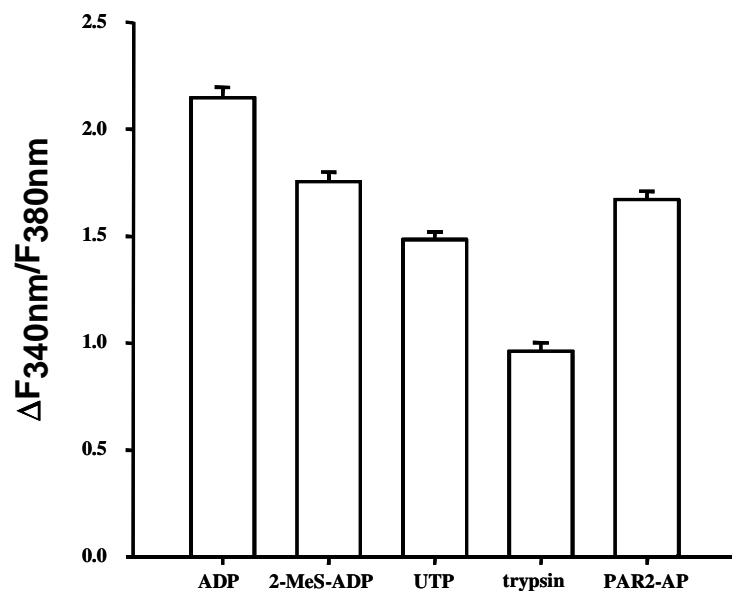


Figure 20: Intracellular calcium rise in HEKP2Y₁₁GFP cells

Peak values of $[Ca^{2+}]_i$ increase in HEKP2Y₁₁GFP cells stimulated with 100 μ M ADP, 10 μ M 2-MeSADP, 100 μ M UTP, 50 nM Trypsin and 100 μ M PAR2-AP. Data represent the mean values \pm s.e.m from 30-90 cells obtained in at least three separate experiments.

Therefore, the specific interaction of the P2Y₁₁ receptor with the P2Y₁ receptor underlies the receptor crosstalk-induced endocytosis of the P2Y₁₁GFP receptor in HEK293 cells.

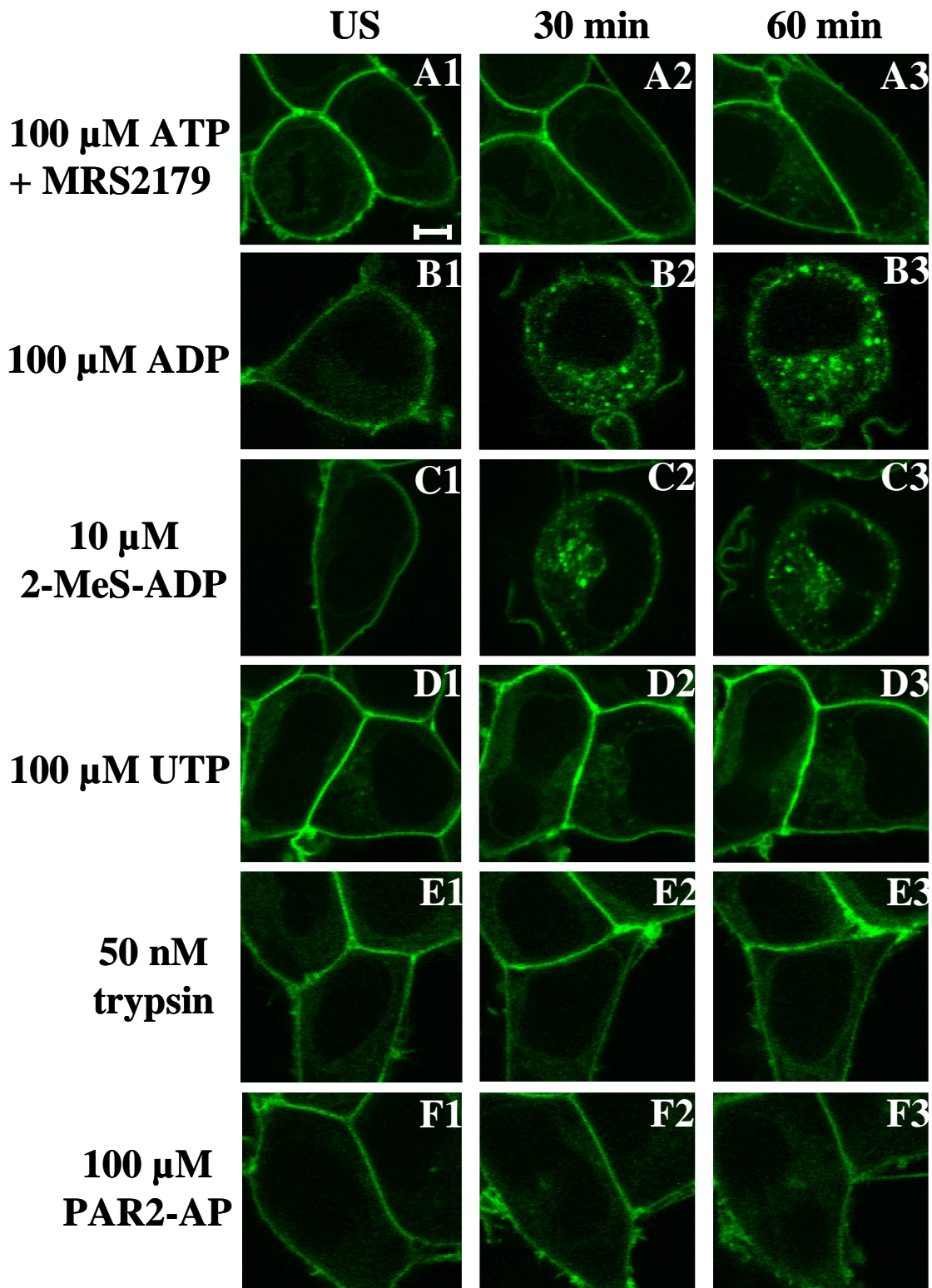


Figure 21: GPCR crosstalk in agonist-induced P2Y₁₁GFP receptor endocytosis

HEK293 cells expressing P2Y₁₁GFP were visualized with a LSM510meta confocal microscope and stimulated with various agonists for up to 60 min at 37°C (5% CO₂) as described in methods. Pictures show unstimulated (US) cells and cells after 30 and 60 min of agonist stimulation. **(A1-3)** Cells preincubated with 100 μ M MRS2179 and stimulated with 100 μ M ATP (n=3). **(B1-3)** Stimulation with 100 μ M ADP (n=5). **(C1-3)** Stimulation with 10 μ M 2-MeS-ADP (n=3). **(D1-3)** Stimulation with 100 μ M UTP (n=4). **(E1-3)** Stimulation with 50 nM trypsin (n=3). **(F1-3)** Stimulation with 100 μ M PAR2-AP (n=3). Scale bar represents 5 μ m. n = number of experiments.

3.3.3 Co-internalization of the P2Y₁ and P2Y₁₁ receptor in 1321N1 cells

Next, we aimed at testing whether the co-internalization of the P2Y₁ and P2Y₁₁ receptor was a general property or a cell type-specific phenomenon of the receptor crosstalk. For this purpose, the P2Y₁ receptor bearing a mycHis tag and the P2Y₁₁GFP receptor were coexpressed in 1321N1 cells. This cell line lacks endogenous functional P2Y receptors, as described in section 3.1.1 and elsewhere (Lazarowski et al., 1995). Thus, stimulation of the cells with nucleotides is affecting only the heterologously expressed P2Y receptors.

Preliminary experiments were made to test the functionality of the endocytosis machinery in the 1321N1 cells. This was addressed by using 1321N1 cells stably expressing the P2Y₁GFP receptor (mentioned in section 3.1). For detection of endocytosis of the GFP tagged receptor, living cells were imaged on a Zeiss inverted LSM 510 META laser scanning confocal microscope before and during agonist stimulation, as described in the methods section. 1321N1-P2Y₁GFP cells were stimulated with 10 μ M 2-MeS-ADP and the receptor trafficking was observed for 60 min. After 30 min of stimulation, a clear beginning of receptor endocytosis was detected (data not shown) that was almost complete at the end of 60 min (Fig. 22, A2). This supports a normal functioning of the GPCR internalization cascade in the 1321N1 cells that resembled previous findings on the endocytosis of the P2Y₁GFP receptor in HEK293 cells (Tulapurkar et al., 2006).

In contrast, 1321N1-P2Y₁₁GFP cells did not show any sign of receptor endocytosis even after 60 min of stimulation with 100 μ M ATP (Fig. 22, B2). This substantiates the conclusion of a lack in agonist-induced receptor internalization of the P2Y₁₁ receptor.

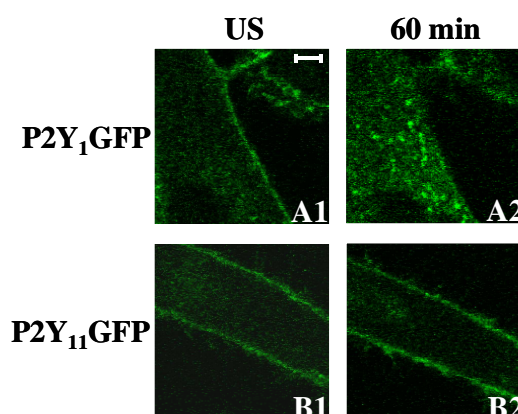


Figure 22: Agonist-induced internalization of the P2Y₁GFP and P2Y₁₁GFP receptor in 1321N1 cells

1321N1 cells were visualized with a LSM510meta confocal microscope and stimulated with various agonists for up to 60 min at 37°C (5% CO₂) as described in methods. Pictures show unstimulated (US) cells and cells after 60 min of agonist stimulation. (A1-2) 1321N1P2Y₁GFP cells stimulated with 10 μ M 2-MeS-ADP. (B1-2) 1321N1P2Y₁₁GFP cells stimulated with 100 μ M ATP.

The next set of experiments was done to analyze whether the P2Y₁₁ receptor internalization could be induced by co-expression of the P2Y₁ receptor. 1321N1 cells were transiently co-transfected with the P2Y₁mycHis and P2Y₁₁GFP receptor. Cells were stimulated with either 100 μ M ATP or 10 μ M 2-MeS-ADP at 48 h post-transfection and fixed after 60 min of stimulation. Fixed cells were stained with anti-myc antibody and visualized on a Zeiss inverted LSM 510 META laser scanning confocal microscope, as described in the methods section.

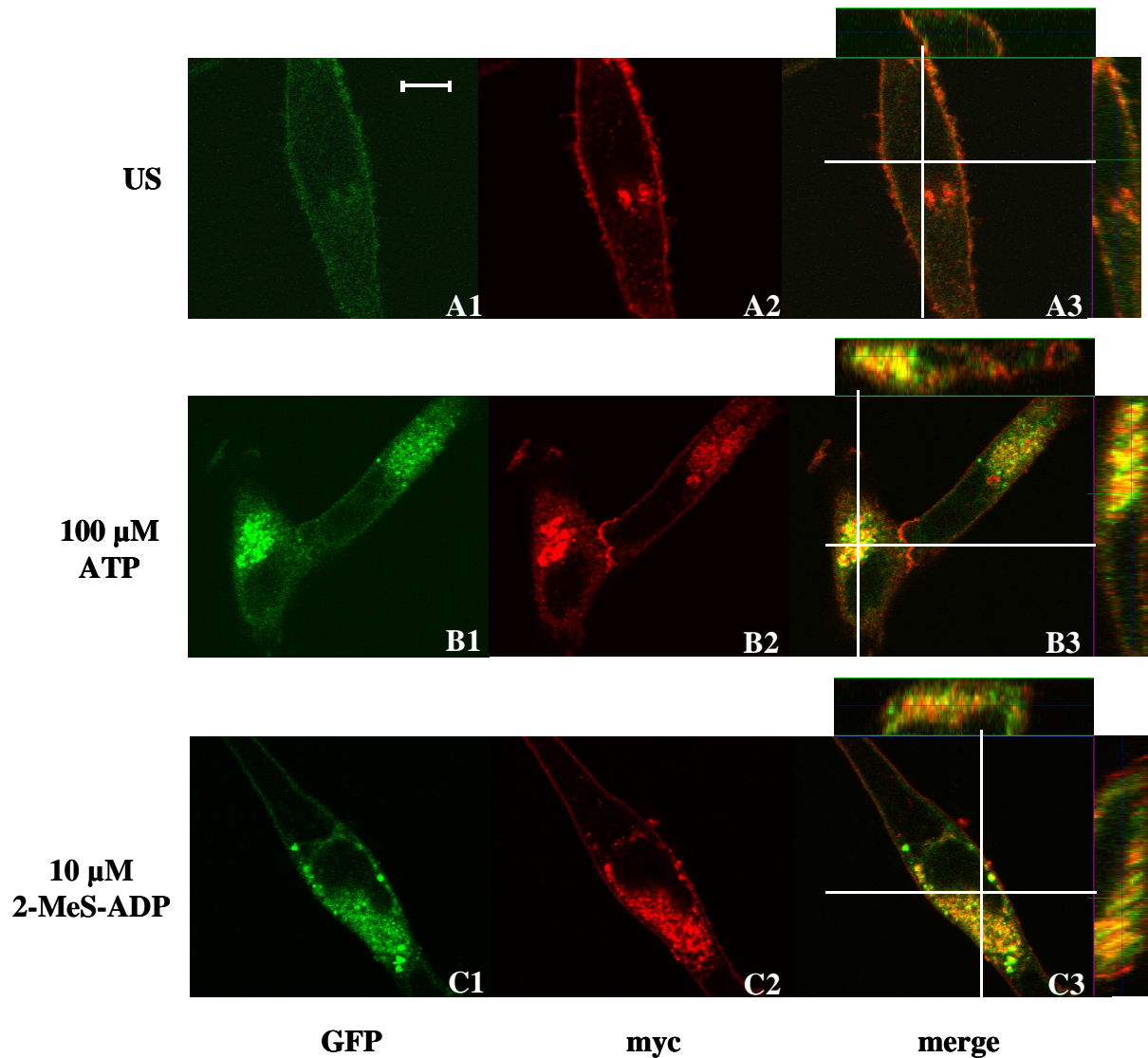


Figure 23: Co-internalization of the P2Y₁mycHis and P2Y₁₁GFP receptor in 1321N1 cells

Transiently co-transfected 1321N1 cells were stimulated with nucleotides for 60 min, fixed with 4% PFA and stained with anti-myc antibody, as described in methods. Images taken on a Zeiss inverted LSM 510 META confocal microscope display the GFP fluorescence (1) and myc-staining (2) separately, as well as a merged picture (3). (A1-3) Unstimulated cells. (B1-3) Stimulation with 100 μ M ATP. (C1-3) Stimulation with 10 μ M 2-MeS-ADP. Scale bar indicates 10 μ m. White lines in the merged picture illustrate the x-z or y-z section-plane displayed in the enlarged view on top and besides the image.

The green fluorescence of the P2Y₁₁GFP receptor (Fig. 23, A1) and the red fluorescence of the Alexa₅₅₅ dye visualizing the myc-staining (Fig. 23 A2) co-localized nicely as shown in the merged image (Fig. 23, A3). Both receptors showed a normal distribution at the plasma membrane. Upon addition of 100 μM ATP for 60 min, endocytosis of the P2Y₁mycHis receptor (Fig. 23, B2) and the P2Y₁₁GFP receptor (Fig. 23, B1) was observed. The receptors co-internalized to intracellular compartments (Fig. 23, B3). The enlarged view in Fig. 23, B3 emphasizes the co-localization of the P2Y₁mycHis and P2Y₁₁GFP receptor in the same intracellular structures. Similar observations were made after stimulation of the co-transfected cells with 10 μM 2-MeS-ADP (Fig. 23, C1-C3). Again the myc-staining of the P2Y₁mycHis receptor and the green fluorescence of the P2Y₁₁GFP receptor co-localized in the same intracellular compartments (Fig. 23, C3). Thus, the results clearly show that the endocytosis-reluctance of the P2Y₁₁ receptor can be overcome upon co-expression and stimulation of the P2Y₁ receptor.

3.3.3.1 Endocytosis-Reluctance of the A₂₆₈P2Y₁₁ receptor mutant stably expressed in HEK293 cells

As 2-MeS-ADP was able to induce the endocytosis of the P2Y₁₁GFP receptor in HEK293 cells (Fig. 21C) and the P2Y₁₁ receptor ligand BzATP was ineffective (Fig. 17A), we examined whether an unresponsive P2Y₁₁ receptor was able to be co-internalized by P2Y₁ receptor activation. The R268A-P2Y₁₁ receptor mutant (A₂₆₈P2Y₁₁) shows a 1000-fold reduced potency for ATP, as we reported recently (Zylberg et al., 2007) and described in section 3.2.4.1. Therefore, we stably expressed the A₂₆₈P2Y₁₁ receptor in HEK293 cells. For detection of receptor endocytosis, the HEK_{A268}P2Y₁₁GFP cells were stimulated on stage with an ATP concentration (100 μM) that was not able to activate the mutant receptor and cells were imaged by confocal microscopy. Live imaging was done for up to 60 min and during the total time period of imaging the GFP tagged A₂₆₈P2Y₁₁ receptor did not show any sign of internalization. The receptor remained at the plasma membrane (Fig. 24). The same was true when cells were stimulated with 2-MeS-ADP (data not shown). A difference in the expression level of the P2Y₁ receptor in HEK_{A268}P2Y₁₁GFP cells, compared to HEK_{P2Y11}GFP cells, was not found in this experiment. The mRNA expression level of the P2Y receptors were comparable in both cell clones (Fig. 19). Therefore, we conclude that a functionally inactive mutant P2Y₁₁ receptor was not able to interact with the P2Y₁ receptor in agonist-induced co-internalization.

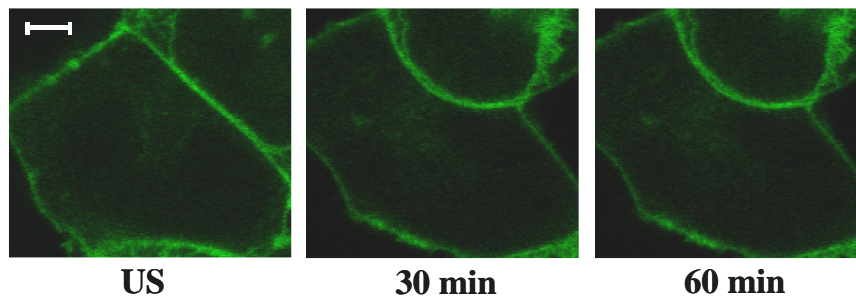


Figure 24: Live-imaging of the $A_{268}P2Y_{11}GFP$ receptor in HEK293 cells

HEK $A_{268}P2Y_{11}GFP$ cells were visualized with a LSM510 meta confocal microscope and stimulated with 100 μ M ATP for up to 60 min at 37°C (5% CO $_2$) as described in methods. Pictures show unstimulated (US) cells and cells after 30 and 60 min of agonist stimulation. Scale bar represents 5 μ m.

3.3.3.2 Knock-down of the endogenous P2Y $_1$ receptor in HEK293 cells with small interfering RNA (siRNA)

The concept that a cross-talk between the P2Y $_1$ and P2Y $_{11}$ receptor is necessary for sufficient endocytosis of the latter receptor was tested by decreasing the expression of the endogenous P2Y $_1$ receptor in HEK293 cells. For this purpose knock-down of the P2Y $_1$ receptor expression was done using siRNA. Oligonucleotides selected against a specific region in the coding sequence of the receptor (section 2.1.11.5 in materials) were applied to HEK $P2Y_{11}GFP$ cells using magnet-assisted transfection (MATra) reagent. This transfection method was already known from our previous experience to achieve nearly quantitative transfection rates. Cells were harvested at 48 h after siRNA transfection. Real-time PCR as well as western blot analysis was done to check for knock-down of the P2Y $_1$ receptor expression, as described in the methods section. Cells treated with the P2Y $_1$ -R siRNA showed approximately 50% knock-down in the mRNA level of the P2Y $_1$ receptor (Fig. 25). The P2Y $_1$ receptor expression remained nearly unaffected when cells were treated with MATra reagent only or with control siRNA (Fig. 25). The decrease in P2Y $_1$ receptor expression after treatment with P2Y $_1$ -R siRNA was also confirmed on the protein level (Fig. 25, inset).

Then HEK $P2Y_{11}GFP$ cells were imaged 48 h post-transfection with siRNA on a LSM510 meta confocal microscope to detect P2Y $_{11}$ receptor internalization after agonist stimulation as described before. Cells not treated with siRNA behaved normally (Fig. 26, A1-3), as they displayed significant internalization of the GFP-tagged P2Y $_{11}$ receptor after 60 min of ATP stimulation (Fig. 26, A3), similar to the already described characteristics in section 3.3.1. The same was true for cells treated only with the transfection reagent (Fig. 26, B2-3) as well as for cells treated with control siRNA (Fig. 26, C2-3). In contrast, treatment with the specific P2Y $_1$ receptor siRNA diminished the agonist-induced endocytosis of the P2Y $_{11}GFP$ receptor (Fig. 26, D2-3).

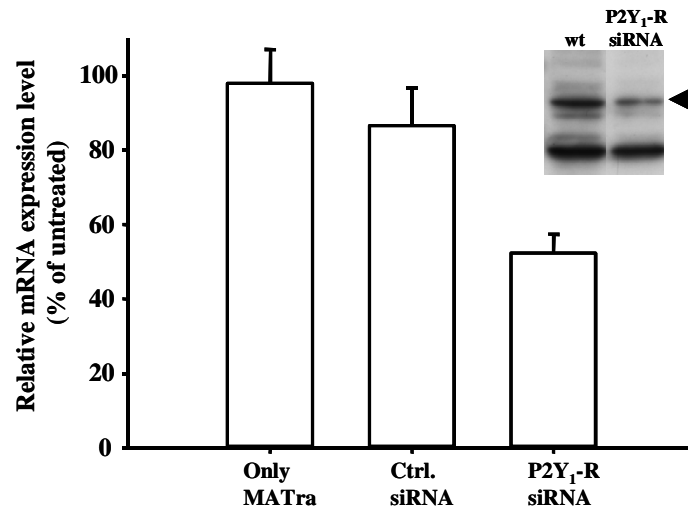


Figure 25: Expression level of P2Y₁ receptor mRNA in HEKP2Y₁₁GFP cells after siRNA treatment

Real time PCR was done using cDNA generated from total RNA of HEKP2Y₁₁GFP cells and specific primers as described in the material and methods section. The expression of the endogenous P2Y₁ receptor was normalized to GAPDH. Bar graphs show expression (%) of the P2Y₁ receptor in cells treated for 48 h with the transfection reagent (MATra) only or siRNA in relation to the P2Y₁ receptor expression in untreated cells. The decrease in protein expression was determined by western blot analysis using a P2Y₁ receptor antibody as shown in the inset.

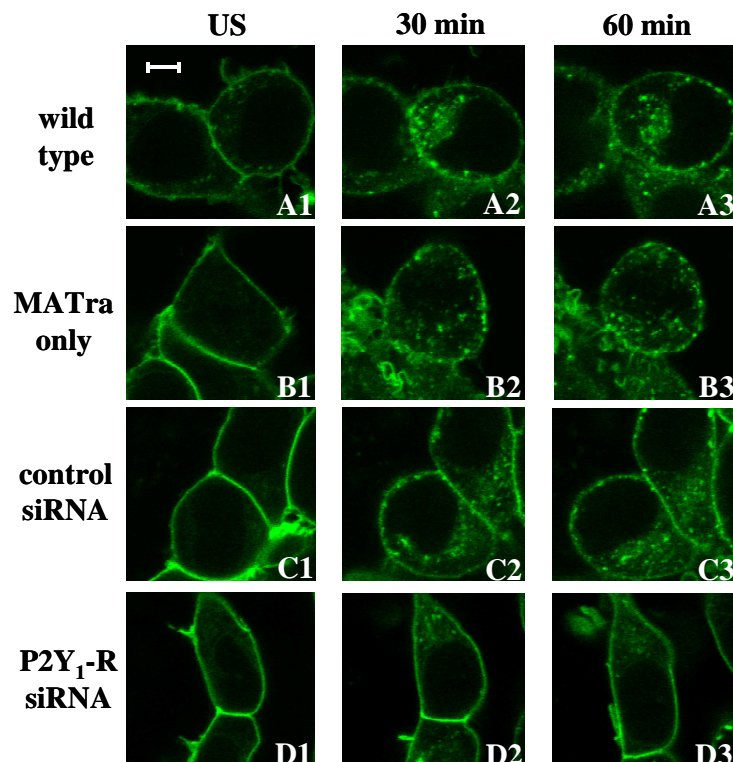


Figure 26: Treatment with P2Y₁-R siRNA reduces internalization of the P2Y₁₁GFP receptor in HEK293 cells

HEKP2Y₁₁GFP cells were monitored on a Zeiss LSM510 meta confocal microscope 48 hours after transfection with siRNA and stimulated with 100 μ M ATP for up to 60 min at 37°C (5% CO₂) as described in methods. Images show unstimulated cells (US), cells after 30 min and 60 min of stimulation. (A1-3) Cells not treated with siRNA or transfection reagent. (B1-3) Cells treated with MATra reagent only. (C1-3) Cells treated with control siRNA. (D1-3) Cells treated with P2Y₁ siRNA. Scale bar represents 5 μ m.

A quantitative analysis of the fluorescence intensities in the cytosol over time is shown in Fig. 27. The increase in fluorescent P2Y₁₁GFP receptor transported to the cytosol was delayed for at least 10 min and then significantly smaller in cells transfected with P2Y₁-R siRNA. The inhibition of the P2Y₁₁ receptor endocytosis amounted to 30 %.

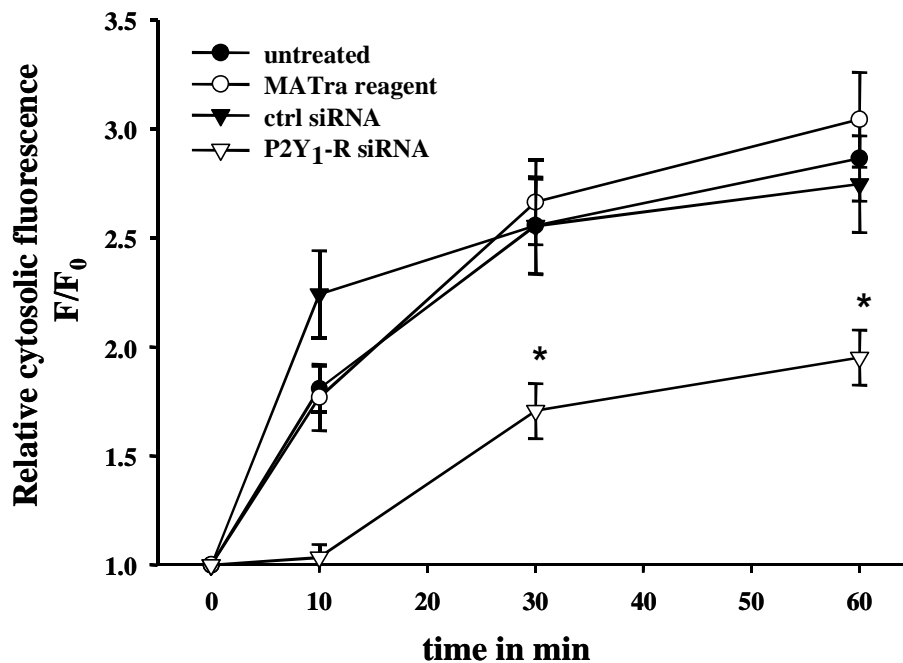


Figure 27: Fluorescence intensities of the P2Y₁₁GFP receptor in cytosol of siRNA transfected HEK293 cells upon agonist stimulation

Images of HEK293 cells transfected with P2Y₁₁GFP and stimulated with 100 μ M ATP for up to 60 min were taken on a Zeiss LSM510 meta confocal microscope 48 h after transfection and fluorescence intensities analyzed using the Zeiss software. Regions of interests were set in the cytosol of n single cells in at least three independent experiments and the average fluorescence intensity determined. Fluorescence intensity values for 10-60 min were normalized to the starting value at 0 min (F_0) which was set to be 1, as described in methods. Curves show the increase in fluorescence intensity in the cytosol of untreated ($n=16$), MATra treated ($n=19$), control siRNA treated ($n=18$) and P2Y₁-R siRNA ($n=21$) treated cells over time. Asterisks indicate significant difference (* $p<0.05$) compared to untreated cells, analyzed using one way ANOVA and the Tukey's test.

3.3.4 Co-Pulldown Experiments

3.3.4.1 Interaction of the heterologously expressed P2Y₁mycHis and P2Y₁₁GST receptors in HEK293 cells

As a next step, we attempted to analyze whether the functional interaction of the P2Y₁ and P2Y₁₁ receptor in internalization was a result of their ability to associate physically. Protein-protein interaction was studied using a co-pulldown approach. The P2Y₁₁ receptor GST fusion-protein and the P2Y₁ receptor bearing a mycHis tag were transiently co-expressed in HEK293 cells. Cells were harvested 48 h post-transfection and total cell lysates were incubated with GSH beads overnight. Samples were resolved by SDS-PAGE and transferred to nitrocellulose membrane, as described in the methods section. Western blot was done using a myc-antibody to check for co-pulldown of the P2Y₁mycHis receptor with the P2Y₁₁GST receptor trapped on the GSH beads.

Western blot analysis of lysates from co-transfected cells revealed smearlike anti-myc reactive bands around 37 kDa and between 75 to 100 kDa (Fig. 28A, lane 1). The molecular mass predicted from amino acid sequence for the P2Y₁ receptor is 42 kDa. The smearlike staining at around 37 kDa probably represents several glycosylated forms of the receptor as reported previously (Yoshioka et al., 2001). The higher molecular mass bands may correspond to oligomerized receptor, as reported before for the A₁-P2Y₁ receptor hetero-oligomer (Yoshioka et al., 2002). Western blot analysis applying a GST-antibody resulted in anti-GST reactive bands of the predicted molecular mass (~65 kDa) for the P2Y₁₁GST receptor (Fig. 28B, lane 1).

Pulldown experiments with lysates of co-expressing cells showed that the P2Y₁mycHis receptor was attached together with the P2Y₁₁GST receptor at the GSH beads (Fig. 28A, lane 5). The interaction of the P2Y₁ and P2Y₁₁ receptor was strong as the myc-staining in the co-pulldown sample was much more intense than in the 10% input (Fig. 28A, compare lanes 5 and 1, respectively). To test for the specificity of the co-pulldown experiment, several control conditions were investigated. The GST pulldown experiment with single transfected HEK293 cells, expressing either the P2Y₁mycHis or the P2Y₁₁GST receptor showed no myc-immunoreaction in the Western blot analysis (data not shown).

The P2Y₁mycHis receptor did not interact with the GST tag as examined using GST preloaded GSH beads and lysate of single P2Y₁ receptor transfected HEK293 cells in a pull-down test. The myc-blot showed no immunoreaction proving that the P2Y₁ receptor could not interact with the GST tag (Fig. 28A, lane 6). This was further confirmed by removing the P2Y₁₁ receptor from the GST fusion protein at the Factor Xa (FXa) cleavage site using this protease. The FXa treatment led to the disappearance of the myc-immunoreaction in the pull-down sample (Fig. 28A, lane 7). The GST-immunoreaction appeared at 27 kDa corresponding to GST only after FXa cleavage (data not shown). When we used mixed lysates from single transfected HEK293 cells (HEKP2Y₁mycHis or HEKP2Y₁₁GST), the pull-down fraction did not show any myc-immunoreaction (Fig. 28A, lane 4). This excludes the formation of aggregates during the pull-down procedure as a possible cause of the positive co-pull-down result.

The specificity of the P2Y₁ and P2Y₁₁ receptor interaction was examined in further experiments. For this, the P2Y₁₁GST receptor was co-transfected with a non-related GPCR, the PAR2 receptor (bearing a HA tag). The PAR2-HA protein showed a smear band (~37-70 kDa) (Fig. 28C, lane 2) which is consistent with our previous results (Luo et al., 2006). The co-pull-down experiment revealed no HA-immunoreactivity, thereby excluding a physical interaction of both receptors (Fig. 28C, lane 8). However, co-transfection of the P2Y₁₁GST receptor with the P2Y₄-HA receptor resulted in a physical interaction of both receptors (Fig. 28C, lane 9), indicating a possible P2Y receptor pooling in HEK293 cells.

Furthermore, we analyzed the probability that the transiently overexpressed receptors were present in small membrane patches of HEK293 cells without direct physical interaction. Therefore, the total lysate of P2Y₁mycHis and P2Y₁₁GST co-transfected cells were extracted for 2 h at 4°C in RIPA buffer and then centrifuged at 50.000 x g for 30 min to remove undissolved membrane patches. These extracts were then used to perform a co-pull-down experiment. After that procedure, the P2Y₁mycHis receptor could still be found together with the P2Y₁₁GST receptor at the GSH beads when we performed a pull-down experiment with these extracts (Fig. 29A, lane 4). These data again support the direct physical interaction of the receptors.

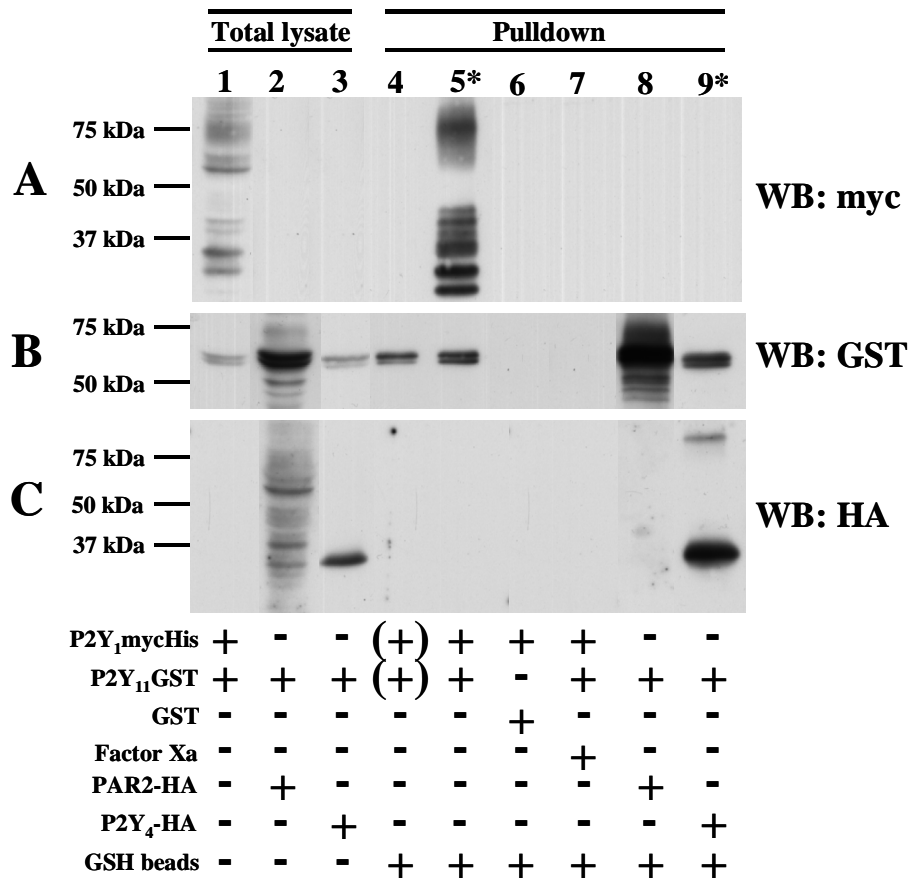


Figure 28: Co-pull-down of the P2Y₁mycHis and P2Y₁₁GST receptor from HEK 293 cells

For pull-down (PD) experiments, total lysates of transfected HEK293 cells expressing the indicated receptors were incubated overnight with GSH beads at 4°C, as described in methods. Samples were resolved by SDS-PAGE and transferred to nitrocellulose. Western blot (WB) analysis was performed using anti-myc (A), anti-GST (B) or anti-HA (C) antibodies. **Lane 1-3:** Input signals from total lysates (10% of PD samples) of P2Y₁mycHis/P2Y₁₁GST (lane 1), PAR2HA/P2Y₁₁GST (lane 2) and P2Y₄HA/P2Y₁₁GST (lane 3) co-expressing HEK293 cells. **Lane 4:** Mixture of lysates from P2Y₁mycHis and P2Y₁₁GST single transfected cells and subsequent incubation with GSH beads. **Lane 5:** Co-pull-down of the P2Y₁mycHis and P2Y₁₁GST receptor from lysates of co-transfected cells. **Lane 6:** Lysate of P2Y₁mycHis single transfected cells incubated with GST preloaded GSH beads. **Lane 7:** P2Y₁mycHis/P2Y₁₁GST receptor co-pull-down beads after incubation with FXa. **Lane 8:** Lysates of PAR2-HA/P2Y₁₁GST co-transfected cells incubated with GSH beads. **Lane 9:** Co-pull-down of the P2Y₄-HA and P2Y₁₁GST receptor from lysates of co-transfected cells. The molecular mass markers are shown in kDa (approximate molecular mass: smearlike staining around 37 and 75 kDa; P2Y₁₁GST ~ 65 kDa; PAR2-HA ~ smearlike bands from 37-70 kDa; P2Y₄-HA ~ 40 kDa). Western blots shown are representative for at least two independent experiments. * indicates positive pull-down signal.

3.3.4.2 Physical interaction of the A₂₆₈P2Y₁₁ receptor mutant with the P2Y₁ receptor in HEK293 cells

The endocytosis-resistant A₂₆₈P2Y₁₁ receptor mutant (section 3.3.3.1) was tested for physical interaction with the P2Y₁ receptor to check if the resistance to internalize was a result of loss in protein-protein interaction. For this, the A₂₆₈P2Y₁₁ receptor was transiently expressed as a GST fusion protein together with the P2Y₁mycHis receptor in HEK293 cells and co-pull-down experiments were done as described above.

Western blot analysis showed that the P2Y₁₁ receptor mutant was still able to physically interact with the P2Y₁ receptor (Fig. 29A, lane 3) similar to the unmutated receptor (Fig. 29A, lane 4). The interaction was still detectable after extracting the receptors from cell membranes (centrifugation at 50.000 x g, 30 min, section 3.3.4.1). Thus, the endocytosis-reluctance of the _{A268}P2Y₁₁ receptor mutant in HEK293 cells is not due its inability to physically interact with the P2Y₁ receptor.

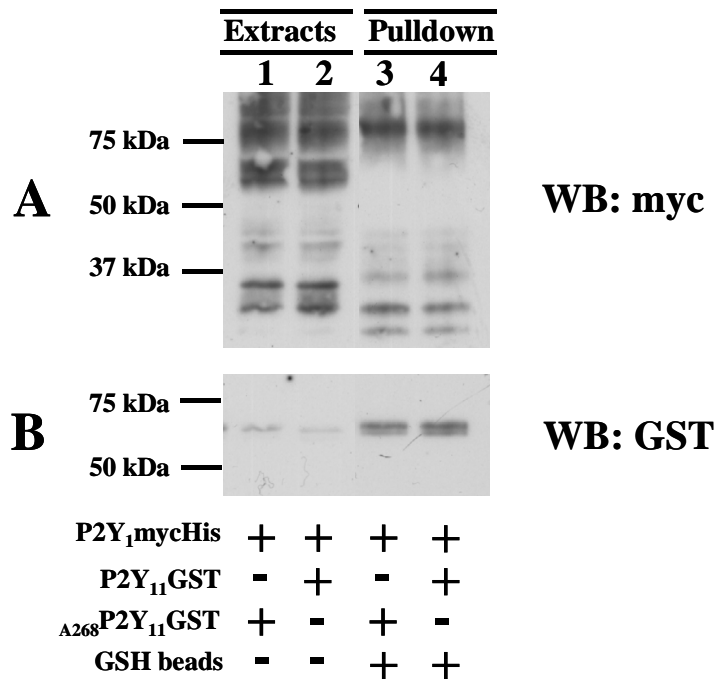


Figure 29: Co-Pulldown of the P2Y₁mycHis and _{A268}P2Y₁₁ receptor from HEK 293 cells

Cell extracts of differently transfected HEK293 cells were obtained by centrifugation at 50.000 x g for 30 min. For pulldown (PD), extracts were incubated overnight with GSH beads at 4°C, as described in methods. Samples were resolved by SDS-PAGE and transferred to nitrocellulose. Western blot (WB) analysis was performed using anti-myc (A) or anti-GST (B) antibodies. **Lane 1-2:** Input signals from extracts (10% of PD samples) of P2Y₁mycHis/_{A268}P2Y₁₁GST (lane 1) and P2Y₁mycHis/P2Y₁₁GST (lane 2) co-expressing cells. **Lane 3-4:** Co-pulldown of the P2Y₁mycHis receptor with the _{A268}P2Y₁₁GST receptor (lane 3) or the wild type P2Y₁₁GST receptor (lane 4) from lysates of co-transfected cells. The molecular mass markers are shown in kDa. Approximate molecular mass: P2Y₁mycHis ~ smearlike staining around 37 and 75 kDa; P2Y₁₁GST ~ 65 kDa. Western blots shown are representative of at least two independent experiments.

3.3.5 Co-immunoprecipitation of P2Y₁mycHis and P2Y₁₁GST receptors

Co-immunoprecipitation of the P2Y₁₁GST receptor by an anti-myc antibody from P2Y₁mycHis receptor co-transfected cells, further proved the stability of the interaction between both receptors. The P2Y₁mycHis receptor was immunoprecipitated from total lysates of HEK293 cells transiently (48 h) expressing both receptors using a myc-antibody. Samples were resolved by SDS-PAGE and transferred to nitrocellulose membrane, as described in the methods section.

The P2Y₁₁GST receptor clearly co-immunoprecipitated together with the myc-tagged P2Y₁ receptor, as detected by Western blot analysis using a GST-antibody (Fig. 30A, lane 3). The signal was specific as lysates precipitated with an unspecific IgG showed no anti-GST reactive bands (Fig. 30A, lane 4). Moreover, when lysates of HEK293 cells single transfected with either the P2Y₁mycHis or P2Y₁₁GST receptor were mixed, immunoprecipitation of the P2Y₁mycHis receptor did not result in co-precipitation of the P2Y₁₁GST receptor (Fig. 30A, lane 2). Thus, the protein-protein interaction of the P2Y₁ and P2Y₁₁ receptor could also be confirmed using an immunoprecipitation approach.

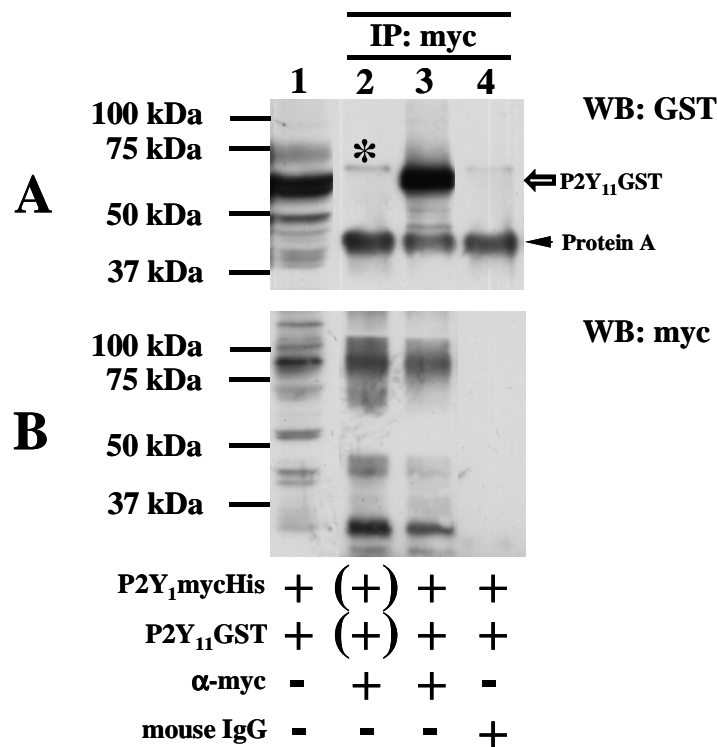


Figure 30: Co-Immunoprecipitation (IP) of the P2Y₁mycHis and P2Y₁₁GST receptors from HEK293 cells

Total lysates of differently transfected HEK293 cells were incubated first overnight with anti-myc antibody and then with Agarose Plus A/G beads at 4°C as described in methods. Samples were resolved by SDS-PAGE and transferred to nitrocellulose. Western blot (WB) analysis was performed using anti-GST (A) or anti-myc (B) antibodies. **Lane 1:** Input signal from total lysate (10% of IP samples) of P2Y₁mycHis /P2Y₁₁GST co-expressing cells. **Lane 2:** Mixture of lysates from P2Y₁mycHis and P2Y₁₁GST single transfected cells immunoprecipitated with anti-myc antibody. **Lane 3:** Co-IP of P2Y₁mycHis and P2Y₁₁GST receptor from lysates of co-transfected cells using anti-myc antibody (arrow points to P2Y₁₁GST protein). **Lane 4:** Precipitation of lysates from P2Y₁mycHis/P2Y₁₁GST cells using unspecific mouse IgG (negative control). The molecular mass markers are shown in kDa. Approximate molecular mass: P2Y₁mycHis ~ smearlike staining around 37 and 75 kDa; P2Y₁₁GST ~ 65 kDa. Here and in Fig. 3, Western blots shown are representative of at least two independent experiments testing the various conditions. The arrowhead indicates a signal corresponding to Protein A. * the indicated band represents non-reduced IgG due to unboiled samples.

3.3.6 Pharmacological characteristics of the receptor hetero-oligomer

3.3.6.1 Intracellular calcium rise

The hetero-oligomerization of the P2Y₁₁GFP receptor with the endogenous P2Y₁ receptor seems to modify the activity of known agonists and antagonists at the P2Y₁₁ receptor, as observed in the endocytosis experiments (section 3.3.1 and 3.3.2). BzATP was ineffective in inducing receptor-endocytosis and NF157 could not inhibit ATP-induced internalization of the P2Y₁₁GFP receptor. Therefore, we also investigated the pharmacology of intracellular calcium rise induced by P2Y₁₁GFP receptor activation in HEK293 cells. As described in methods, cells were subjected to single-cell calcium measurement applying the calcium indicator fura-2. Results are summarized in Fig. 31 and 32.

P2Y₁₁GFP receptor-expressing HEK293 cells responded to the potent P2Y₁₁ receptor agonist BzATP, but the recently developed P2Y₁₁ receptor antagonist NF157 was not able to inhibit this response (Fig. 31A). However, when HEK293 cells were preincubated with the specific P2Y₁ receptor antagonist MRS2179 (100 μM) no response to BzATP (100 μM) could be detected (Fig. 31A).

This antagonist sensitivity was different at the single P2Y₁₁GFP receptor expressed in 1321N1 cells, where MRS2179 showed no effect on the activity of BzATP, but preincubation with NF157 totally abolished the activity of BzATP at the P2Y₁₁ receptor (Fig. 31A). Thus, the interaction of the P2Y₁₁GFP receptor with the endogenous P2Y₁ receptor in HEK293 cells seems to influence the pharmacology of the receptor.

As the A₂₆₈P2Y₁₁GFP receptor did not functionally interact with the endogenous P2Y₁ receptor in HEK293 cells with regard to internalization, we examined the influence of this mutant P2Y₁₁ receptor on the pharmacological interaction with the P2Y₁ receptor. Therefore, the intracellular calcium rise in HEK_{A268}P2Y₁₁GFP cells was measured. The cells responded to 100 μM ATP (Fig. 31B) in the same way as mock-transfected cells confirming the inability of 100 μM ATP to stimulate the P2Y₁₁ receptor mutant. However, the more potent P2Y₁₁ receptor agonist BzATP elicited a significant response at a concentration of 100 μM at the R268A mutant (Fig. 31A) which was not seen in the mock-transfected cells (Fig. 31A). Nevertheless, the amplitude of the response to 100 μM BzATP of the HEK_{A268}P2Y₁₁GFP cells was clearly smaller (25%) than the [Ca²⁺]_i increase in HEK293 cells (Fig. 31A).

Pretreatment of the HEK_{A268}P2Y₁₁GFP cells with MRS2179 did not affect the action of BzATP at the P2Y₁₁ receptor (Fig. 31A) in contrast to the observations made at the unmutated receptor (Fig. 31A). Thus, the R268A mutation of the P2Y₁₁ receptor seems to disrupt the interaction with the P2Y₁ receptor concerning the P2Y₁ receptor mediated internalization of the P2Y₁₁ receptor (section 3.3.3.1) and the ligand selectivities in inducing $[Ca^{2+}]_i$ rise.

Moreover, real-time PCR showed that the differently transfected HEK293 cells display a comparable expression profile of P2Y receptor mRNAs, as depicted in the above figure at page 70 (Fig. 19). HEK_{A268}P2Y₁₁GFP, mock-transfected, as well as HEKP2Y₁₁GFP cells all showed similar levels of P2Y₁ receptor mRNA. The P2Y₁₁ receptor expression was significantly increased in the accordingly transfected HEK293 cells compared to mock-transfected cells. The P2Y₂ receptor expression was very weak and only clearly detectable in HEKP2Y₁₁GFP cells. The P2Y₆ receptor was not expressed in any of these cell clones. Thus, different P2Y receptor expression profiles apparently are not the reason for the diversity in the ligand selectivities at the unmutated and R268A mutated P2Y₁₁ receptor in HEK293 cells.

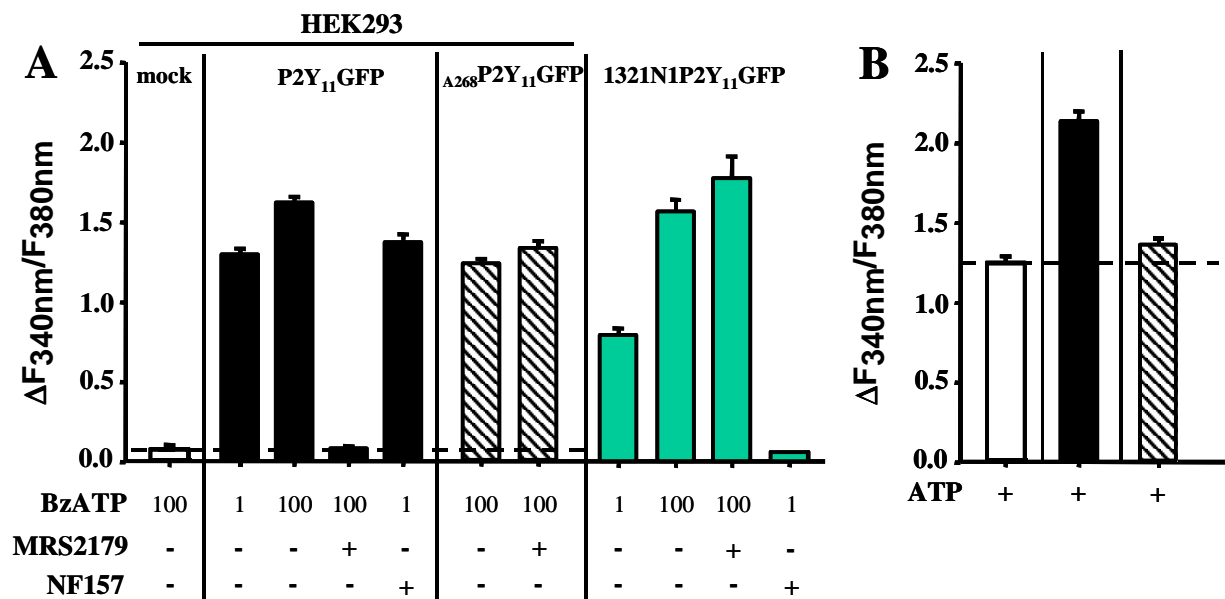


Figure 31: Peak values of intracellular calcium rise induced by P2Y receptor stimulation

(A) Bar graphs display the $[Ca^{2+}]_i$ rise in HEK293 cells transfected with GFP only (mock) (blank bar), P2Y₁₁GFP (black bars), A₂₆₈P2Y₁₁GFP (striped bars) and the calcium rise in 1321N1P2Y₁₁GFP cells (green bars). Cells were stimulated with BzATP at the indicated concentrations (μ M). Preincubation with 100 μ M MRS2179 or 1 μ M NF157 is also indicated. $[Ca^{2+}]_i$ rise was detected using fura-2 as described in methods. (B) Bar graphs display the $[Ca^{2+}]_i$ rise in response to 100 μ M ATP of HEK293 cells transfected with GFP only (blank bar), P2Y₁₁GFP (black bar), A₂₆₈P2Y₁₁GFP (striped bar). Data represent the mean \pm s.e.m obtained in at least three independent experiments analyzing 20-100 cells. The dashed lines in (A) and (B) give the comparison of the responses to that of mock transfected HEK293 cells.

Furthermore, a significant increase in intracellular calcium upon stimulation of the cells with 100 μ M UDP was observed (Fig. 32). UDP is known to activate the P2Y₆ receptor (Nicholas et al., 1996) but this receptor was not expressed in our HEK293 cells. Interestingly, only the green fluorescent, i.e. positively P2Y₁₁GFP transfected, cells responded. After preincubation with MRS2179, the response was dramatically reduced (Fig. 32). The P2Y₁₁ receptor antagonist NF157 was able to inhibit 46 % of the calcium response to 100 μ M UDP. When HEK_{A268}P2Y₁₁GFP cells were challenged with UDP, the intracellular calcium concentration was only slightly increased (Fig. 32), which was comparable to the value in HEK293P2Y₁₁GFP cells after incubation with MRS2179. Mock-transfected HEK293 cells (Fig. 32) and 1321N1P2Y₁₁GFP cells (data not shown) showed no significant calcium response to UDP.

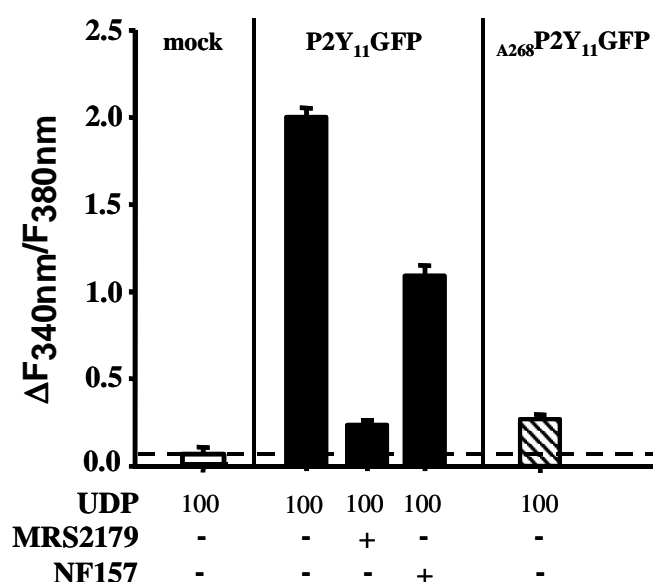


Figure 32: Peak values of intracellular calcium rise induced by UDP in HEK293 cells

Bar graphs display the $[Ca^{2+}]_i$ rise in HEK293 cells transfected with GFP only (blank bars), P2Y₁₁GFP (black bars), A₂₆₈P2Y₁₁GFP (striped bars). Cells were stimulated with 100 μ M UDP. Preincubation with 100 μ M MRS2179 or 10 μ M NF157 is indicated. $[Ca^{2+}]_i$ rise was detected using fura-2 as described in methods. Data represent the mean \pm s.e.m obtained in at least three independent experiments analyzing 40-100 cells.

3.3.6.2 Determination of cAMP accumulation

The P2Y₁₁ receptor not only couples to the G_q protein, but also to the G_s protein, thereby inducing the activation of adenylyl cyclase and subsequent cAMP production in the cells. Therefore, it was interesting to know whether the interaction of the P2Y₁₁ receptor with the P2Y₁ receptor also influences the receptor pharmacology with respect to cAMP accumulation. HEK293P2Y₁₁GFP cells were stimulated with various agonists and/or antagonists, the reaction was stopped by addition of 0.1 M HCl and the cAMP content was measured after cell lysis, as explained in the methods section.

Stimulation of the cells with 100 μM BzATP led to a substantial increase in the cAMP concentration that was about 17-fold as compared to that of unstimulated cells (Fig. 33). Preincubation with 100 μM MRS2179 did not affect the response to BzATP. In contrast, cells preincubated with 10 μM NF157 showed a significantly reduced (by 40 %) response to BzATP. No cAMP accumulation was induced when cells were treated with 100 μM UDP or 10 μM 2-MeSADP. Thus, the pharmacology of adenylyl cyclase activation found in HEKP2Y₁₁GFP cells represents the profile known for the P2Y₁₁ receptor ligands.

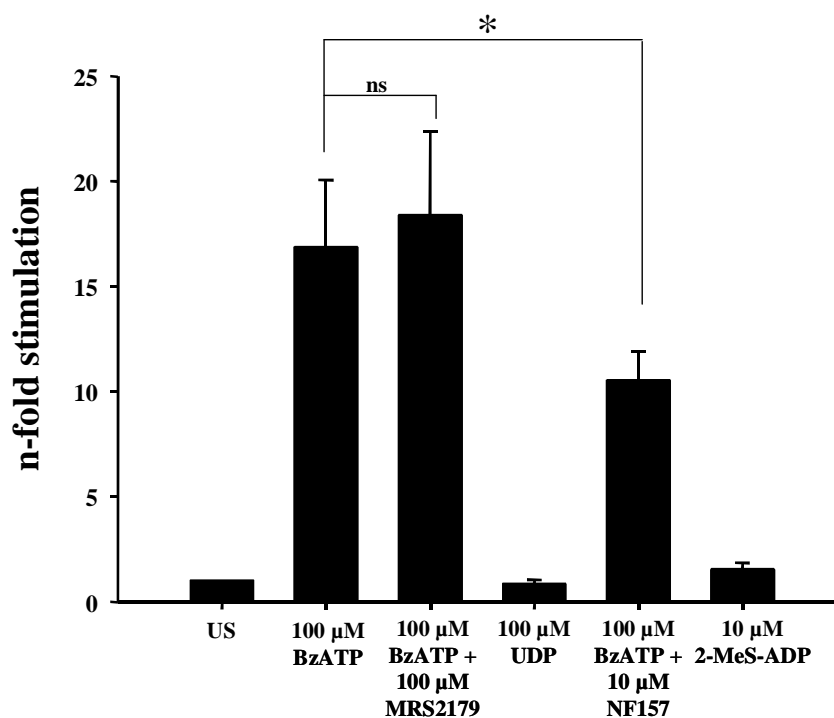


Figure 33: Stimulation of cAMP accumulation in HEKP2Y₁₁GFP cells

Cells preincubated with IBMX (500 μM) and antagonists (as indicated) were stimulated with various nucleotides. The cAMP content was measured using an Enzyme-Linked-Immunoassay (EIA) as described in methods. Bar graphs represent the average stimulation (normalized to unstimulated cells) and s.e.m from at least three independent experiments. Asterisks indicate significance (* $p < 0.05$) and 'ns' indicates non significant differences analyzed using one-side ANOVA and the Tukey's test.

4 DISCUSSION

The purinergic P2Y receptors are a family of GPCRs that respond to a variety of nucleotides. Thereby body tissues can react to extracellular nucleotides. Among the P2Y receptors, the P2Y₁ and P2Y₁₁ receptor are closely related (Costanzi et al., 2004). Agonists acting at the P2Y₁₁ receptor are also capable of activating the P2Y₁ receptor. Therefore, mechanisms are required to regulate activation of one or the other receptor in tissues or cells where both are expressed. One mechanism can be the desensitization of the receptor responses. Interestingly, the P2Y₁ receptor can be rapidly desensitized (Bourdon et al., 2006), whereas the P2Y₁₁ receptor can not (Communi et al., 1999). A regulated activation of the P2Y₁ or the P2Y₁₁ receptor can also be realized by appropriate pharmacological tools. The design and synthesis of these pharmacological tools relies on sufficient experimental evaluation of the agonist and antagonist selectivities of the receptors.

The present study focussed on the detailed characterization of the less studied P2Y₁₁ receptor in terms of pharmacology, ligand recognition, desensitization and P2Y receptor crosstalk. The results are discussed in the same order.

4.1 Diastereoselective activation is opposite for the P2Y₁ receptor and the P2Y₁₁ receptor

The potency of different novel diastereomeric analogues of ATP at the P2Y₁₁ receptor was investigated. Through substitution of one of the non-bridging oxygen atoms of P_α by borane or sulfur a new chiral centre in the ATP molecule was introduced. The resulting diastereoisomers were separated and the absolute configuration around the P_α was assigned (Major et al., 2004). The R_p configuration was attributed to the (A) isomers of the borano-modified and the (B) isomers of the thio-substituted analogues. This difference in assignment is due to the group priorities around P_α, which are opposite for the borane derivatives (ATP-α-B) and sulfur derivatives (ATP-α-S). Sulfur is of higher priority in the chemical nomenclature compared to oxygen, and borane is of lower priority than oxygen. The increase in intracellular [Ca²⁺]_i in 1321N1 astrocytoma cells stably expressing a P2Y₁₁ receptor GFP fusion protein was determined upon stimulation with these analogues. The successful expression of the P2Y₁₁GFP receptor in 1321N1 cells was confirmed by western blot analysis. Moreover, the 1321N1-P2Y₁₁GFP cells showed the typical pharmacology profile of agonists that had already been described for this receptor. The novel diastereoisomeric compounds tested, activated the P2Y₁₁ receptor with EC₅₀ values in the low micromolar range.

☞ **Introduction of a borane or sulfur group at P α of ATP results in potent P2Y₁₁ receptor agonists**

The diastereoisomers showed striking differences in the potencies at the P2Y₁₁ receptor as compared to their parent compounds ATP, 2-MeS-ATP, and 2-Cl-ATP. Specifically, the introduction of a borane/sulfur group resulted in more potent ligands at the P2Y₁₁ receptor. The effect of the borane substitution on the potency of the ATP derivatives for the P2Y₁₁ receptor is in contrast to the findings at the P2Y₁ receptor. At the P2Y₁ receptor the introduction of borane into ATP or 2-MeS-ATP did not create more potent ligands (Nahum et al., 2002), while the introduction of sulfur at P α of ATP led to an increase in potency at the P2Y₁ receptor (Major et al., 2004). However, the 2-MeS-ATP- α -S analogues were as potent as 2-MeS-ATP itself. This demonstrates that the introduction of sulfur at P α leads to an increased potency of ATP at the P2Y₁ receptor but is not able to further increase the potency of 2-methylthioether derivatives, which are already very potent agonists at this receptor. This underlines that the 2-methylthio substitution plays a pivotal role in the potency of the ATP derivatives at the P2Y₁ receptor (Schachter et al., 1996; Palmer et al., 1998).

In contrast, at the P2Y₁₁ receptor both sulfur- and borano-substitution increased the potency of ATP as well as 2-MeS-ATP and 2-Cl-ATP. Moreover, the shift in potency was more distinct for the (B) isomers of 2-MeS-ATP- α -B/S derivatives, compared to the parent compound than for the (B) isomers of the 2-unsubstituted ATP- α -B/S analogues compared to ATP. This shows that the introduction of a borane/sulfur group at P α determines the potency of the derivative at the P2Y₁₁ receptor, overriding the negative influence of a substituent at position 2 of the ATP molecule.

☞ **The P2Y₁ and P2Y₁₁ receptors prefer different diastereoisomers**

Interestingly, at the P2Y₁₁ receptor, for all P α substituted derivatives the corresponding (B) diastereoisomers were found to be more potent than the (A) isomers. This stereoselective action of the ligands is opposite at the P2Y₁ receptor. The latter prefers the (A) isomers (Nahum et al., 2002; Major et al., 2004). In contrast, the P2Y₂ and P2Y₄ receptor display the same stereoselectivity as P2Y₁₁ receptor regarding the activity of α -thio diastereoisomers. At both P2Y₂ and P2Y₄ receptors the Rp-UTP- α -S isomer was more potent than the Sp isomer but their potency was weak compared to that of UTP (Jacobson et al., 2006). All the receptors mentioned above belong to one phylogenetic subgroup (Costanzi et al., 2004).

Surprisingly, the amino acid sequence of the P2Y₁₁ receptor protein is more closely related to the P2Y₁ receptor, although besides the P2Y₂ receptor the human P2Y₁₁ receptor is an “ATP-receptor”. Still, the pharmacological profiles of both ATP-preferring receptors differ much more than the profiles of the P2Y₁₁ and P2Y₁ receptor (Burnstock and Knight, 2004). Both receptors are activated by adenine nucleotides exclusively and are blocked by Reactive Blue, whereas the P2Y₂ receptor can also be activated by uridine nucleotides and shows an affinity for PPADS which is not shared by the P2Y₁ and P2Y₁₁ receptors (Burnstock and Knight, 2004).

Another P2Y receptor at which the action of α -thio diastereoisomers had been investigated is the P2Y₁₂ receptor. The ATP- α -S isomers were found to be antagonists at the P2Y₁₂ receptor with only a slightly higher affinity for the (A) isomer (Cusack and Hourani, 1982). Since the determination of the antagonistic action of the ATP- α -S isomers at the P2Y₁₂ receptor was done by measurement of adenylyl cyclase activity in platelets it is rather difficult to compare these results with our investigations (Cusack and Hourani, 1982).

Furthermore, the P2Y₁₁ receptor displays the same diastereoselectivity for borano-/thiophosphate nucleotide analogues like the catalytic site of ecto-nucleotidase NTPDase 1 (CD39, EC 3.6.1.5) (Cusack et al., 1983; Nahum et al., 2002). The ATP- α -B (B) isomers were found to be about ten times less stable in an assay to test the enzymatic stability regarding NTPDase 1 than the corresponding (A) isomers, but they showed a hydrolysis rate that was still two times slower than that of ATP itself. The 1321N1 cells possess an ecto-nucleotidase activity characteristic for NTPDase 1, with a high micromolar range K_m value of 66 μ M \pm 13 for ATP hydrolysis (Lazarowski et al., 1997). If this is taken into consideration, the potencies found for all (B) isomers tested in this study might be influenced by a competitive binding of the substances to the receptor and the ecto-nucleotidase. However, if the experimental design of the measurements in this study is considered, where we have a continuous flow application of the agonists, and the much higher affinity of the P2Y₁₁ receptor for ATP as compared to the NTPDase 1, competition in binding does certainly not affect our analysis.

An interesting observation made here is that the ATP- α -B/-S analogues appear to be more potent at the P2Y₁ receptor than at the P2Y₁₁ receptor. As both receptors, the P2Y₁ and P2Y₁₁ receptor, were expressed in different cell systems, it is difficult to make an absolute comparison of the EC₅₀ values. Therefore, the P2Y₁-GFP receptor was also stably expressed in 1321N1 cells. In these cells, a comparable rank order of potency for the 2-Cl-ATP- α -B and ATP- α -S analogues was found as in HEK293 cells. The tendency that the ligands are overall more potent at the P2Y₁ receptor than at the P2Y₁₁ receptor was also observed. This underlines the conclusion that our data definitely show the stereoselectivity and receptor subtype selectivity of the compounds tested.

☞ **Borano-substituted ATP derivatives are suitable to distinguish the functional contribution of the two ATP-activated P2Y receptors**

The (A) isomer of the 2-MeS-ATP- α -B derivatives is the most selective of all the analogues tested here, being more active at the P2Y₁ receptor. This substantial receptor-subtype selectivity is due to the combination of modifications on both C2 and the phosphate chain of the ATP scaffold. In addition, our previous report showed the lack of any activity of the 2-MeS-ATP- α -B diastereoisomers at the P2Y₂ receptor (Tulapurkar et al., 2004). This suggests the possibility of a selective activation of the P2Y₁ receptor by the (A) isomer of these compounds in cells/organs, which also express P2Y₁₁ and P2Y₂ receptor. Moreover, the ATP- α -B derivatives that had no activity at the P2Y₂ receptor are compounds suitable to distinguish the functional contribution of the two ATP-activated P2Y receptors, the P2Y₂ and P2Y₁₁ receptor, in physiological or pathophysiological responses of cells to ATP.

4.2 Ligand binding site characteristics of the P2Y₁₁ receptor deduced from mutational analysis

The amino acid residues [Arg 106 (TM3), Phe109 (TM3), Glu186 (EL2), Arg268 (TM6) and Arg307 (TM7)] putatively involved in ligand recognition at the P2Y₁₁ receptor were mutated to test our binding mode hypothesis. 1321N1 cells were used to stably express the wild type and the mutant receptors, respectively, both as GFP fusion proteins. The expression level of the receptors was analyzed by flow cytometry. Wild type and mutant receptors displayed comparable fluorescence intensities.

The subcellular localization of the mutant receptors was found to be comparable to that of the unmutated receptor for the Glu186Ala, Arg268Ala, Arg268Gln, Ala313Asn mutant receptors. Although the Phe109Ile mutant receptor was only partially located at the plasma membrane, it still exhibited a significant potency for ATP. Similar observations were made in a different mutagenesis approach, where a 90% reduction in surface expression levels of the wild type P2Y₁ receptor had no significant influence on the EC₅₀ values of the investigated agonist (Hoffmann et al., 1999). Therefore, the potency of ATP found at the Phe109Ile mutant as well as the potency at the mutants with a similar subcellular localization (Arg106Ala, Tyr261Ala, and Arg307Ala) likely reflects the intrinsic activity of these constructs. Functional activity of the mutated receptors was determined in stably transfected cells by monitoring the intracellular [Ca²⁺]_i rise induced by agonist stimulation.

☞ **Three arginine residues in TM3, 6 and 7 are involved in the recognition of ATP**

The arginine residues in TM3 (Arg106, 3.29) and TM7 (Arg307, 7.39) were found to be most critical for P2Y₁₁ receptor activation. The arginine at position 7.39 is believed to take part in an H-bond through its backbone carbonyl with the N⁶ of the ATP molecule. Besides this interaction, Arg7.39 is also thought to stabilize the bound ATP through electrostatic interaction with ATP-P α and P γ of the phosphate moiety together with the Arg3.29. These hypothesis were confirmed by detecting a loss-of-function after mutation of these arginine residues in the P2Y₁₁ receptor. The corresponding residues in the human P2Y₁ receptor (Arg128, Arg310) are similarly essential for ligand recognition. Their mutation resulted in functionally inactive receptors (Jiang et al., 1997). A model of the human P2Y₆ receptor showed the involvement of these conserved arginine residues in binding of the phosphate moiety of the nucleotide to the receptor (Costanzi et al., 2005). Surprisingly, at the human P2Y₂ receptor only the mutation of the corresponding arginine in TM7 (Arg292, 7.39) resulted in loss of function of the receptor, but mutation of the arginine in TM3 (Arg110, 3.29) to leucine had little effect on the potency of the agonists (Erb et al., 1995). The arginine in TM7 is part of a conserved motif (Q/KxxR) within the G_q-coupled subgroup of P2Y receptors. This motif is thought to be important for receptor activation.

Another cationic residue (Arg268, 6.55) that was thought to be involved in ATP-P α,β recognition is also part of a conserved motif. For members belonging to the G_q-coupled subgroup of P2Y receptors the motif is HxxR/K, the G_i-coupled receptors have all arginine and not lysine. P1 receptors lack these arginine/ lysine residues, indicating the role of the positively charged amino acids in coordination of the phosphate moiety.

The Arg268Ala mutant receptor displayed a clearly reduced potency for ATP, compared to the wild type receptor, indicating the significance of an intact motif in TM6. When this arginine was substituted by glutamine, the potency of ATP could be partially rescued. These findings are consistent with the interpretation of a partial recovery of the Arg268 interaction with the phosphate moiety of ATP, which results in the partially restored activity. However, one cannot ignore the importance of a conserved pattern in TM6. Indeed, it has been suggested that at least one mechanism of GPCR activation originates in TM6, being the "aromatic zipper" (Rosenkilde et al., 2007). Although in cases where that mechanism of activation is clearly missing, the existence of alternative mechanisms, which could involve Arg268 cannot be ruled out.

For ATP γ S the loss in potency was not as drastic as for ATP at the Arg268 receptor mutants compared to the wild type receptor. This indicates that there is a favorable interaction with P γ -S, as compared to P γ -O, that still remains in the mutant which might be due to a tighter fit of the larger P γ -S moiety.

The corresponding residues in the P2Y₁ receptor (Lys280, 6.55) and the P2Y₂-R (Arg265, 6.55) were also found to be essential for activation at low ATP concentrations, because a clear decrease in potency was found by substitution of Lys280 or Arg265 by uncharged amino acids (Erb et al., 1995; Jiang et al., 1997). In the P2Y₆-R model this position (Lys259, 6.55) was part of a positively charged subpocket that bound the phosphate moiety of docked UDP, again highlighting the importance of this residue (Costanzi et al., 2005). For a member of the G_i-coupled subgroup of P2Y receptors the P2Y₁₂-R, the significance of this arginine residue (Arg256, 6.55) in TM6 was also confirmed (Cattaneo et al., 2003; Hoffmann, 2006).

☞ **A tyrosine residue in TM6 seems to be important for receptor activation**

The importance of an aromatic residue in TM6 (Tyr261) for ligand recognition was investigated. The Tyr261Ala mutant P2Y₁₁ receptor was incapable of being activated by ATP at concentrations up to 10 mM. Tyr261 (6.48) was not found to be directly interacting with the ATP molecule docked in the proposed P2Y₁₁-R model. However, it has been shown that a comparable residue (Tyr273) in the P2Y₁ receptor located at the same position (6.48) seems to act as a molecular switch for receptor activation (Costanzi et al., 2004). A Tyr273Ala mutation led to a functionally inactive receptor that was still able to bind agonist/antagonist with the same affinity as the wild type receptor. This is in accordance with the "aromatic zipper" theory proposing a probable mechanism of activation.

It can be assumed that Tyr261 is also solely involved in P2Y₁₁ receptor activation, since it was not found to significantly take part in the binding of ATP in the computed model. Due to the lack of a selective radioligand at the P2Y₁₁ receptor it was not possible to prove directly this hypothesis.

☞ **The EL2 is involved in ligand recognition whereas interactions of the P2Y₁₁ receptor with the adenine ring of ATP are only weak**

Besides the TM regions a role of the ELs for nucleotide binding by P2Y receptors has been suggested before (Hoffmann et al., 1999), and the importance of the EL2 Asp204 residue in ligand recognition has been already shown for the P2Y₁ receptor (Hoffmann et al., 1999; Costanzi et al., 2004; Major and Fischer, 2004). For the P2Y₁₁ receptor the residue Glu186 in the EL2 was also predicted to be involved in ligand recognition. Mutation of this glutamate to alanine resulted in a decreased potency of ATP at the receptor, consistent with the finding at the P2Y₁ receptor. However, for the more potent P2Y₁₁ receptor agonist ATP γ S the shift in potency was not as pronounced. This implies that Glu186 interacts with phosphates P _{α,β} of the triphosphate moiety because the tight fit of the P γ -S is less affected at the receptor mutant. Interaction of the glutamate with the phosphate chain occurs probably also via coordination of a Mg²⁺ ion, as proposed for the corresponding residue in the P2Y₁ receptor (Major and Fischer, 2004). The relatively small shift in potency for agonists at the Glu186 mutant implies a modulatory function of this residue in receptor functionality, similar to the observations at the P2Y₁ receptor (Hoffmann et al., 1999; Moro et al., 1999).

The involvement of the Phe109 residue that was proposed to interact with bound ATP in the P2Y₁₁-R model could not be confirmed. The aromatic amino acid in TM3 (Phe109, 3.32) seems to be not very critical for agonist recognition. There was no major effect on the potency of ATP at the receptor after substitution of this phenylalanine by isoleucine. However, this phenylalanine is highly conserved throughout the P2Y receptor family (Fig. 4A). In the P2Y₁ receptor, mutation of this residue to alanine caused a loss in potency for 2-MeS-ADP of about one order of magnitude but was still less critical for ligand recognition than other sites of the receptor (Jiang et al., 1997; Moro et al., 1998). Moreover, in a molecular model of the P2Y₆ receptor this phenylalanine (3.32) is possibly involved in hydrophobic interactions with the uracil ring of docked UDP (Costanzi et al., 2005).

The mutation of Phe109 to isoleucine in the P2Y₁₁ receptor did probably not much disturb the recognition of ATP at the receptor, since isoleucine is also a bulky, hydrophobic amino acid and therefore the loss in potency was only 4-fold. Thus, the prediction of π -stacking between the adenine and the phenyl ring could not be verified experimentally.

☞ **Arg268 in TM6 plays an important role in the determination of the diastereoselectivity of the P2Y₁₁ receptor**

Two of the residues (Glu186, Arg268) discussed here as being possibly involved in ligand recognition at the P2Y₁₁ receptor were also shown to influence the diastereoselectivity of the receptor. The glutamate in EL2 seems to be important for the activity of the ATP- α -S (A) isomers. Substitution of Glu186 by an uncharged, nonpolar amino acid (alanine) clearly reduced the potency of the (A) isomer, whereas the potency of the (B) isomers was more or less conserved. Therefore, the difference in potency between both ATP- α -S diastereoisomers was increased at the Glu186Ala receptor mutant as compared to the wild type P2Y₁₁ receptor.

The corresponding amino acid in the EL2 of the P2Y₁ receptor (Asp204) is believed to be responsible for the preference of the (A) isomers of the P $_{\alpha}$ borane/sulfur substituted ATP derivatives. Computational docking studies showed that Asp204 coordinates a Mg²⁺ ion which in turn interacts with the phosphate chain of a docked ATP molecule. In this process, the (A) isomers of the ATP- α -B,S analogues show the greatest interaction energies with the Mg²⁺ ion, clearly demonstrating the chiral discrimination of the P2Y₁ receptor (Major et al., 2004). If this is considered, the corresponding residue in the P2Y₁₁ receptor might play a similar role. The fact that the (A) isomer shows a reduced potency at the Glu186Ala receptor mutant seems to confirm this hypothesis. However, the EL2 of the P2Y₁₁ receptor is much longer than that of the P2Y₁ receptor (35 aa vs. 25 aa, resp.). Therefore, different mechanisms may account for the observed differences in potency.

The other residue influencing the diastereoselectivity of the P2Y₁₁ receptor is an arginine in TM6 (Arg268, 6.55). Mutation of this basic residue to alanine or glutamine resulted in a loss of the chiral discrimination at the receptor. The ATP- α -S (A) and (B) isomers were found to be equipotent at these mutant receptors. This was mainly caused by a severe loss of potency of the (B) isomers at the receptor whereas the activity of the (A) isomer was less affected. Thus, the arginine at position 6.55 seems to be essential for a preferred recognition of the (B) isomers at the P2Y₁₁ receptor. Interestingly, this arginine is also necessary for the preference of adenosine triphosphate over diphosphate at the receptor. The canine P2Y₁₁ receptor displays a glutamine at position 6.55 and is activated more potently by ADP than ATP (Qi et al., 2001) which could be confirmed in our study (data not shown). In addition, this residue (Arg268) is also involved in the stereoselective preference of the ATP- α -S (B) isomer at the P2Y₁₁ receptor, indicating the necessity of a basic residue at this position for proper chiral discrimination.

The positive charge of the Arg268 residue and its ability to contribute to H-bonds might induce a more tight interaction with the oxygen at P_α than the sulfur, thereby leading to the preference of one diastereoisomer at the receptor. Sulfur forms relatively weak H-bonds and has a lower potential in participating in electrostatic interactions than oxygen (Major et al., 2004).

☞ **Minor role of Ala313 in the recognition of 2-alkythio-ATP analogues**

Another characteristic of the P2Y₁₁ receptor besides its stereoselectivity is the weak potency of ATP derivatives carrying a substituent at the C2 position. To decipher the molecular basis of this property the unique alanine residue in TM7 (7.45) was mutated to asparagine as found in all the other P2Y receptors (Fig. 4A). This Ala313 (7.45) is situated at the entrance to a hydrophobic pocket located in the vicinity of the ATP C2 position in the P2Y₁₁-R model. The potency of ATP remained nearly unaffected at the Ala313Asn receptor mutant whereas 2-MeS-ATP showed a slight gain in function. This finding could support the hypothesis of this residue being a key player in the interactions involving ATP-C2 substitutions. However, 2-neopentylS-ATP with a bulkier substituent at C2 of the ATP molecule did not show a gain in function at the Ala313Asn receptor mutant. Therefore, it cannot be concluded that the unique alanine in TM7 of the P2Y₁₁ receptor is a true element in the determination of the weak potency of C2-substituted ATP analogues, but rather appears to be a 'supporting actor'.

4.3 Crosstalk between two P2Y receptors: the P2Y₁ and P2Y₁₁ receptor

The present study provides convincing evidence for a physical and functional interaction of the P2Y₁ and P2Y₁₁ receptor. The existence of GPCR homo- or heterooligomers is now largely accepted. Their formation as either constitutive or ligand-dependent complexes is still discussed and data are published for both variants (Terrillon and Bouvier, 2004). The functional relevance of GPCR oligomers includes modulation of internalization processes or alteration of their agonists/antagonists potency, which has to be considered regarding drug development (Milligan, 2006).

Interaction of two members of the P2Y receptor family has been investigated in the current study. The P2Y₁ and P2Y₁₁ receptor are found to be very close homologues in their receptor family. So far a crosstalk between both receptors has not been hypothesized. For the P2Y₁ receptor the ability to interact with other GPCRs became obvious in a study exploring the hetero-dimerization of the receptor with the A₁ adenosine receptor (Yoshioka et al., 2001).

The A₁ receptor was also found to interact with the P2Y₂ receptor (Suzuki et al., 2006) showing that the process of hetero-oligomerization was not only restricted to one subtype of the P2Y receptor family.

☞ **The P2Y₁ and P2Y₁₁ receptor associate physically thereby mediating the agonist-induced endocytosis of the P2Y₁₁ receptor**

In the current study the P2Y₁ and P2Y₁₁ receptor were discovered to show a strong physical interaction. This was determined by co-pulldown or co-immunoprecipitation experiments. The signal for the P2Y₁mycHis receptor could be clearly detected in the pulldown fraction of the P2Y₁₁GST receptor on GSH beads. There, the signal was much stronger than in the lane of the 10 % input (Fig. 28A, lane 5 and 1 respectively) indicating a robust complexation of both receptors. Precipitation of the P2Y₁mycHis receptor by an anti-myc antibody and detection of the P2Y₁₁GST receptor in a western blot of the precipitate further proved this fact. Moreover, this interaction of the receptors was not due to their presence in small membrane patches as the P2Y₁mycHis receptor could also be found in the pulldown fraction of the P2Y₁₁GST receptor from cellular extracts.

The hetero-oligomerization of the P2Y₁ receptor with the P2Y₁₁ receptor apparently has a great impact on the desensitization of the P2Y₁₁ receptor. When expressed alone, the P2Y₁₁ receptor does not internalize upon stimulation, as shown in this study. The P2Y₆ receptor behaves similarly and shows only slight reduction in cell surface expression after long-time exposure to agonists (Brinson and Harden, 2001). In contrast, the other members of the G_q-coupled P2Y receptor subgroup are able to undergo agonist-induced internalization as shown in studies concerning the P2Y₁ receptor (Tulapurkar et al., 2006), the P2Y₂ receptor (Tulapurkar et al., 2005), or the P2Y₄ receptor (Brinson and Harden, 2001).

In the present study, we show that the endocytosis of the P2Y₁₁ receptor is clearly dependent on the presence of its interaction with the partner, the P2Y₁ receptor, as shown in the current study. Knock-down of the endogenous P2Y₁ receptor in HEK293 cells by specific siRNA significantly diminished the agonist-induced internalization of the P2Y₁₁GFP receptor. The extent of reduction in P2Y₁ receptor mRNA transcripts correlated with the reduction of endocytosed P2Y₁₁ receptor.

Moreover, the P2Y₁₁GFP receptor stably expressed in 1321N1 cells could not be internalized by its natural agonist ATP. These cells, opposed to HEK293 cells which are known to express several endogenous P2Y receptors including the P2Y₁, P2Y₂ and P2Y₄ receptor (Schafer et al., 2003), do not express any P2Y receptor endogenously (Lazarowski et al., 1995). Interestingly, when the P2Y₁mycHis receptor was co-expressed with the P2Y₁₁GFP receptor in 1321N1 cells, clear signs of endocytosis of the P2Y₁₁ receptor were found. The endocytosed P2Y₁₁ receptor co-localized with the immunostaining of the P2Y₁mycHis receptor.

This functional interaction with the P2Y₁₁ receptor was specific for the P2Y₁ receptor. Agonists or antagonists of the P2Y₁ receptor were able to induce or block the endocytosis of the P2Y₁₁GFP receptor in HEK293 cells, respectively. In contrast, stimulation of the P2Y₂ receptor with UTP or the non-related PAR-2 receptor with trypsin or PAR2-AP did not lead to internalization of the P2Y₁₁ receptor. As the PAR2-HA receptor did also not physically interact with the P2Y₁₁GST receptor, as determined by co-pulldown experiments, it is obvious that the physical interaction is the prerequisite for a functional interaction.

However, the endocytosis of the P2Y₁₁ receptor is not only dependent on the interaction with the P2Y₁ receptor but also on a normal P2Y₁₁ receptor functioning. The A₂₆₈P2Y₁₁ receptor mutant that was unresponsive to ATP concentrations up to 100 μM showed endocytosis-resistance, when expressed in HEK293 cells. This was not due to a loss of interaction with the P2Y₁ receptor in HEK293 cells as shown by co-pulldown experiments. A difference in P2Y receptor expression profile of the HEKP2Y₁₁GFP or HEK_{A268}P2Y₁₁GFP cells did also not account for this observation. This was analyzed by RT-PCR. Thus, the R268A mutation of the P2Y₁₁ receptor seems to disrupt the ATP-induced functional interaction with the P2Y₁ receptor if co-internalization is considered.

The phenomenon of co-internalization may be a general and important functional consequence of hetero-oligomerization to control desensitization and resensitization of GPCRs (Prinster et al., 2005). Hetero-oligomerization among GPCRs can induce internalization of receptors previously considered endocytosis-reluctant. The somatostatin receptor (SSTR) SSTR1 failed to internalize upon agonist stimulation in several cell lines. However, the SSTR1 present in a hetero-dimer with the SSTR5 was found to display sufficient agonist-induced internalization (Rocheville et al., 2000).

Similar findings are presented here for the P2Y₁ and P2Y₁₁ receptor. The P2Y₁₁ receptor expressed alone lacks any desensitization, as shown here and reported previously by others (Communi et al., 1999). This property seems to be important for normal receptor function in the maturation process of dendritic cells (DC). These antigen-presenting cells are attracted by low concentrations of ATP to migrate to the site of inflammation. Once in the epicenter of inflammation, activation of the P2Y₁₁ receptor by high ATP concentrations leads to arrest in cell movement to prolong exposure to maturation-inducing factors (Schnurr et al., 2003). Thereby, the inability of the P2Y₁₁ receptor to desensitize seems to be important in overriding the chemotactic effects of nucleotides acting on other P2Y receptors. However, distinct DC subsets respond differently to ATP in terms of migration. DCs directly isolated from human blood show no arrest in migration in response to ATP treatment (Schnurr et al., 2003). Interestingly, these DC subpopulations display significant mRNA expression levels for the P2Y₁ receptor opposed to a negligible PCR signal in DCs (Langerhans cells, monocyte-derived DCs) which do not migrate in the presence of high ATP concentrations. It can be hypothesized that the presence of the P2Y₁ receptor in DCs isolated from human blood enables the desensitization of the P2Y₁₁ receptor in response to ATP, thereby controlling the chemotactic behavior and maturation of the cells. After all, distinct DC subsets were found to differentially regulate T cell responses in vivo (Pulendran et al., 2000). Therefore, a changed function of the P2Y₁₁ receptor by hetero-oligomerization with the P2Y₁ receptor might contribute to the differences observed in initiating T cell immunity by distinct DC subpopulations.

- **The P2Y₁-P2Y₁₁ receptor hetero-oligomer shows a pharmacology different to that of the receptor monomers**

Hetero-oligomerization of the P2Y₁₁ receptor with the endogenous P2Y₁ receptor in HEK293 cells has an impact on the receptor pharmacology. So far there is evidence that formation of hetero-oligomers can result in a distinct pharmacology of GPCRs (Carrillo et al., 2003). The A₁-P2Y₁ receptor hetero-dimer was found to have no affinity for MRS2179, a specific P2Y₁ receptor antagonist, whereas A₁ receptor antagonists could still bind. In contrast, the modified ligand binding pocket in the hetero-dimer appears to fit well to a P2Y₁ receptor agonist (ADPβS) but slightly less well to A₁ receptor ligands (Yoshioka et al., 2001).

In case of the P2Y₁-P2Y₁₁ receptor oligomer, the P2Y₁ receptor antagonist MRS2179 still showed an affinity for the hetero-oligomer, whereas the specific P2Y₁₁ receptor antagonist NF157 did not. MRS2179 was able to interfere with the BzATP-stimulated [Ca²⁺]_i rise and the ATP-induced internalization of the P2Y₁₁GFP receptor, whereas NF157 was not able to inhibit any of these effects. BzATP shows normally no activity at the P2Y₁ receptor (von Kugelgen, 2006). Therefore, it can be concluded that BzATP and MRS2179 both bind to the hetero-dimer. However, there are some discrepancies regarding the activity of BzATP. This ligand could induce a [Ca²⁺]_i increase in HEKP2Y₁₁GFP cells but was not able to stimulate receptor endocytosis. Such inconsistencies in the action of BzATP have also been found by other groups (Feng et al., 2004; Lee et al., 2005). Taken together, this indicates that BzATP can only induce specific receptor conformations in accordance with the probabilistic model of GPCR function. Different conformations of GPCRs are defined in the probabilistic model, where the pharmacological activity of a ligand is defined by the quantity and type of receptor conformations that are stabilized by the ligand (Kenakin, 2004).

Another interesting observation in HEKP2Y₁₁GFP cells is that UDP induced a drastic increase in [Ca²⁺]_i. UDP is known to activate the P2Y₆ receptor but this receptor was not expressed in our HEK293 cells, as analyzed by RT-PCR. The lack of P2Y₆ receptor expression in HEK293 cells was further confirmed by an unresponsiveness of mock-transfected cells to UDP. Moreover, the effect of UDP in the HEKP2Y₁₁GFP cells could be prevented by preincubation with MRS2179. This indicates an action of UDP at the P2Y₁-P2Y₁₁ receptor hetero-dimer that would have far-reaching consequences. Physiological effects of UDP that were assigned to the action at the P2Y₆ receptor would have to be reconsidered.

However, as the action of UDP in the HEKP2Y₁₁GFP cells could also be partially blocked by the P2Y₁₁ receptor antagonist NF157 some other reasons than affinity at the hetero-dimer have to be considered. NF157 was shown here in the endocytosis experiments and the BzATP-induced calcium responses to have no affinity at the P2Y₁-P2Y₁₁ receptor hetero-dimer.

The influence of lack of P2Y₁₁ receptor activity on its endocytosis was discussed above for the R268A receptor mutant. This mutation also influenced the pharmacology of the P2Y₁-P2Y₁₁ receptor hetero-oligomer. Heterologous expression of the A₂₆₈P2Y₁₁GFP receptor in HEK293 cells abolished the calcium response to UDP. Moreover, MRS2179 also lost its activity. This was not due to a loss of interaction with the P2Y₁ receptor in HEK293 cells as shown by co-pulldown experiments. A different mRNA expression profile for endogenous P2Y receptors in the differently transfected cells was also not the reason. Thus, the ligand selectivity of the P2Y₁-A₂₆₈P2Y₁₁ receptor hetero-oligomer was apparently different from that of the P2Y₁-P2Y₁₁ receptor hetero-dimer. Therefore, the R268 arginine seems to be a critical residue in the nucleotide binding pocket of the hetero-oligomer.

Two theories are currently discussed as to how GPCR oligomers are formed. One is the 'contact dimerization' and the other is the 'domain swapping' theory (Fig. 5b) (Kroeger et al., 2003). In the case of the P2Y₁-P2Y₁₁ receptor heterodimer our indications suggest that it is formed as a 'domain swapped' dimer because the pharmacological profile of P2Y receptor ligands implies the creation of a newly formed binding pocket.

Interestingly, investigations of [cAMP] increase in HEK293/P2Y₁₁GFP cells revealed the pharmacology profile known for the P2Y₁₁ receptor. Hetero-oligomerization of GPCRs is known to promote changes in the selectivity of the receptors to certain G proteins. A loss of coupling to G_i proteins has been reported following co-expression of μ - and δ -opioid receptors (Terrillon and Bouvier, 2004). We cannot be sure that the P2Y₁-P2Y₁₁ receptor hetero-dimer was unable to couple to G_s proteins, as we only investigated the pharmacology of cAMP elevation. However, it can be assumed that the coupling to activation of adenylyl cyclase was only possible for the non-oligomerized portion of the heterologously expressed P2Y₁₁GFP receptor. Therefore, the ligand selectivities resembled a profile that was representative for the P2Y₁₁ receptor monomer.

☞ **P2Y receptors can be pooled in cellular microdomains**

The importance of GPCR oligomerization becomes apparent when the relation between organization and signaling is considered. Organization of receptors and elements of the signal transduction pathway clearly affects cellular communication processes (Woolf and Linderman, 2004). The homo- or hetero-dimerization of GPCRs thereby allows fine tuning in the response to extracellular signals.

Functional compartmentation of P2Y receptors into cholesterol-rich signaling microdomains has been described for endothelial cells of the aorta. These endothelial cells may recruit different nucleotide receptors into different signaling domains in order to distinguish stimuli and regulate signal transduction (Kaiser et al., 2002). Such cholesterol-rich microdomains are also found in HEK293 cells and cholesterol depletion was found to affect the agonist-induced internalization of the P2Y₂ receptor heterologously expressed in these cells (Tulapurkar et al., 2005). In the present study some indication was gained as to suggest that P2Y receptors are pooled in these microdomains. The P2Y₁mycHis as well as the P2Y₄HA receptor could be found in the pulldown fraction of the P2Y₁₁GST receptor by western blot. The organization of the receptors in such microdomains seems to enable sufficient interaction to form oligomers and might be important for the integration of nucleotide signals.

Importantly, the hetero-oligomerization of the P2Y₁ or P2Y₂ receptor with the A₁ receptor was also found to take place in HEK293 cells (Yoshioka et al., 2001; Suzuki et al., 2006). The spatial organization of the whole purinergic signaling machinery might be an advantage for the cells to respond to extracellular nucleotides in a controlled manner.

5 ZUSAMMENFASSUNG

Die Signalübertragung durch extrazelluläre Nukleotide und Nukleoside ist ein weit verbreitetes System zur Anpassung an physiologische oder pathophysiologische Zustände in den unterschiedlichsten Geweben oder Organen. Die ‚Signalempfänger‘ auf zellulärer Ebene können, sowohl ionotrope Rezeptoren, als auch G-Protein-gekoppelte Rezeptoren sein und werden als purinerge Rezeptoren zusammengefasst. Die metabotropen Rezeptoren gliedern sich weiterhin in die Nukleosid-Rezeptoren (P1-Rezeptoren) und die Nukleotid-Rezeptoren (P2-Rezeptoren). Die Familie der G-Protein-gekoppelten Nukleotid-Rezeptoren (P2Y) ist sehr komplex. Bisher wurden acht verschiedene Rezeptor-Subtypen identifiziert, welche diverse Funktionen im menschlichen Körper übernehmen. Die gezielte Aktivierung oder Inhibition einzelner Rezeptor-Subtypen im Zuge einer therapeutischen Intervention benötigt daher spezifische Agonisten bzw. Antagonisten. Die Selektivität der P2Y-Rezeptor Subtypen für einzelne Nukleotide ist teilweise sehr divers, kann sich andererseits aber auch nur geringfügig unterscheiden. Die P2Y₁- und P2Y₁₁-Rezeptoren bevorzugen beide Adenin-Nukleotide, wobei der P2Y₁-Rezeptor stärker durch Diphosphate (ADP) und der P2Y₁₁-Rezeptor mehr durch Triphosphate (ATP) aktiviert wird. Zahlreiche Studien und die daraus resultierenden Erkenntnisse haben bereits zur Entwicklung von P2Y₁-Rezeptor-spezifischen Liganden geführt, welche keine Affinität am P2Y₁₁-Rezeptor oder an anderen Subtypen haben. Allerdings konnten für den P2Y₁₁-Rezeptor bisher keine selektiven Liganden entwickelt werden, da sich die Strukturmerkmale der bekannten Agonisten an diesem Rezeptor meist mit denen der P2Y₁-Rezeptor-Agonisten decken.

In der Absicht feinste Unterschiede in der Ligandenerkennung zwischen dem P2Y₁- und P2Y₁₁-Rezeptor aufzudecken, untersuchten wir die Stereoselektivität des Letzteren. Die bereits beschriebene stereoselektive Präferenz des P2Y₁-Rezeptors wurde nun in dieser Arbeit mit der Präferenz des P2Y₁₁-Rezeptors verglichen. Dafür haben wir den P2Y₁₁-Rezeptor als GFP Fusionsprotein stabil in 1321N1 Astrozytomzellen exprimiert, welche endogen keine funktionellen P2-Rezeptoren aufweisen. In Einzelzell-Kalziummessungen wurden die Zellen mit ATP Analoga, bei denen ein Sauerstoffatom am P_α durch Bor (ATP-α-B) oder Schwefel (ATP-α-S) substituiert war, stimuliert. Die Substitution am P_α schafft ein neues chirales Zentrum im Molekül. Die beiden resultierenden Diastereoisomere (A- und B-Isomere) testeten wir auf Aktivität am P2Y₁₁-Rezeptor. Wir identifizierten die Stereoselektivität des P2Y₁₁-Rezeptors und stellten fest, dass der Rezeptor die B-Isomere der jeweiligen ATP-α-B/S Derivate bevorzugt.

Dieses Ergebnis steht im Kontrast zu der bereits bekannten Stereoselektivität des P2Y₁ Rezeptors, welcher die A-Isomere bevorzugt. Weiterhin fanden wir heraus, dass die Substitution am P_α zu einem klaren Potenzgewinn der ATP Derivate am P2Y₁₁-Rezeptor führt. Da die getesteten ATP- α -B/S Analoga nahezu keine Aktivität am P2Y₂-Rezeptor (ein weiterer 'ATP-Rezeptor') aufweisen, stellen die B-Isomere wichtige Leitstrukturen für die Entwicklung eines selektiven P2Y₁₁ Rezeptor Agonisten dar. Diese könnten dann zum Beispiel als Adjuvantien in Impfstoffen eingesetzt werden, um deren Effizienz zu verbessern.

Das rationale Ligandendesign verwendet heutzutage computergestützte Modelle der therapeutischen Targets (z.B. Rezeptorproteine). Die berechneten Modelle sind allerdings ohne zusätzliche Information aus Mutagenese-Studien nicht genügend validiert. Wir haben die Ligandenbindungstasche des P2Y₁₁-Rezeptors mittels Computer-Modelling (in Kooperation mit der Bar-Ilan Universität, Israel) und zielgerichteter Mutagenese charakterisiert. Wie erwartet, ähneln sich die Nukleotidbindungstaschen des P2Y₁₁- und P2Y₁-Rezeptors sehr. Drei positiv geladene Aminosäuren im P2Y₁₁-Rezeptor (Arg106, Arg268, Arg307) koordinieren die Phosphatkette eines gebundenen ATP Moleküls und sind somit für die Nukleotidbindung essentiell. Die zweite extrazelluläre Schleife (EL2) ist auch beim P2Y₁₁-Rezeptor wie beim P2Y₁-Rezeptor an der Ligandenerkennung beteiligt. Wir entdeckten in der EL2 des P2Y₁₁ Rezeptors einen Glutamarest (Glu186), welcher die Potenz von ATP am Rezeptor deutlich mitbestimmt. Die Interaktion des Adeninrings mit der aromatischen Aminosäure Phe109 scheint nur eine schwache Wechselwirkung zu sein. Uns wurde klar, dass im Gegensatz zum P2Y₁-Rezeptor der P2Y₁₁-Rezeptor nur geringfügige Interaktionen mit dem Adeninring von gebundenem ATP zeigt. Weiterhin erhielten wir bei der Analyse der Mutanten erste Hinweise auf die mögliche molekulare Ursache der Diastereoselektivität des Rezeptors. Nach Mutation des Arginins Arg268 in der Transmembrandomäne 6 zu Alanin verloren die B-Isomere der ATP- α -S Analoga ihre verstärkte Potenz gegenüber den A-Isomeren.

Der Einsatz von P2Y₁₁-Rezeptor selektiven Agonisten zu therapeutischen Zwecken verlangt ausreichend Kenntnis über die Desensibilisierung des Rezeptors und eine sich daraus möglicherweise entwickelnde Toleranz gegenüber dem Therapeutikum. Daher haben wir die Agonist-induzierte Internalisierung des P2Y₁₁GFP Rezeptors untersucht. Bei diesen Experimenten wurde deutlich, dass der P2Y₁₁-Rezeptor allein nicht zur Endozytose fähig ist. Interessanterweise war die Internalisierung des Rezeptors eindeutig abhängig von der Präsenz des P2Y₁-Rezeptors. In weiteren Experimenten stellte wir fest, dass beide Rezeptoren interagieren und in den Zellen ein Hetero-Oligomer bilden.

Die Hetero-Oligomerisierung der P2Y₁- und P2Y₁₁-Rezeptoren wurde durch 'Pull-down'-Experimente und Immunopräzipitation nachgewiesen. Wir zeigten, dass die Interaktion mit dem P2Y₁-Rezeptor nicht nur Einfluß auf die Desensibilisierung des P2Y₁₁-Rezeptors, sondern auch auf dessen Pharmakologie hat. Der spezifische P2Y₁₁-Rezeptor-Antagonist NF157 zeigte keinerlei Affinität am Hetero-Oligomer. Dagegen war der P2Y₁-Rezeptor-Antagonist MRS2179 in der Lage sowohl die Internalisierung des P2Y₁₁-Rezeptors, als auch die rezeptor-vermittelte Calcium-Antwort zu inhibieren.

Letztendlich läßt sich sagen, dass die Erkenntnisse des gesamten Projektes sowohl Einblicke in die Stereoselektivität, als auch die Struktur des P2Y₁₁-Rezeptors geben und die Existenz von P2Y₁-P2Y₁₁-Rezeptor Oligomeren eindeutig nachweisen.

6 ABSTRACT

Purinergic signaling represents a primitive signaling system that employs widespread receptors which serve many different tissues. The purinergic receptor family consists of two different subgroups, the nucleoside (P1) and nucleotide (P2) receptors. The P2 receptors are further divided into ionotropic (P2X) and metabotropic (P2Y) receptors and till date seven P2X subtypes and eight human P2Y receptor subtypes have been discovered. Among the P2Y receptor subtypes, the P2Y₁ and P2Y₁₁ receptor are closely related. Agonists acting at the P2Y₁₁ receptor are also capable of activating the P2Y₁ receptor whereas the P2Y₁ receptor already responds to very low concentrations of these nucleotides. Therefore, it is important to identify mechanisms, which can regulate activation of one or the other receptor in tissues or cells where both are expressed. Pharmacological intervention provides one alternative to regulate the activation of individual P2Y receptors. For this, chemically modified agonists have to be studied to characterize agonist preferences of different receptor subtypes.

The focus of the present study was to elucidate differences in the ligand recognition between the less explored P2Y₁₁ receptor and the more widely studied P2Y₁ receptor. Therefore, we first investigated the diastereoselectivity of the P2Y₁₁ receptor stably expressed as GFP fusion protein in 1321N1 cells. These cells lack any functional expression of endogenous P2 receptors. Different diastereoisomers were tested at the stably expressed P2Y₁₁ receptor. These isomers show substitution of one of the non-bridging oxygen atoms of P_α by borane or sulfur (ATP- α -B/S). Thereby, a new chiral centre in the ATP molecule is introduced. In summary, a diastereoselective activity of ATP- α -B and ATP- α -S diastereoisomers with a preference for the (B) isomers was found at the P2Y₁₁ receptor. This diastereoselectivity is opposite to that of the P2Y₁ receptor which prefers the (A) isomers of these compounds. This shows that both receptors prefer different diastereoisomers of the chiral ATP analogues, in spite of being close homologues in the P2Y receptor family, sharing >50% of the amino acid residues involved in ligand recognition. These findings add to the understanding of the structural and conformational determinants of nucleotides which activate different P2Y receptors. The difference in diastereoselectivity allows a more detailed insight into the structure-activity relationships of these P2Y receptors.

Such a detailed insight can be realized by studying the binding mode of nucleotides at the P2Y receptors using mutagenesis analysis in combination with molecular modeling. As a next step in the thesis study, we analyzed amino acid residues putatively involved in ligand recognition at the P2Y₁₁ receptor.

During the course of this study, it became obvious that the nucleotide binding pockets of the P2Y₁ and P2Y₁₁ receptors are very similar, as expected. Three cationic amino acid residues in the TM regions of the P2Y₁₁ receptor (Arg106, Arg268, Arg307) coordinate the phosphate chain of a bound ATP molecule. Interaction with the adenine ring via the aromatic amino acid Phe109 seems to be a minor interaction. A glutamate (Glu186) in the EL2 of the P2Y₁₁ receptor also proved significant for ligand recognition. Moreover, further analysis of the mutant receptors gave the first indications about the molecular determinants of the stereoselective preference of ATP derivatives at the P2Y₁₁ receptor. Upon mutation of the arginine residue Arg268 in TM6 the preference of the (B)-isomers of ATP- α -S analogues at the receptor was lost. This finding is of considerable importance, particularly for the development of subtype-specific agonists or antagonists at the P2Y₁₁ receptor as potentially attractive drug candidates.

The use of such drugs for therapeutic intervention requires information on the desensitization of the P2Y₁₁ receptor induced by agonists. Therefore, we studied the agonist-induced endocytosis of the receptor in living cells. To our surprise we found that the internalization of the P2Y₁₁ receptor was clearly dependent on the presence of the P2Y₁ receptor. Further experiments using pulldown and immunoprecipitation techniques showed that both receptors associate physically in HEK293 cells to form a hetero-oligomer. These hetero-oligomers showed a distinct pharmacology. The specific P2Y₁₁ receptor antagonist had no affinity at the P2Y₁-P2Y₁₁ receptor hetero-oligomer whereas the P2Y₁ receptor antagonist MRS2179 could still interfere with signaling. The importance of GPCR oligomerization becomes apparent when the spatial organization of purinergic receptors and signaling are considered. The receptor oligomerization might be an advantage for the cell to respond to extracellular nucleotides in a well-regulated manner.

Taken together, the present thesis study has provided new insights into the structural determinants of ligands acting at the P2Y₁₁ receptor and insights into the ligand binding mode of the receptor. The study gives also convincing evidence for the existence of P2Y receptor hetero-oligomers.

7 REFERENCES

- Abbracchio MP, Burnstock G, Boeynaems JM, Barnard EA, Boyer JL, Kennedy C, Knight GE, Fumagalli M, Gachet C, Jacobson KA, Weisman GA (2006) International Union of Pharmacology LVIII: update on the P2Y G protein-coupled nucleotide receptors: from molecular mechanisms and pathophysiology to therapy. *Pharmacol Rev* 58:281-341.
- Amisten S, Melander O, Wihlborg AK, Berglund G, Erlinge D (2007) Increased risk of acute myocardial infarction and elevated levels of C-reactive protein in carriers of the Thr-87 variant of the ATP receptor P2Y₁₁. *Eur Heart J* 28:13-18.
- Balogh J, Wihlborg AK, Isackson H, Joshi BV, Jacobson KA, Arner A, Erlinge D (2005) Phospholipase C and cAMP-dependent positive inotropic effects of ATP in mouse cardiomyocytes via P2Y₁₁-like receptors. *J Mol Cell Cardiol* 39:223-230.
- Berchtold S, Ogilvie AL, Bogdan C, Muhl-Zurbes P, Ogilvie A, Schuler G, Steinkasserer A (1999) Human monocyte derived dendritic cells express functional P2X and P2Y receptors as well as ecto-nucleotidases. *FEBS Lett* 458:424-428.
- Besada P, Shin DH, Costanzi S, Ko H, Mathe C, Gagneron J, Gosselin G, Maddileti S, Harden TK, Jacobson KA (2006) Structure-activity relationships of uridine 5'-diphosphate analogues at the human P2Y₆ receptor. *J Med Chem* 49:5532-5543.
- Bourdon DM, Mahanty SK, Jacobson KA, Boyer JL, Harden TK (2006) (N)-methanocarb-2MeSADP (MRS2365) is a subtype-specific agonist that induces rapid desensitization of the P2Y₁ receptor of human platelets. *J Thromb Haemost* 4:861-868.
- Brinson AE, Harden TK (2001) Differential regulation of the uridine nucleotide-activated P2Y₄ and P2Y₆ receptors. SER-333 and SER-334 in the carboxyl terminus are involved in agonist-dependent phosphorylation desensitization and internalization of the P2Y₄ receptor. *J Biol Chem* 276:11939-11948.
- Bulenger S, Marullo S, Bouvier M (2005) Emerging role of homo- and heterodimerization in G-protein-coupled receptor biosynthesis and maturation. *Trends Pharmacol Sci* 26:131-137.
- Burnstock G (1971) Neural nomenclature. *Nature* 229:282-283.
- Burnstock G (1976) Do some nerve cells release more than one transmitter? *Neuroscience* 1:239-248.
- Burnstock G (2006) Purinergic P2 receptors as targets for novel analgesics. *Pharmacol Ther* 110:433-454.
- Burnstock G, Kennedy C (1985) Is there a basis for distinguishing two types of P2-purinoceptor? *Gen Pharmacol* 16:433-440.
- Burnstock G, Knight GE (2004) Cellular distribution and functions of P2 receptor subtypes in different systems. *Int Rev Cytol* 240:31-304.
- Buscher R, Hoerning A, Patel HH, Zhang S, Arthur DB, Grasemann H, Ratjen F, Insel PA (2006) P2Y₂ receptor polymorphisms and haplotypes in cystic fibrosis and their impact on Ca²⁺ influx. *Pharmacogenet Genomics* 16:199-205.
- Buvinic S, Poblete MI, Donoso MV, Delpiano AM, Briones R, Miranda R, Huidobro-Toro JP (2006) P2Y₁ and P2Y₂ receptor distribution varies along the human placental vascular tree: role of nucleotides in vascular tone regulation. *J Physiol* 573:427-443.
- Carrillo JJ, Pediani J, Milligan G (2003) Dimers of class A G protein-coupled receptors function via agonist-mediated trans-activation of associated G proteins. *J Biol Chem* 278:42578-42587.

- Cattaneo M, Zighetti ML, Lombardi R, Martinez C, Lecchi A, Conley PB, Ware J, Ruggeri ZM (2003) Molecular bases of defective signal transduction in the platelet P2Y₁₂ receptor of a patient with congenital bleeding. *Proc Natl Acad Sci U S A* 100:1978-1983.
- Chhatriwala M, Ravi RG, Patel RI, Boyer JL, Jacobson KA, Harden TK (2004) Induction of novel agonist selectivity for the ADP-activated P2Y₁ receptor versus the ADP-activated P2Y₁₂ and P2Y₁₃ receptors by conformational constraint of an ADP analog. *J Pharmacol Exp Ther* 311:1038-1043.
- Colquhoun D (2006) The quantitative analysis of drug-receptor interactions: a short history. *Trends Pharmacol Sci* 27:149-157.
- Communi D, Robaye B, Boeynaems JM (1999) Pharmacological characterization of the human P2Y₁₁ receptor. *Br J Pharmacol* 128:1199-1206.
- Communi D, Govaerts C, Parmentier M, Boeynaems JM (1997) Cloning of a human purinergic P2Y receptor coupled to phospholipase C and adenylyl cyclase. *J Biol Chem* 272:31969-31973.
- Conigrave AD, Fernando KC, Gu B, Tasevski V, Zhang W, Luttrell BM, Wiley JS (2001) P2Y(11) receptor expression by human lymphocytes: evidence for two cAMP-linked purinoceptors. *Eur J Pharmacol* 426:157-163.
- Cooper DR, Lewis GP, Lieberman GE, Webb H, Westwick J (1979) ADP metabolism in vascular tissue, a possible thrombo-regulatory mechanism. *Thromb Res* 14:901-914.
- Costanzi S, Mamedova L, Gao ZG, Jacobson KA (2004) Architecture of P2Y nucleotide receptors: structural comparison based on sequence analysis, mutagenesis, and homology modeling. *J Med Chem* 47:5393-5404.
- Costanzi S, Joshi BV, Maddileti S, Mamedova L, Gonzalez-Moa MJ, Marquez VE, Harden TK, Jacobson KA (2005) Human P2Y(6) receptor: molecular modeling leads to the rational design of a novel agonist based on a unique conformational preference. *J Med Chem* 48:8108-8111.
- Cusack NJ, Hourani SM (1982) Adenosine 5-diphosphate antagonists and human platelets: no evidence that aggregation and inhibition of stimulated adenylate cyclase are mediated by different receptors. *Br J Pharmacol* 76:221-227.
- Cusack NJ, Pearson JD, Gordon JL (1983) Stereoselectivity of ectonucleotidases on vascular endothelial cells. *Biochem J* 214:975-981.
- Erb L, Garrad R, Wang Y, Quinn T, Turner JT, Weisman GA (1995) Site-directed mutagenesis of P2U purinoceptors. Positively charged amino acids in transmembrane helices 6 and 7 affect agonist potency and specificity. *J Biol Chem* 270:4185-4188.
- Evans RJ, Lewis C, Virginio C, Lundstrom K, Buell G, Surprenant A, North RA (1996) Ionic permeability of, and divalent cation effects on, two ATP-gated cation channels (P2X receptors) expressed in mammalian cells. *J Physiol* 497 (Pt 2):413-422.
- Feng C, Mery AG, Beller EM, Favot C, Boyce JA (2004) Adenine nucleotides inhibit cytokine generation by human mast cells through a G_s-coupled receptor. *J Immunol* 173:7539-7547.
- Ferre S, Fredholm BB, Morelli M, Popoli P, Fuxe K (1997) Adenosine-dopamine receptor-receptor interactions as an integrative mechanism in the basal ganglia. *Trends Neurosci* 20:482-487.
- Fotiadis D, Liang Y, Filipek S, Saperstein DA, Engel A, Palczewski K (2003) Atomic-force microscopy: Rhodopsin dimers in native disc membranes. *Nature* 421:127-128.
- Gallagher JA (2004) ATP P2 receptors and regulation of bone effector cells. *J Musculoskelet Neuronal Interact* 4:125-127.
- Gallego D, Hernandez P, Clave P, Jimenez M (2006) P2Y₁ receptors mediate inhibitory purinergic neuromuscular transmission in the human colon. *Am J Physiol Gastrointest Liver Physiol* 291:G584-594.

- Gendron FP, Neary JT, Theiss PM, Sun GY, Gonzalez FA, Weisman GA (2003) Mechanisms of P2X₇ receptor-mediated ERK1/2 phosphorylation in human astrocytoma cells. *Am J Physiol Cell Physiol* 284:C571-581.
- Gever JR, Cockayne DA, Dillon MP, Burnstock G, Ford AP (2006) Pharmacology of P2X channels. *Pflugers Arch* 452:513-537.
- Granstein RD, Ding W, Huang J, Holzer A, Gallo RL, Di Nardo A, Wagner JA (2005) Augmentation of cutaneous immune responses by ATP gamma S: purinergic agonists define a novel class of immunologic adjuvants. *J Immunol* 174:7725-7731.
- Hansen JL, Sheikh SP (2004) Functional consequences of 7TM receptor dimerization. *Eur J Pharm Sci* 23:301-317.
- Hechler B, Nonne C, Roh EJ, Cattaneo M, Cazenave JP, Lanza F, Jacobson KA, Gachet C (2006) MRS2500 [2-iodo-N6-methyl-(N)-methanocarba-2'-deoxyadenosine-3',5'-bisphosphate], a potent, selective, and stable antagonist of the platelet P2Y₁ receptor with strong antithrombotic activity in mice. *J Pharmacol Exp Ther* 316:556-563.
- Hoffmann C, Moro S, Nicholas RA, Harden TK, Jacobson KA (1999) The role of amino acids in extracellular loops of the human P2Y₁ receptor in surface expression and activation processes. *J Biol Chem* 274:14639-14647.
- Hoffmann KA, I. von Kugelgen, I. (2006) Evidence for the involvement of basic amino acid residues in transmembrane regions 6 and 7 of the human platelet P2Y₁₂-receptor in ligand recognition. *Purinergic Signalling* 2:199-200.
- Horckmans M, Marcet B, Marteau F, Bulte F, Maho A, Parmentier M, Boeynaems JM, Communi D (2006) Extracellular adenine nucleotides inhibit the release of major monocyte recruiters by human monocyte-derived dendritic cells. *FEBS Lett* 580:747-754.
- Ivanov AA, Costanzi S, Jacobson KA (2006) Defining the nucleotide binding sites of P2Y receptors using rhodopsin-based homology modeling. *J Comput Aided Mol Des* 20:417-426.
- Jacobson KA, Costanzi S, Ohno M, Joshi BV, Besada P, Xu B, Tchilibon S (2004) Molecular recognition at purine and pyrimidine nucleotide (P2) receptors. *Curr Top Med Chem* 4:805-819.
- Jacobson KA, Costanzi S, Ivanov AA, Tchilibon S, Besada P, Gao ZG, Maddileti S, Harden TK (2006) Structure activity and molecular modeling analyses of ribose- and base-modified uridine 5'-triphosphate analogues at the human P2Y₂ and P2Y₄ receptors. *Biochem Pharmacol* 71:540-549.
- Jenner P (2005) Istradefylline, a novel adenosine A_{2A} receptor antagonist, for the treatment of Parkinson's disease. *Expert Opin Investig Drugs* 14:729-738.
- Jiang Q, Guo D, Lee BX, Van Rhee AM, Kim YC, Nicholas RA, Schachter JB, Harden TK, Jacobson KA (1997) A mutational analysis of residues essential for ligand recognition at the human P2Y₁ receptor. *Mol Pharmacol* 52:499-507.
- Kaiser RA, Oxhorn BC, Andrews G, Buxton IL (2002) Functional compartmentation of endothelial P2Y receptor signaling. *Circ Res* 91:292-299.
- Kenakin T (2004) Principles: receptor theory in pharmacology. *Trends Pharmacol Sci* 25:186-192.
- Kenakin T, Onaran O (2002) The ligand paradox between affinity and efficacy: can you be there and not make a difference? *Trends Pharmacol Sci* 23:275-280.
- Khakh BS, North RA (2006) P2X receptors as cell-surface ATP sensors in health and disease. *Nature* 442:527-532.
- Khakh BS, Burnstock G, Kennedy C, King BF, North RA, Seguela P, Voigt M, Humphrey PP (2001) International union of pharmacology. XXIV. Current status of the nomenclature and properties of P2X receptors and their subunits. *Pharmacol Rev* 53:107-118.

- Kim HS, Ravi RG, Marquez VE, Maddileti S, Wihlborg AK, Erlinge D, Malmsjo M, Boyer JL, Harden TK, Jacobson KA (2002) Methanocarba modification of uracil and adenine nucleotides: high potency of Northern ring conformation at P2Y₁, P2Y₂, P2Y₄, and P2Y₁₁ but not P2Y₆ receptors. *J Med Chem* 45:208-218.
- Korcok J, Raimundo LN, Du X, Sims SM, Dixon SJ (2005) P2Y₆ nucleotide receptors activate NF-kappaB and increase survival of osteoclasts. *J Biol Chem* 280:16909-16915.
- Kristiansen K (2004) Molecular mechanisms of ligand binding, signaling, and regulation within the superfamily of G-protein-coupled receptors: molecular modeling and mutagenesis approaches to receptor structure and function. *Pharmacol Ther* 103:21-80.
- Kroeger KM, Pflieger KD, Eidne KA (2003) G-protein coupled receptor oligomerization in neuroendocrine pathways. *Front Neuroendocrinol* 24:254-278.
- Lazarowski ER, Homolya L, Boucher RC, Harden TK (1997) Identification of an ecto-nucleoside diphosphokinase and its contribution to interconversion of P2 receptor agonists. *J Biol Chem* 272:20402-20407.
- Lazarowski ER, Watt WC, Stutts MJ, Boucher RC, Harden TK (1995) Pharmacological selectivity of the cloned human P2U-purinoceptor: potent activation by diadenosine tetraphosphate. *Br J Pharmacol* 116:1619-1627.
- Lee BC, Cheng T, Adams GB, Attar EC, Miura N, Lee SB, Saito Y, Olszak I, Dombkowski D, Olson DP, Hancock J, Choi PS, Haber DA, Luster AD, Scadden DT (2003) P2Y-like receptor, GPR105 (P2Y14), identifies and mediates chemotaxis of bone-marrow hematopoietic stem cells. *Genes Dev* 17:1592-1604.
- Lee H, Jun DJ, Suh BC, Choi BH, Lee JH, Do MS, Suh BS, Ha H, Kim KT (2005) Dual roles of P2 purinergic receptors in insulin-stimulated leptin production and lipolysis in differentiated rat white adipocytes. *J Biol Chem* 280:28556-28563.
- Limbird LE (2004) The receptor concept: a continuing evolution. *Mol Interv* 4:326-336.
- Luo W, Wang Y, Reiser G (2005) Two types of protease-activated receptors (PAR-1 and PAR-2) mediate calcium signaling in rat retinal ganglion cells RGC-5. *Brain Res* 1047:159-167.
- Luo W, Wang Y, Hanck T, Stricker R, Reiser G (2006) Jab1, a novel protease-activated receptor-2 (PAR-2)-interacting protein, is involved in PAR-2-induced activation of activator protein-1. *J Biol Chem* 281:7927-7936.
- Major DT, Fischer B (2004) Molecular recognition in purinergic receptors. 1. A comprehensive computational study of the h-P2Y₁-receptor. *J Med Chem* 47:4391-4404.
- Major DT, Nahum V, Wang Y, Reiser G, Fischer B (2004) Molecular recognition in purinergic receptors. 2. Diastereoselectivity of the h-P2Y₁-receptor. *J Med Chem* 47:4405-4416.
- Marshall FH, Jones KA, Kaupmann K, Bettler B (1999) GABAB receptors - the first 7TM heterodimers. *Trends Pharmacol Sci* 20:396-399.
- Marteau F, Communi D, Boeynaems JM, Suarez Gonzalez N (2004) Involvement of multiple P2Y receptors and signaling pathways in the action of adenine nucleotides diphosphates on human monocyte-derived dendritic cells. *J Leukoc Biol* 76:796-803.
- Marteau F, Gonzalez NS, Communi D, Goldman M, Boeynaems JM, Communi D (2005) Thrombospondin-1 and indoleamine 2,3-dioxygenase are major targets of extracellular ATP in human dendritic cells. *Blood* 106:3860-3866.
- Matos JE, Robaye B, Boeynaems JM, Beauwens R, Leipziger J (2005) K⁺ secretion activated by luminal P2Y₂ and P2Y₄ receptors in mouse colon. *J Physiol* 564:269-279.
- Milligan G (2006) G-protein-coupled receptor heterodimers: pharmacology, function and relevance to drug discovery. *Drug Discov Today* 11:541-549.

- Moore D, Chambers J, Waldvogel H, Faull R, Emson P (2000) Regional and cellular distribution of the P2Y₁ purinergic receptor in the human brain: striking neuronal localisation. *J Comp Neurol* 421:374-384.
- Moore DJ, Chambers JK, Wahlin JP, Tan KB, Moore GB, Jenkins O, Emson PC, Murdock PR (2001) Expression pattern of human P2Y receptor subtypes: a quantitative reverse transcription-polymerase chain reaction study. *Biochim Biophys Acta* 1521:107-119.
- Moreschi I, Bruzzone S, Nicholas RA, Fruscione F, Sturla L, Benvenuto F, Usai C, Meis S, Kassack MU, Zocchi E, De Flora A (2006) Extracellular NAD⁺ is an agonist of the human P2Y₁₁ purinergic receptor in human granulocytes. *J Biol Chem* 281:31419-31429.
- Moro S, Hoffmann C, Jacobson KA (1999) Role of the extracellular loops of G protein-coupled receptors in ligand recognition: a molecular modeling study of the human P2Y₁ receptor. *Biochemistry* 38:3498-3507.
- Moro S, Guo D, Camaioni E, Boyer JL, Harden TK, Jacobson KA (1998) Human P2Y₁ receptor: molecular modeling and site-directed mutagenesis as tools to identify agonist and antagonist recognition sites. *J Med Chem* 41:1456-1466.
- Nahum V, Zundorf G, Levesque SA, Beaudoin AR, Reiser G, Fischer B (2002) Adenosine 5'-O-(1-boranotriphosphate) derivatives as novel P2Y₁ receptor agonists. *J Med Chem* 45:5384-5396.
- Nicholas RA, Watt WC, Lazarowski ER, Li Q, Harden K (1996) Uridine nucleotide selectivity of three phospholipase C-activating P2 receptors: identification of a UDP-selective, a UTP-selective, and an ATP- and UTP-specific receptor. *Mol Pharmacol* 50:224-229.
- Oury C, Toth-Zsomboki E, Vermylen J, Hoylaerts MF (2006) The platelet ATP and ADP receptors. *Curr Pharm Des* 12:859-875.
- Palmer RK, Boyer JL, Schachter JB, Nicholas RA, Harden TK (1998) Agonist action of adenosine triphosphates at the human P2Y₁ receptor. *Mol Pharmacol* 54:1118-1123.
- Pearson JD, Carleton JS, Gordon JL (1980) Metabolism of adenine nucleotides by ectoenzymes of vascular endothelial and smooth-muscle cells in culture. *Biochem J* 190:421-429.
- Prinster SC, Hague C, Hall RA (2005) Heterodimerization of G protein-coupled receptors: specificity and functional significance. *Pharmacol Rev* 57:289-298.
- Pulendran B, Banchereau J, Burkeholder S, Kraus E, Guinet E, Chalouni C, Caron D, Maliszewski C, Davoust J, Fay J, Palucka K (2000) Flt3-ligand and granulocyte colony-stimulating factor mobilize distinct human dendritic cell subsets in vivo. *J Immunol* 165:566-572.
- Qi AD, Zambon AC, Insel PA, Nicholas RA (2001) An arginine/glutamine difference at the juxtaposition of transmembrane domain 6 and the third extracellular loop contributes to the markedly different nucleotide selectivities of human and canine P2Y₁₁ receptors. *Mol Pharmacol* 60:1375-1382.
- Ralevic V, Burnstock G (1998) Receptors for purines and pyrimidines. *Pharmacol Rev* 50:413-492.
- Rang H, Dale MM, Ritter JM, Moore PK (2003) *Pharmacology, Section One, How drugs act: General Principles*: Churchill-Livingstone.
- Ravi RG, Kim HS, Servos J, Zimmermann H, Lee K, Maddileti S, Boyer JL, Harden TK, Jacobson KA (2002) Adenine nucleotide analogues locked in a Northern methanocarpa conformation: enhanced stability and potency as P2Y₁ receptor agonists. *J Med Chem* 45:2090-2100.
- Robaye B, Ghanem E, Wilkin F, Fokan D, Van Driessche W, Schurmans S, Boeynaems JM, Beauwens R (2003) Loss of nucleotide regulation of epithelial chloride transport in the jejunum of P2Y₄-null mice. *Mol Pharmacol* 63:777-783.

- Rocheville M, Lange DC, Kumar U, Sasi R, Patel RC, Patel YC (2000) Subtypes of the somatostatin receptor assemble as functional homo- and heterodimers. *J Biol Chem* 275:7862-7869.
- Rodrigues RJ, Almeida T, Richardson PJ, Oliveira CR, Cunha RA (2005) Dual presynaptic control by ATP of glutamate release via facilitatory P2X₁, P2X_{2/3}, and P2X₃ and inhibitory P2Y₁, P2Y₂, and/or P2Y₄ receptors in the rat hippocampus. *J Neurosci* 25:6286-6295.
- Rosenkilde MM, Andersen MB, Nygaard R, Frimurer TM, Schwartz TW (2007) Activation of the CXCR3 chemokine receptor through anchoring of a small molecule chelator ligand between TM-III, -IV, and -VI. *Mol Pharmacol* 71:930-941.
- Schachter JB, Li Q, Boyer JL, Nicholas RA, Harden TK (1996) Second messenger cascade specificity and pharmacological selectivity of the human P2Y₁-purinoceptor. *Br J Pharmacol* 118:167-173.
- Schafer R, Sedehizade F, Welte T, Reiser G (2003) ATP- and UTP-activated P2Y receptors differently regulate proliferation of human lung epithelial tumor cells. *Am J Physiol Lung Cell Mol Physiol* 285:L376-385.
- Schnurr M, Toy T, Stoitzner P, Cameron P, Shin A, Beecroft T, Davis ID, Cebon J, Maraskovsky E (2003) ATP gradients inhibit the migratory capacity of specific human dendritic cell types: implications for P2Y₁₁ receptor signaling. *Blood* 102:613-620.
- Suzuki T, Namba K, Tsuga H, Nakata H (2006) Regulation of pharmacology by hetero-oligomerization between A1 adenosine receptor and P2Y₂ receptor. *Biochem Biophys Res Commun* 351:559-565.
- Terrillon S, Bouvier M (2004) Roles of G-protein-coupled receptor dimerization. *EMBO Rep* 5:30-34.
- Tsim KW, Barnard EA (2002) The signaling pathways mediated by P2Y nucleotide receptors in the formation and maintenance of the skeletal neuromuscular junction. *Neurosignals* 11:58-64.
- Tulapurkar ME, Zundorf G, Reiser G (2006) Internalization and desensitization of a green fluorescent protein-tagged P2Y nucleotide receptor are differently controlled by inhibition of calmodulin-dependent protein kinase II. *J Neurochem* 96:624-634.
- Tulapurkar ME, Laubinger W, Nahum V, Fischer B, Reiser G (2004) Subtype specific internalization of P2Y₁ and P2Y₂ receptors induced by novel adenosine 5'-O-(1-boranotriphosphate) derivatives. *Br J Pharmacol* 142:869-878.
- Tulapurkar ME, Schafer R, Hanck T, Flores RV, Weisman GA, Gonzalez FA, Reiser G (2005) Endocytosis mechanism of P2Y₂ nucleotide receptor tagged with green fluorescent protein: clathrin and actin cytoskeleton dependence. *Cell Mol Life Sci* 62:1388-1399.
- Ubl JJ, Vöhringer C, Reiser G (1998) Co-existence of two types of [Ca²⁺]_i-inducing protease-activated receptors (PAR-1 and PAR-2) in rat astrocytes and C6 glioma cells. *Neuroscience* 86:597-609.
- Ullmann H, Meis S, Hongwiset D, Marzian C, Wiese M, Nickel P, Communi D, Boeynaems JM, Wolf C, Hausmann R, Schmalzing G, Kassack MU (2005) Synthesis and structure-activity relationships of suramin-derived P2Y₁₁ receptor antagonists with nanomolar potency. *J Med Chem* 48:7040-7048.
- Vigne P, Hechler B, Gachet C, Breittmayer JP, Frelin C (1999) Benzoyl ATP is an antagonist of rat and human P2Y₁ receptors and of platelet aggregation. *Biochem Biophys Res Commun* 256:94-97.
- Vöhringer C, Schäfer R, Reiser G (2000) A chimeric rat brain P2Y₁ receptor tagged with green-fluorescent protein: high-affinity ligand recognition of adenosine diphosphates and triphosphates and selectivity identical to that of the wild-type receptor. *Biochem Pharmacol* 59:791-800.

- von Kugelgen I (2006) Pharmacological profiles of cloned mammalian P2Y-receptor subtypes. *Pharmacol Ther* 110:415-432.
- Vonend O, Grote T, Oberhauser V, Von Kugelgen I, Rump LC (2003) P2Y-receptors stimulating the proliferation of human mesangial cells through the MAPK42/44 pathway. *Br J Pharmacol* 139:1119-1126.
- Wang L, Olivecrona G, Gotberg M, Olsson ML, Winzell MS, Erlinge D (2005) ADP acting on P2Y₁₃ receptors is a negative feedback pathway for ATP release from human red blood cells. *Circ Res* 96:189-196.
- White PJ, Webb TE, Boarder MR (2003) Characterization of a Ca²⁺ response to both UTP and ATP at human P2Y₁₁ receptors: evidence for agonist-specific signaling. *Mol Pharmacol* 63:1356-1363.
- Wilkin F, Duhant X, Bruyns C, Suarez-Huerta N, Boeynaems JM, Robaye B (2001) The P2Y₁₁ receptor mediates the ATP-induced maturation of human monocyte-derived dendritic cells. *J Immunol* 166:7172-7177.
- Woolf PJ, Linderman JJ (2004) An algebra of dimerization and its implications for G-protein coupled receptor signaling. *J Theor Biol* 229:157-168.
- Yoshioka K, Saitoh O, Nakata H (2001) Heteromeric association creates a P2Y-like adenosine receptor. *Proc Natl Acad Sci U S A* 98:7617-7622.
- Yoshioka K, Saitoh O, Nakata H (2002) Agonist-promoted heteromeric oligomerization between adenosine A₁ and P2Y₁ receptors in living cells. *FEBS Lett* 523:147-151.
- Yoshioka K, Hosoda R, Kuroda Y, Nakata H (2002) Hetero-oligomerization of adenosine A₁ receptors with P2Y₁ receptors in rat brains. *FEBS Lett* 531:299-303.
- Zylberg J, Ecke D, Fischer B, Reiser G (2007) Structure and ligand binding site characteristics of the human P2Y₁₁ nucleotide receptor deduced from computational modelling and mutational analysis. *Biochem J*.

8 ABBREVIATIONS

2-Cl-ATP- α -B	2-chloro-adenosine-5'-(1-boranotriphosphate)
2-MeSADP	2-methylthio-adenosine-5'-diphosphate
2-MeSATP	2-methylthio-adenosine-5'-triphosphate
2-MeS-ATP- α -B	2-methylthio-adenosine-5'-(1-boranotriphosphate)
2-MeS-ATP- α -S	2-methylthio-adenosine-5'-(1-thiotriphosphate)
2-neopentyl-thio-ATP	2-neopentylthio-adenosine-5'-triphosphate
5-Br-UDP	5-bromo-uridine-5'-diphosphate
ADP	adenosine-5'-diphosphate
ADPRC	ADP-ribosylcyclase
ADP β S	adenosine-5'-(2-thiodiphosphate)
AMP	adenosine-5'-monophosphate
Ap4A	diadenosine 5',5''-P1,P4-tetraphosphate
ARC67085	2-propylthio- β , γ -dichloromethylene-D-ATP
ATP	adenosine-5'-triphosphate
ATP- α -B	adenosine-5'-(1-boranotriphosphate)
ATP β S	adenosine-5'-(2-thiotriphosphate)
ATP γ S	adenosine-5'-(3-thiotriphosphate)
B2AR	β_2 adrenergic receptor
BRET	Bioluminescence Resonance Energy Transfer
BRHO	bovine rhodopsin
BzATP	2'-and 3'-O-(4-benzoyl-benzoyl)adenosine 5'-triphosphate
CaCl ₂	calcium chloride
cADPR	cyclic adenosine diphosphate ribose
cAMP	cyclic Adenosinemonophosphate
CF	Cystic Fibrosis
CGS21680	2-[p-(2-carboxyethyl)phenylethylamino]-5'-N-ethyl-carboxamidoadenosine
CPA	N ⁶ -cyclopentyladenosine
C-terminus	carboxyl terminus
D2	D ₂ dopamine receptor
DC	dendritic cells
DMEM	Dulbecco's Modified Eagle Medium
DMSO	dimethylsulfoxide
DNA	desoxyribonucleic acid
DPCPX	1,3-dipropyl-8-cyclopentylxanthine
D-receptor	dopamine receptor
DTT	dithiothreitol
ECL	enhanced chemiluminescence

Abbreviations

EDTA	ethylene-diamine-tetra-acetic acid
EIA	enzyme-linked immuno assay
ER	endoplasmic reticulum
FACS	fluorescence activated cell sorting
FCS	fetal calf serum
G418 Sulphate	geneticin disulfate
GAPDH	glyceraldehyde-3-phosphate-dehydrogenase
GFP	green fluorescent protein
GPCR	G protein-coupled receptor
G protein	guanine nucleotide-binding protein
GSH	glutathione sepharose
HBSS	Hank's Buffered Salt Solution
HEPES	N- (2-Hydroxyethyl)-piperazin-N'-2- ethansulfonic acid
IB-MECA	N ⁶ -(3-iodo-benzyl)-5'-(N-methylcarbamoyl)adenosine
IBMX	3-Isobutyl-1-methylxanthine
INS37217	denufosol tetrasodium
KCl	potassium chloride
kDA	kilo Dalton
KF17837	1,3-dipropyl-8-(3,4-dimethoxystyryl)-7-methylxanthine
KH ₂ PO ₄	potassium dihydrogenphosphate
L-DOPA	L-3,4-Dihydroxyphenylalanin
MATra	Magnet Assisted Transfection
MgCl ₂	magnesium chloride
MgSO ₄	magnesium sulphate
MRS1067	3,6-dichloro-2'-isopropoxy-4'-isopropylflavone
MRS2179	N ⁶ -methyl-2'-deoxyadenosine-3',5'-bisphosphate
MRS2365	(N)-Methanocarba-2-MeS-ADP
MRS2500	2-iodo-N ⁶ -methyl-(N)-methanocarba-2'-deoxyadenosine-3',5'-bisphosphate
MRS2567	1,2-di-(4-isothiocyanatophenyl)ethane
Na ₂ HPO ₄ *2H ₂ O	sodium hydrogenphosphate-Dihydrate
NaCl	sodium chloride
NaF	sodium fluoride
NaHCO ₃	sodium hydrogencarbonate
NC	nitrocellulose
NECA	5'-N-ethyl-carboxamidoadenosine
NF157	8,8'-[Caronylbis[imino-3,1-phenylenecarbonylimino (4-fluoro-3,1-phenylene)carbonylimino]]bis-1,3,5-naphtalenetrisulfonic acid
NK1	tachykinin receptor
NO	Nitrogenmonooxide
N-terminus	amino-terminus
P1	Purinergic receptor family 1

Abbreviations

P2	Purinergic receptor family 2
P2X	ionotropic P2 receptor
P2Y	metabotropic P2 receptor
PAGE	polyacrylamide gel electrophoresis
PAR2	protease activated receptor 2
PAR2-AP	PAR2- activating peptide
PCR	polymerase chain reaction
PEG	polyethyleneglycol
PFA	paraformaldehyde
PPADS	pyridoxal-phosphate-6-azophenyl-2',4'-disulfonate
RBC	red blood cells
RNA	ribonucleic acid
Rp/Sp-ATP- α -S	Rp/Sp-adenosine-5'-(1-thiotriphosphate)
SDS	sodiumdodecylsulphate
siRNA	small interfering RNA
SSTR	somatostatin receptor
TEMED	tetramethylethylenediamine
TM	Transmembrane domain
TNP-ATP	2'(or 3')-O-(2, 4, 6-trinitrophenyl)adenosine 5'-triphosphate
UDP	uridine-5'-diphosphate
UDP β S	uridine-5'-(2-thiodiphosphate)
UTP	uridine-5'-triphosphate
UTP γ S	uridine-5'-(3-thiotriphosphate)
HA	hemagglutinin
α -receptor	α adrenergic receptor
β -NAD ⁺ _e	extracellular NAD ⁺ (β -form)
β -receptor	β adrenergic receptor

Verzeichnis der wissenschaftlichen Leistungen

Publikationen:

1. Demographic variation in the use of antibiotics in a New Zealand town. Norris P, Becket G, Ecke D; New Zealand Medical Journal 2005 Mar 11; 118 (1211):U1352
2. How many prescriptions are unsubsidised in New Zealand? Norris P, Funke S, Becket G, Ecke D, Reiter L, Herbison P; New Zealand Medical Journal 2006 May 5; 119 (1233):U1951
3. Fluorescent N²,N³-epsilon-adenine nucleoside and nucleotide probes: synthesis, spectroscopic properties, and biochemical evaluation. Sharon E, Levesque SA, Munkonda MN, Sevigny J, Ecke D, Reiser G, Fischer B; CHEMBIOCHEM 2006 Sep; 7(9):1361-1374
4. Opposite diastereoselective activation of P2Y₁ and P2Y₁₁ nucleotide receptors by adenosine 5'-O-(alpha-boranotriphosphate) analogues. Ecke D, Tulapurkar ME, Nahum V, Fischer B, Reiser G; British Journal of Pharmacology 2006 Oct; 149(4):416-423
5. Characterization of the human P2Y₁₁ nucleotide receptor by computational and mutational analysis. Zylberg J*, Ecke D*, Fischer B, Reiser G; Biochemical Journal 2007 Jul; 405(2):277-86. *gleicher Beitrag
6. Hetero-oligomerization of the P2Y₁ and P2Y₁₁ receptor controls receptor internalization and ligand selectivity of the P2Y₁₁ receptor. Ecke D, Hanck T, Tulapurkar ME, Schäfer R, Stricker R, Kassack M, Reiser G; Biochemical Journal 2007 Sep; [Epub ahead of print].

Lebenslauf

Name: Denise Ecke
Anschrift: Marderweg 11
39120 Magdeburg
Telefon: 0391/6713892
geboren: 25. September 1978 in Halle/S.
Staatsangehörigkeit: deutsch

Schulausbildung

1985-1991 Makarenko-Schule Halle/S.
1991-1997 Tor-Gymnasium in Halle/S.
09.07.1997 Abitur

Arbeitszeiten

09/1997-02/1998 Freiwilliges Soziales Jahr, Altenheim Akazienhof Halle/S.

Studium

04/1998 - 05/2002 Pharmaziestudium, Technische Universität Braunschweig
06/2002 - 11/2002 Pharmaziepraktikantin in der Rudolf-Apotheke Braunschweig
01/2003 - 06/2003 Postgraduate Certificate in Pharmacy mit dem Thema: „The use of antibiotics in a small New Zealand town“ an der School of Pharmacy, University of Otago, Dunedin, Neuseeland unter Anleitung von Pauline Norris, Ph.D und Gordon Becket, Ph.D
10/2003 Prüfung und Approbation zur Apothekerin
10/2003-05/2007 Dissertation: „Characteristics of the P2Y₁₁ nucleotide receptor: Ligand binding characteristics and the interaction of the P2Y₁₁-P2Y₁ receptor interaction“ am Institut für Neurobiochemie, Otto-von-Guericke Universität, Magdeburg
01/2005-12/2005 BMBF NBL3-Doktorandenstipendium des Magdeburger Forschungsverbunds „Neurowissenschaften“ & „Immunologie und Molekulare Medizin der Entzündung“

Magdeburg, Mai 2007

Denise Ecke